

Tutorial: Introduction to Research in Magnetic Resonance Imaging

Tutorial authors:

- **Fábio Augusto Menocci Cappabianco** – Institute of Science and Technology, Federal University of São Paulo
- **Claudio Saburo Shida** – Institute of Science and Technology, Federal University of São Paulo
- **Jaime Shinsuke Ide** – Department of Biomedical Engineering, Stony Brook University

Tutorial Presentation:

- **Fábio Augusto Menocci Cappabianco** – Institute of Science and Technology, Federal University of São Paulo
- **Claudio Saburo Shida** – Institute of Science and Technology, Federal University of São Paulo
- **Gilson Vieira** – Faculty of Medicine, University of São Paulo
- **Kelly Cotosck** – Faculty of Medicine, University of São Paulo

Overview

Part I: Magnetic Resonance Image Acquisition – Cláudio Subaru Shida – Pages 3-49

Part II: Magnetic Resonance Image Processing and Analysis – Fábio Augusto Menocci Cappabianco – Page 50-96

Part III: Magnetic Resonance Image Spatial Normalization – Cláudio Subaru Shida – Page 97-120

Part IV: Functional Magnetic Resonance Image Acquisition and Analysis – Gilson Vieira and Kelly Cotosck – Page 121-138

Aquisição

Magnetic Resonance Imaging (MRI)



Sibigrapi 16 – São José dos
Campos

2016

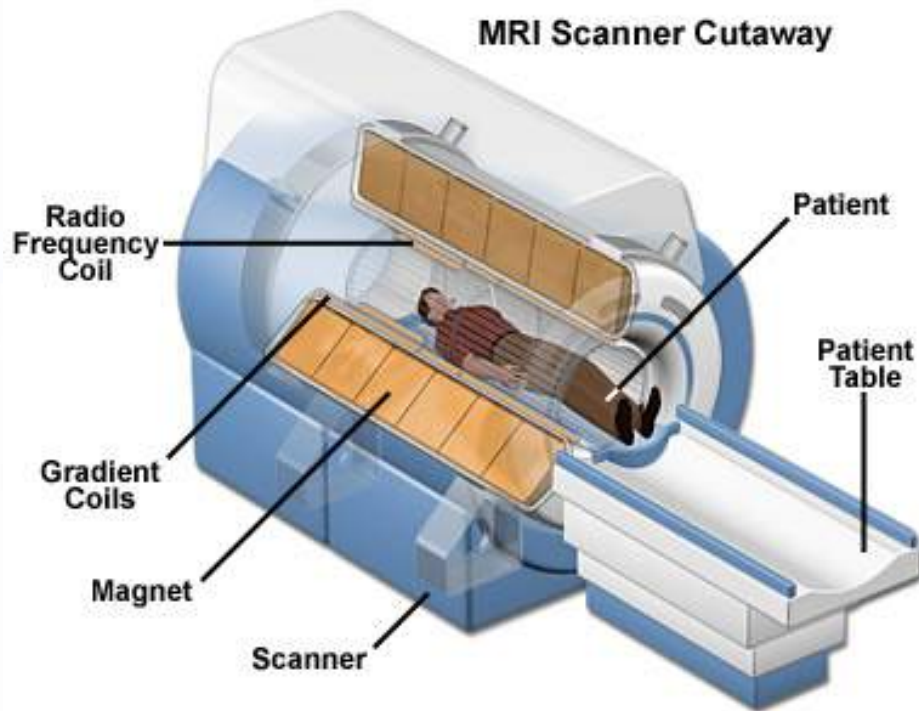
Claudio Shida

Email: shida@unifesp.br

Summary

- Introduction to MRI
- MRI scanner
- NMR phenomenon
- Relaxation times T_1 and T_2
- Image formation: Spin-echo technique (TR and TE)

Introduction to MRI



<https://pancreaticcanceraction.org/about-pancreatic-cancer/diagnosis/second-line-investigations/mri-scan>

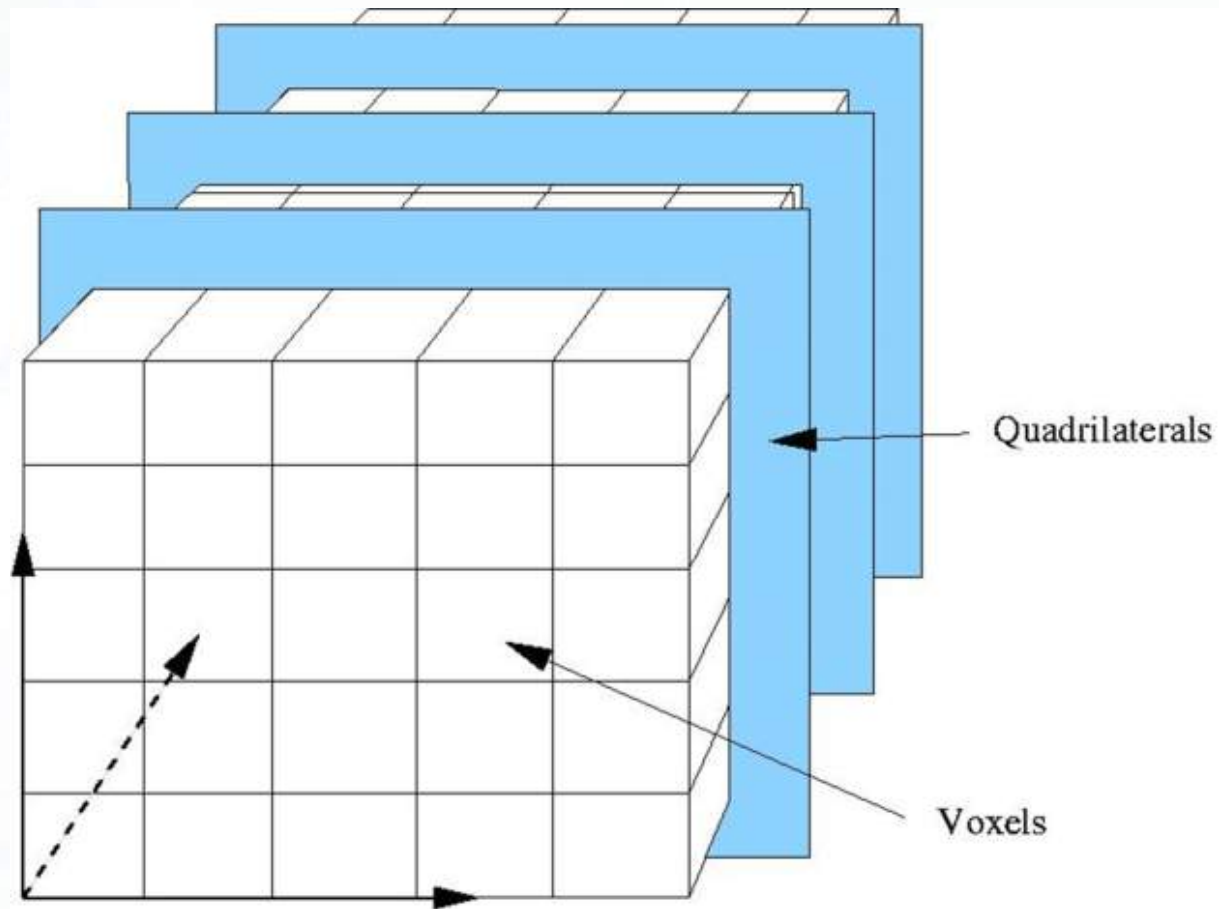


<http://london-imaging.co.uk/growing-use-mri-mental-health/>

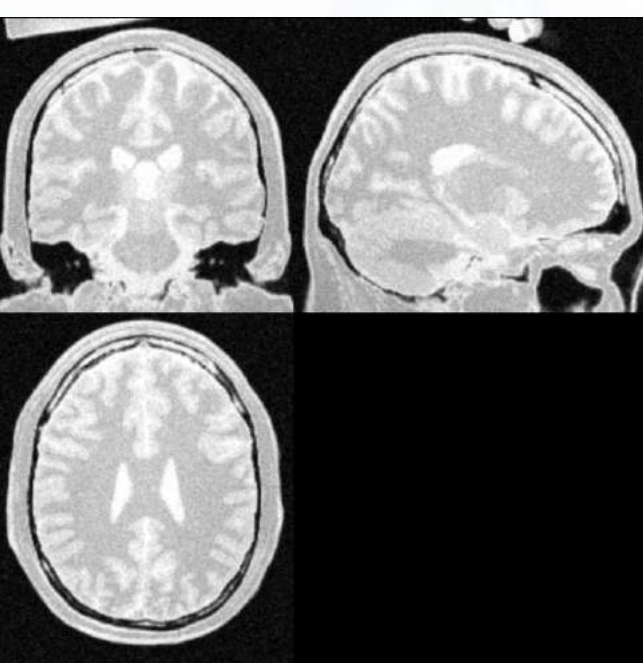
Typical magnetic field 1T a 4T (1T= 10.000G 100.000x earth magnetic field).

Eletrico motor:3000G (max). Supercondutor coils.

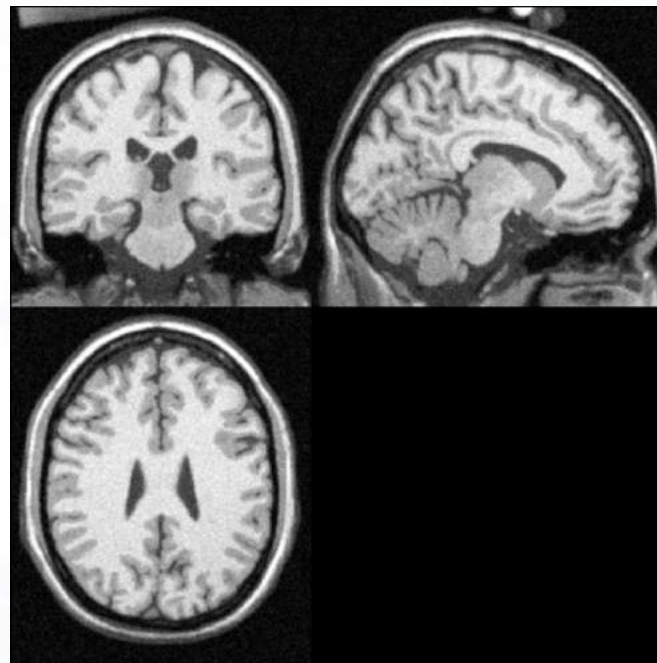
MRI: acquisition - voxel ($\sim 1 \text{ mm}^3$)



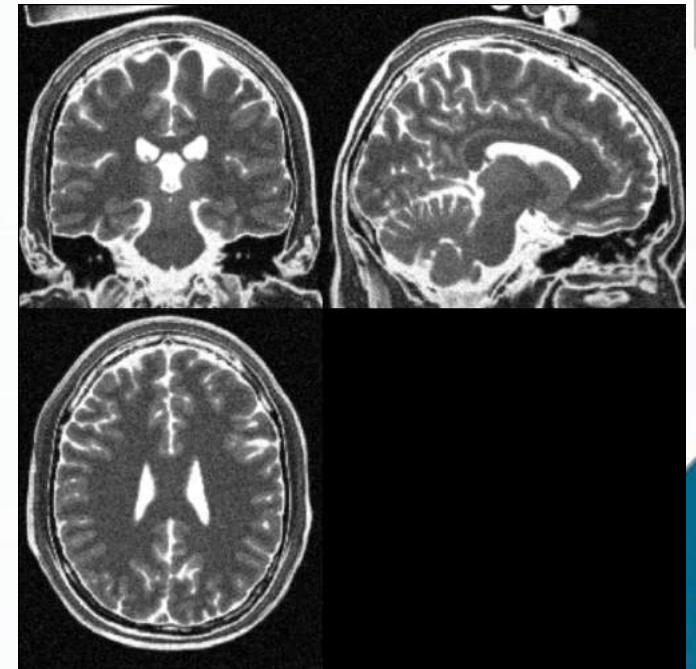
MRI modalities slices



Proton Density



T1-weighted



T2-weighted

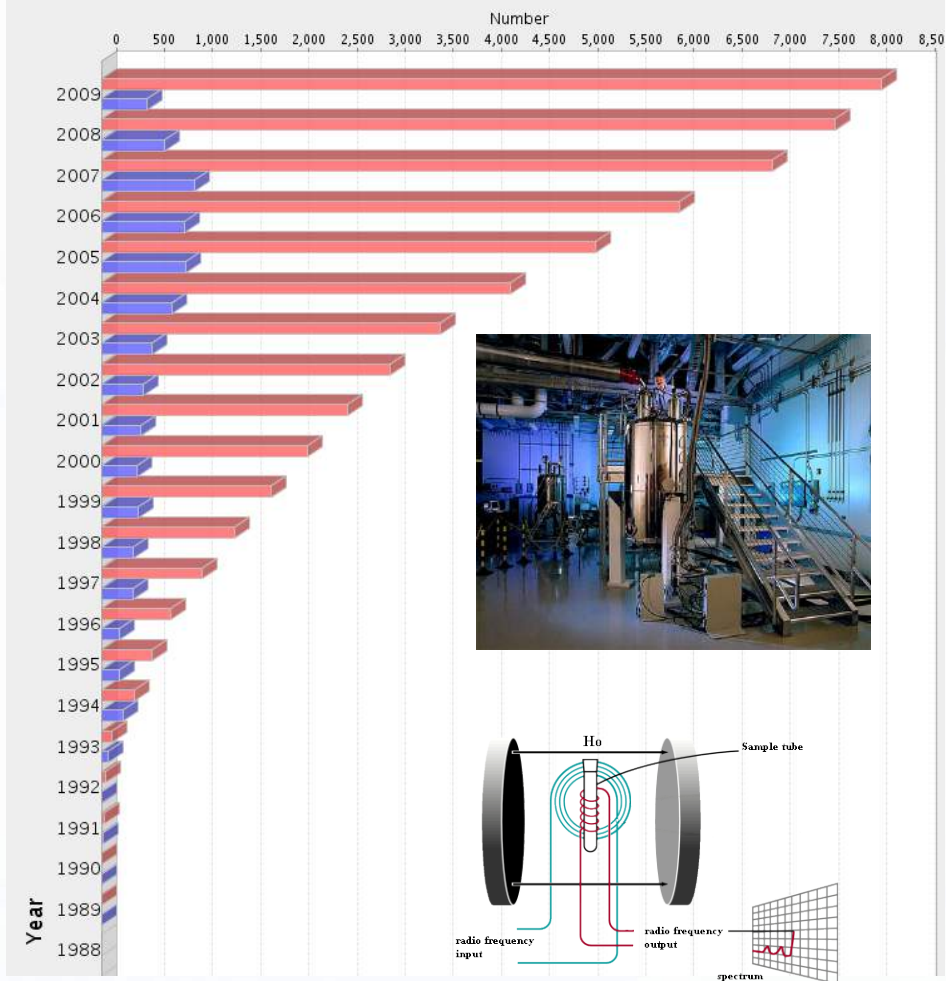
Each modality depends on TR and TE – MRI scanner acquisition parameter

<http://www.bic.mni.mcgill.ca/brainweb/>



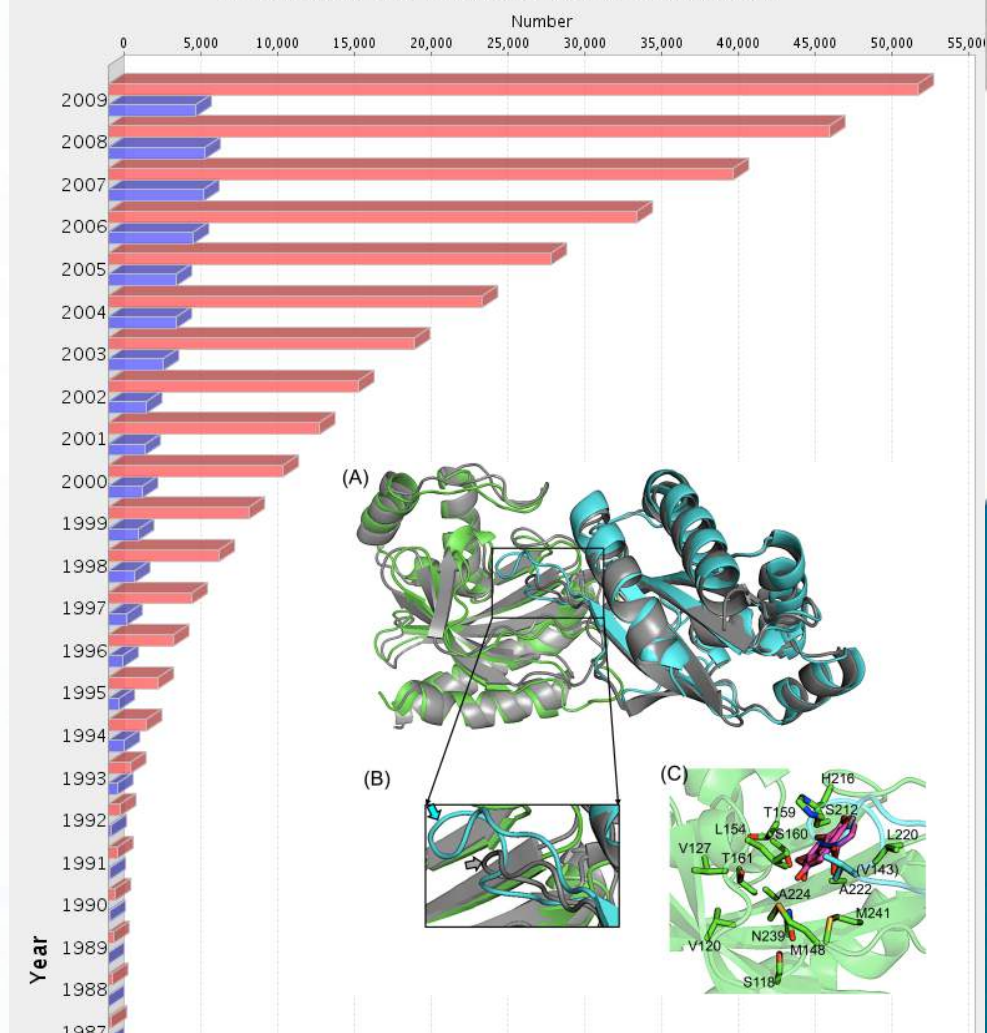
Curiosity: NMR spectroscopy – macromolecules structure

Yearly Growth of Structures Solved By NMR
number of structures can be viewed by hovering mouse over the bar



<http://www.mhhe.com/physsci/chemistry/carey/student/olc/ch13nmr.html>

Yearly Growth of Structures Solved By X-ray
number of structures can be viewed by hovering mouse over the bar



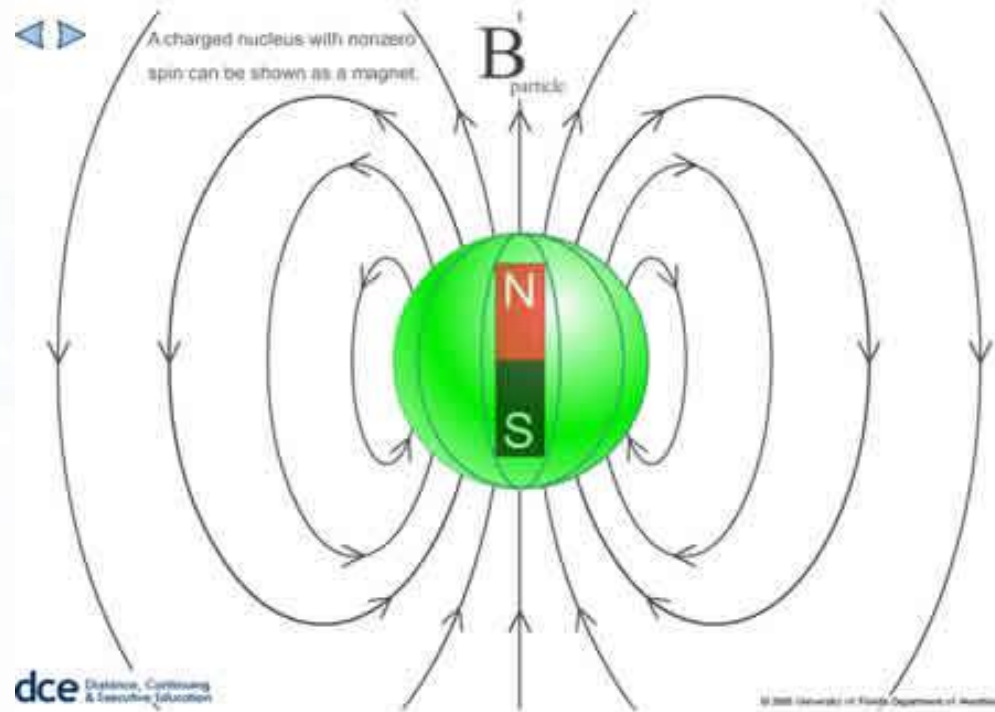
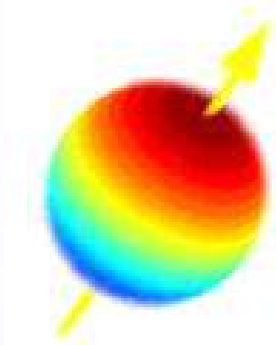
NMR phenomenon

Nuclear Magnetic Resonance

1946 - NMR phenomenon was first observed by Bloch and Purcell et al.

1973 - first MR image was only obtained by P.C. Lautenbur in 1973

N: Spin nuclear



Electron: spin $\frac{1}{2}$

Proton: spin $\frac{1}{2}$

Neutron: spin $\frac{1}{2}$ (despite zero electric charge!!! Quantum phenomenon)

<http://www.chm.bris.ac.uk/pt/polymer/techniques.shtml>

<https://vam.anest.ufl.edu/simulations/nuclearmagneticresonance>



N: Spin nuclear

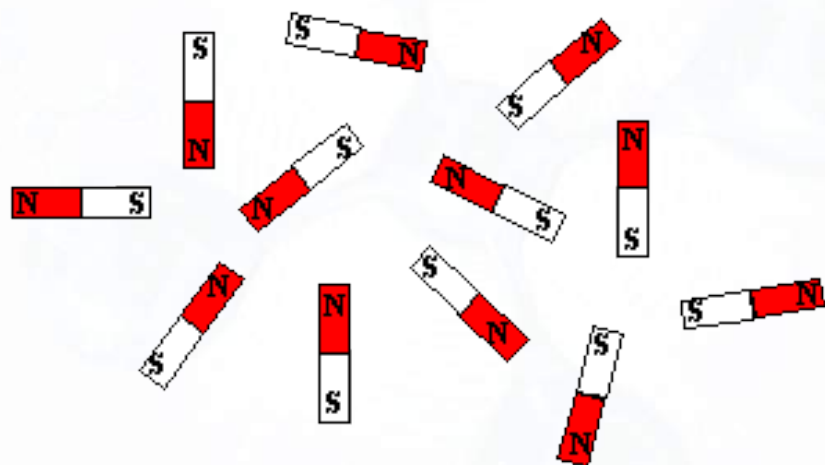
NMR Properties of Various Isotopes

Nucleus	Spin (42)	Gyromagnetic ratio (MHz/T) (42)	Natural abundance (42)	Concentration in human tissue (41)
Hydrogen ^1H	1/2	42.58	~100%	88M
Deuterium ^2H	1	6.53	0.015%	13 mM
Sodium ^{23}Na	3/2	11.27	~100%	80 mM
Phosphorous ^{31}P	1/2	1.131	~100%	75 mM
Oxygen ^{17}O	5/2	-5.77	0.04%	16 mM
Fluorine ^{19}F	1/2	2.627	~100%	4 mM

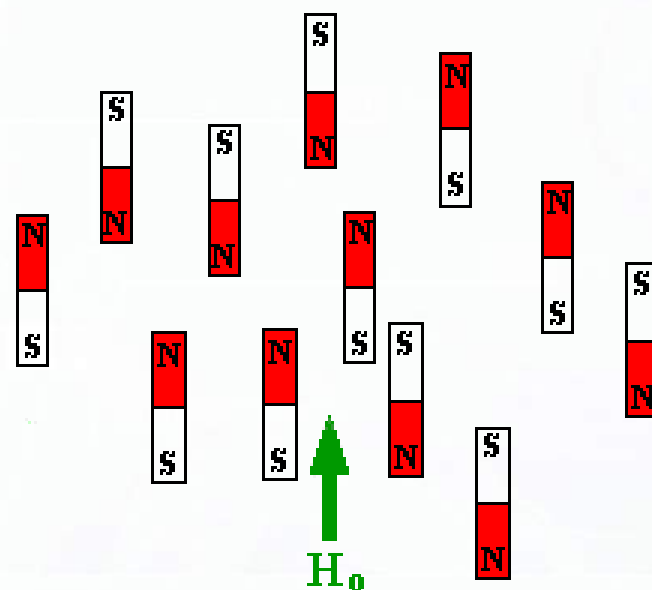
- Criteria:
Must have ODD number of protons or ODD number of neutrons.

M: Magnetic Field

Magnets in a magnetic field

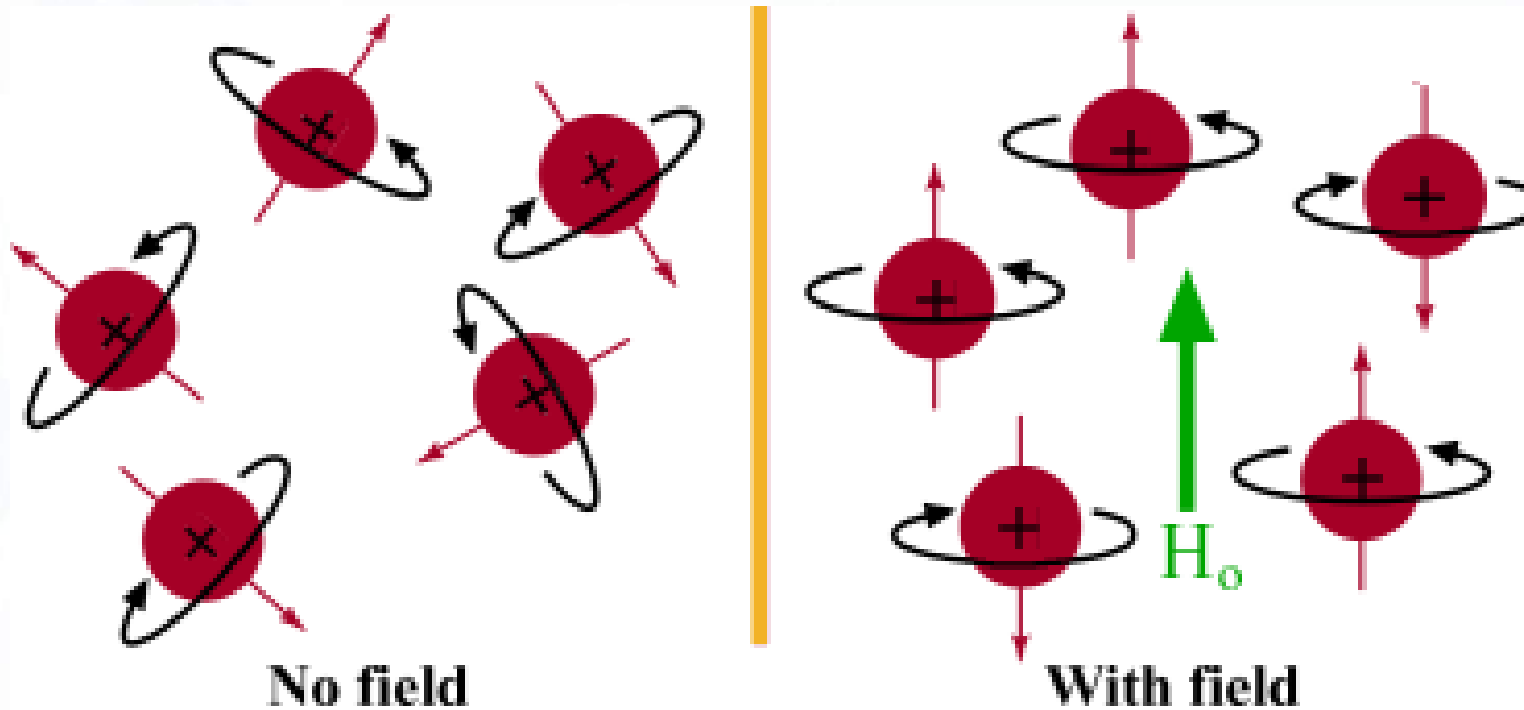


No Field

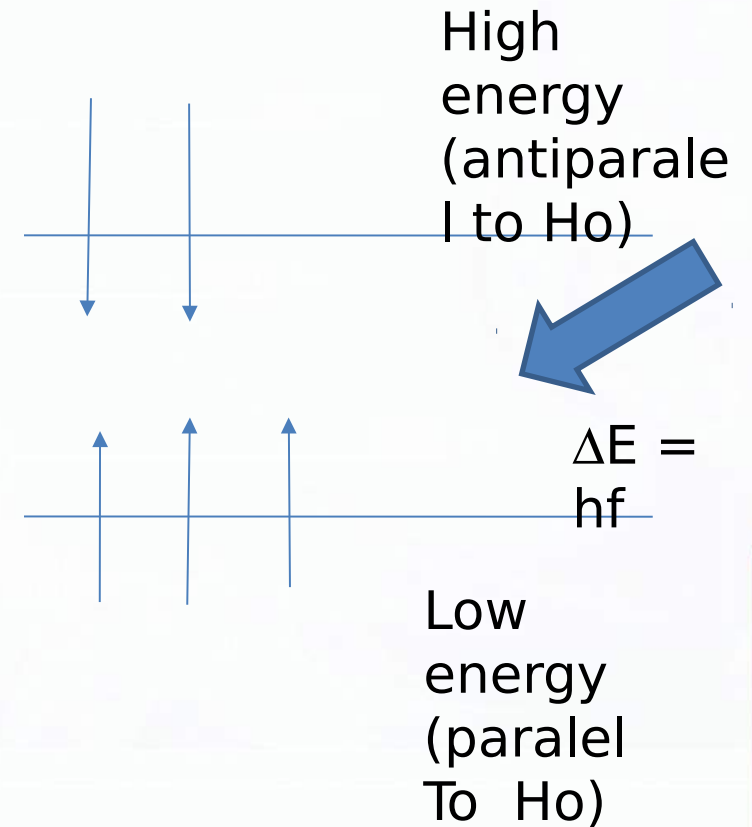
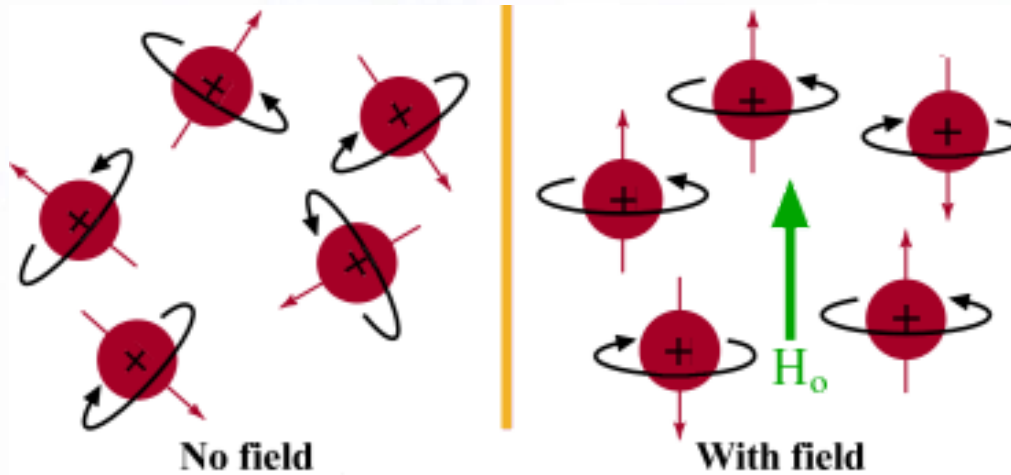


With Field

M: Magnetic Field

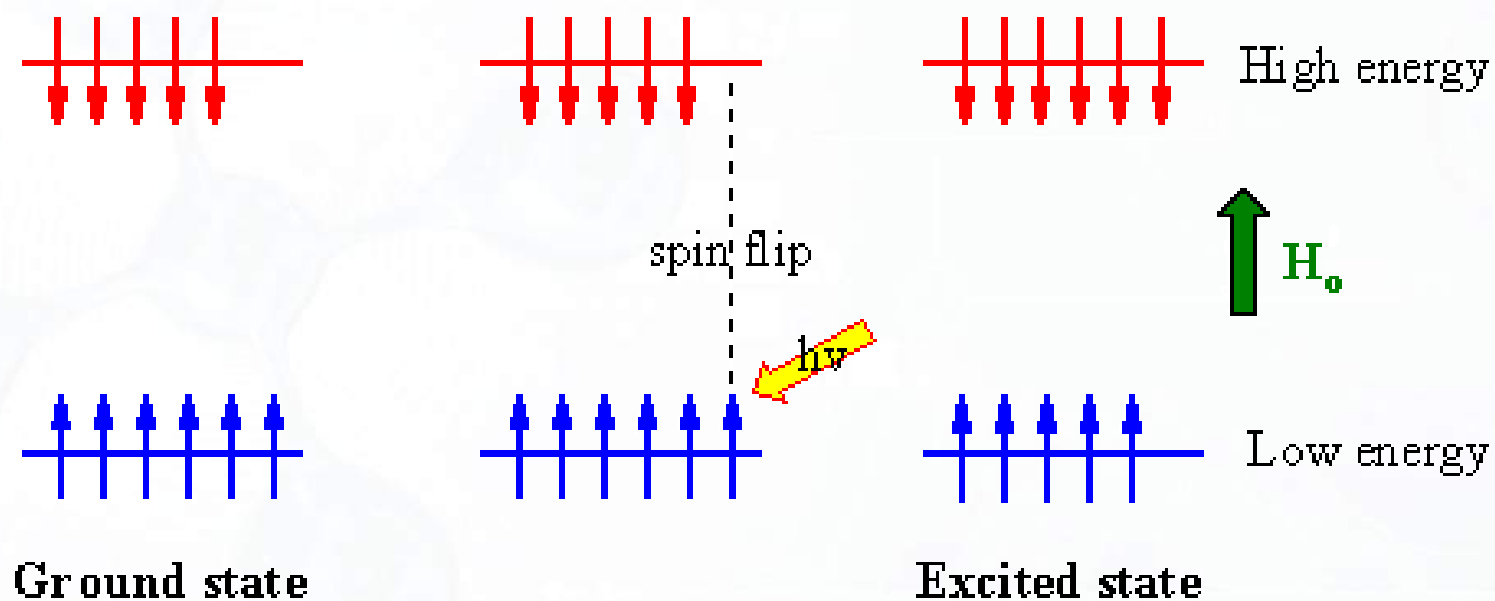


R: Resonance



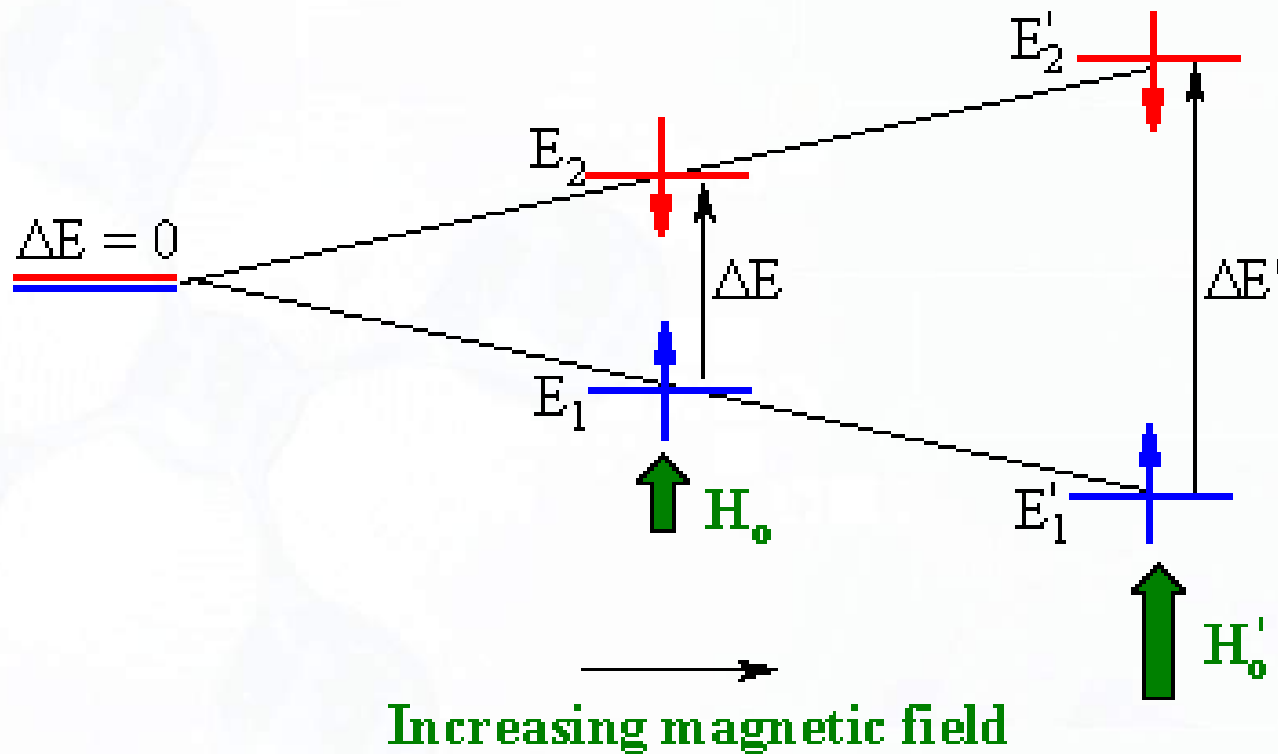
$\Delta E = hf$ - resonance condition
 $\Delta E = k H_0$

R: Resonance



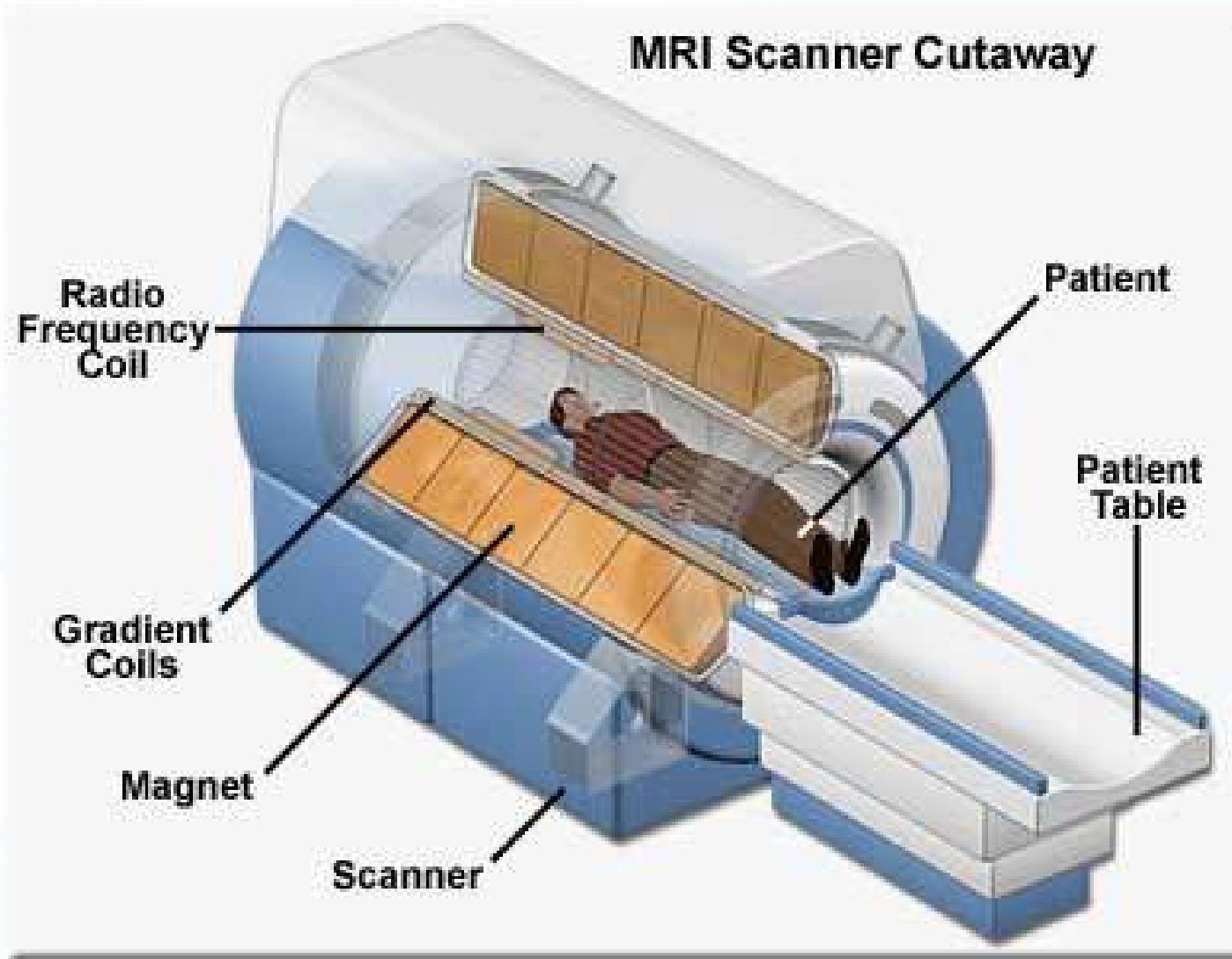
$$\frac{N_{upper}}{N_{lower}} = e^{-\Delta E/kT} = e^{-h\nu/kT}$$

Resonance

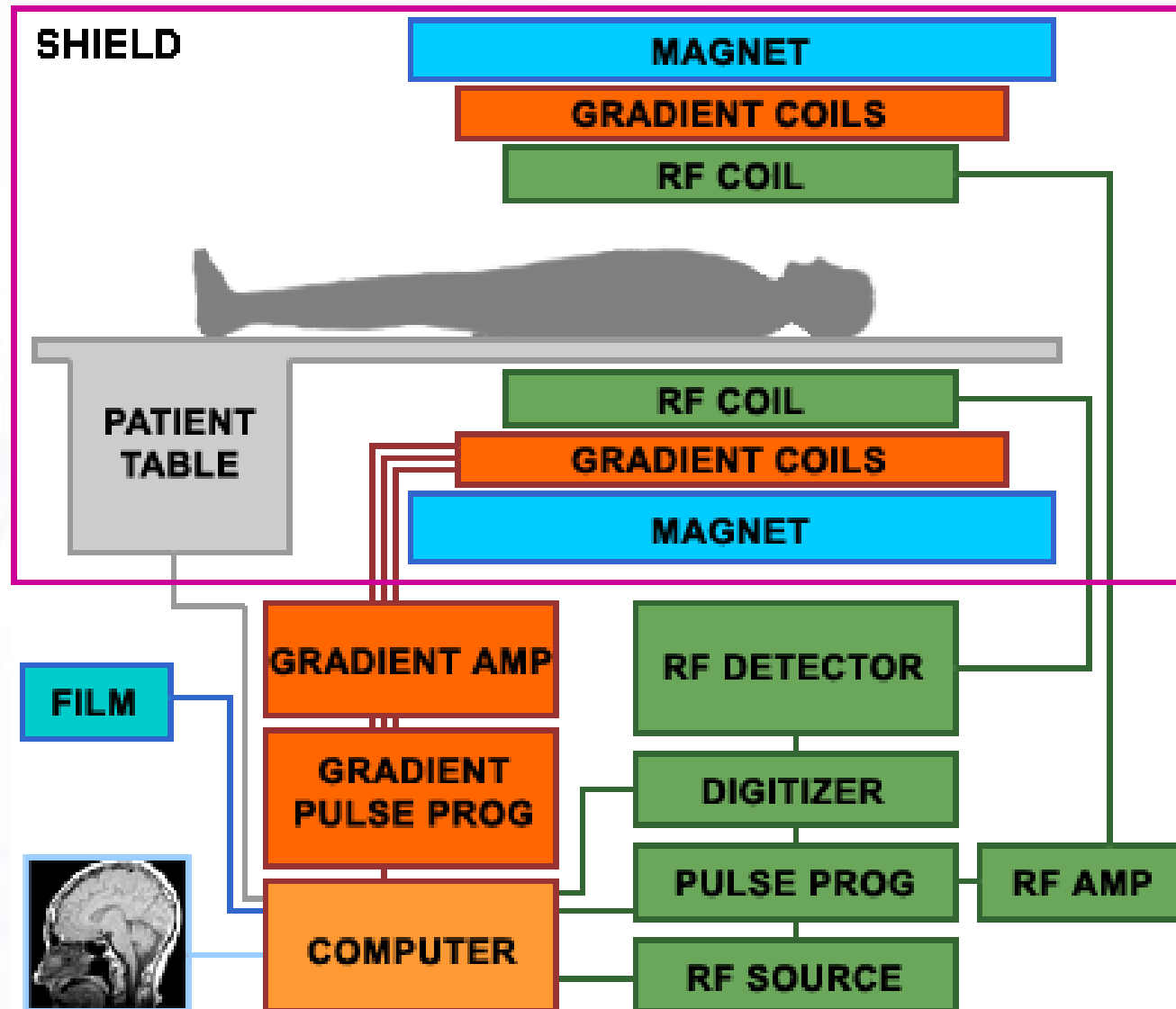


$\Delta E = hf$ - condição de
ressonância
 $\Delta E = k H_0$

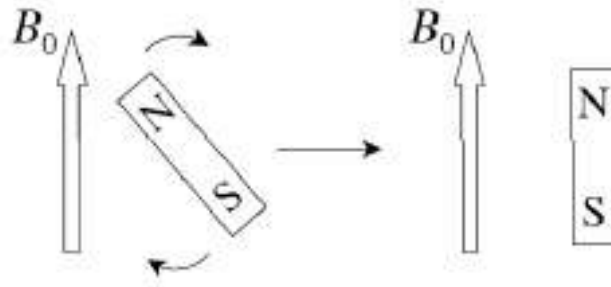
MRI (pulsed RF)



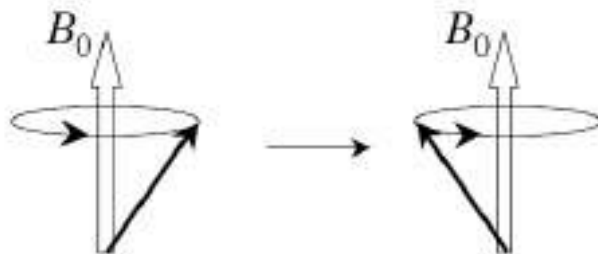
Block diagram of MRI scanner



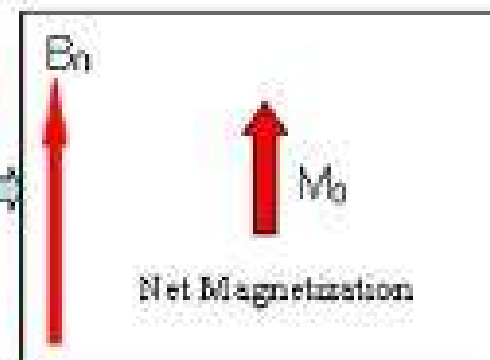
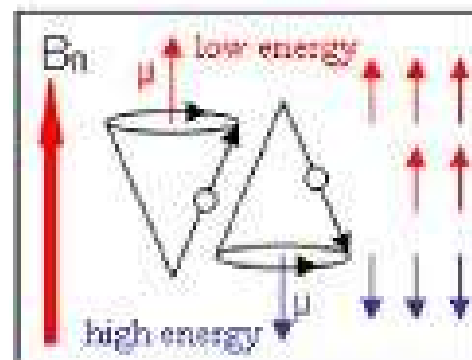
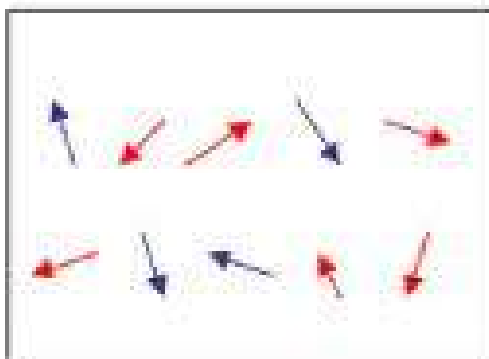
Precession of Nuclear spin in a magnetic field



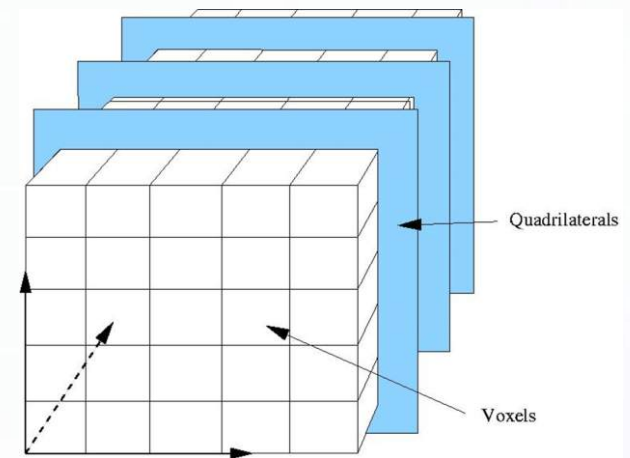
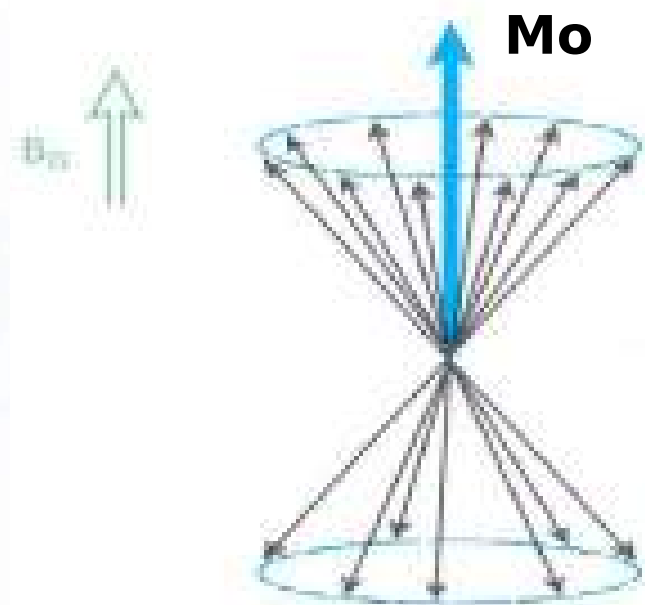
- Put a bar magnet in a magnetic field and it rotates to minimize the energy



- Put a nuclear spin in a magnetic field, and the torque on the magnetic moment (angular momentum) imposed by the field causes the spin to move around the field on a cone with a constant angle between the moment and the field (*precession* or *Larmor precession*)

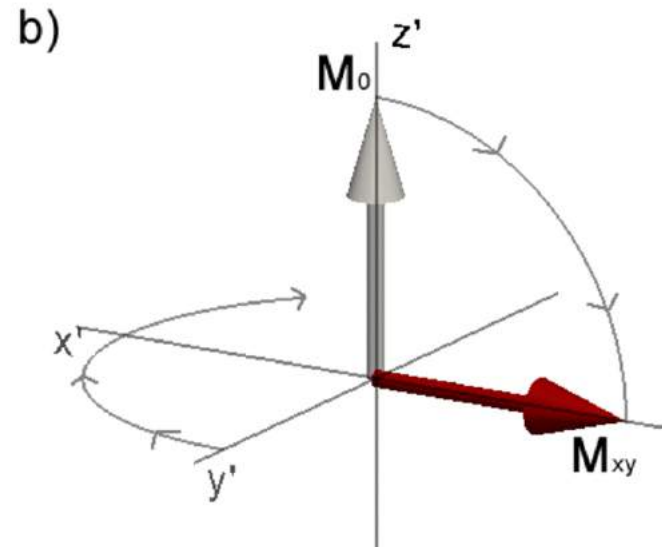
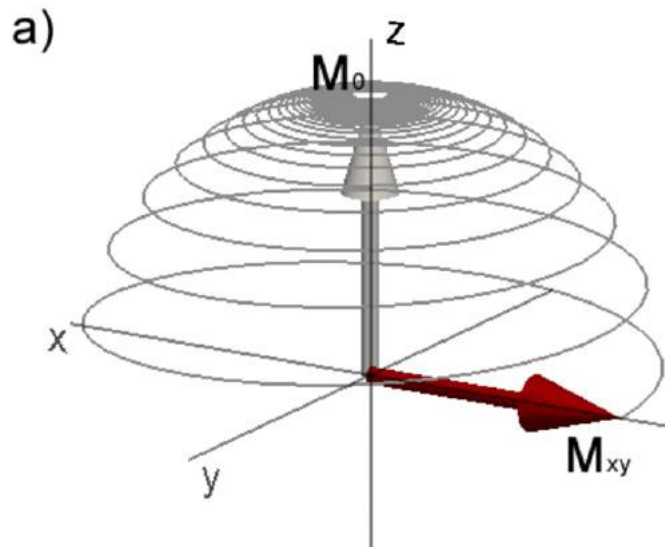
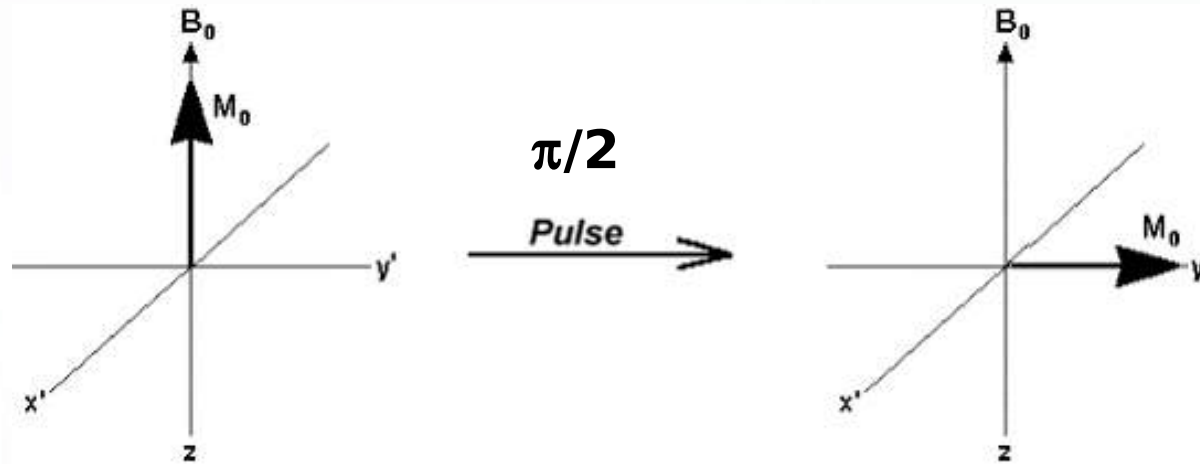


Net magnetization of nuclear spins in each voxel



voxel ($\sim 1 \text{ mm}^3$)

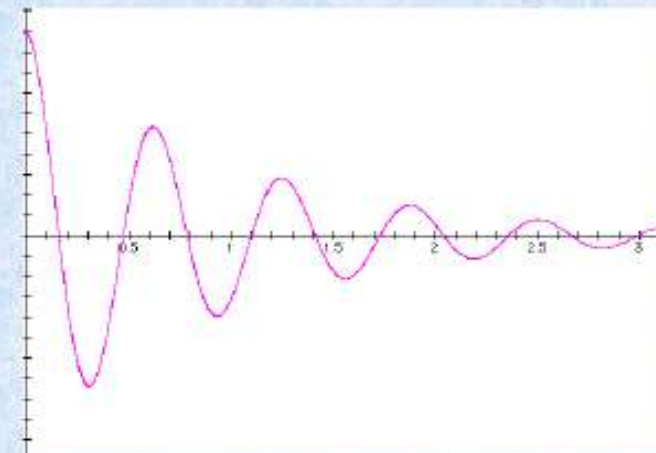
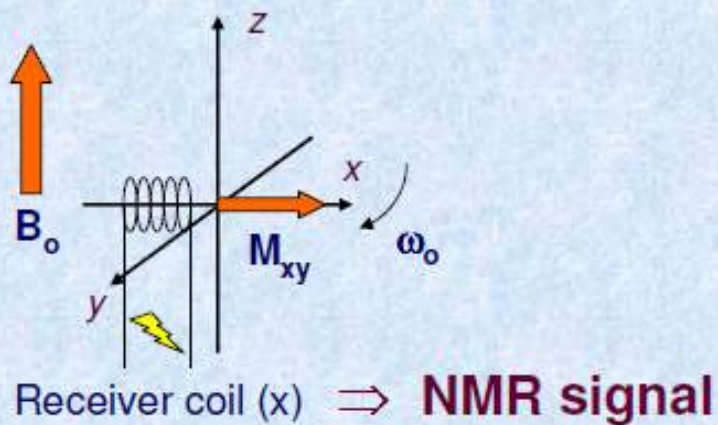
Net magnetization after a RF pulse (excitation)



Net magnetization after a RF pulse

Detection of M_{xy} and return to equilibrium

The oscillation of M_{xy} generates a fluctuating magnetic field which can be used to generate a current in a coil:



Free Induction Decay

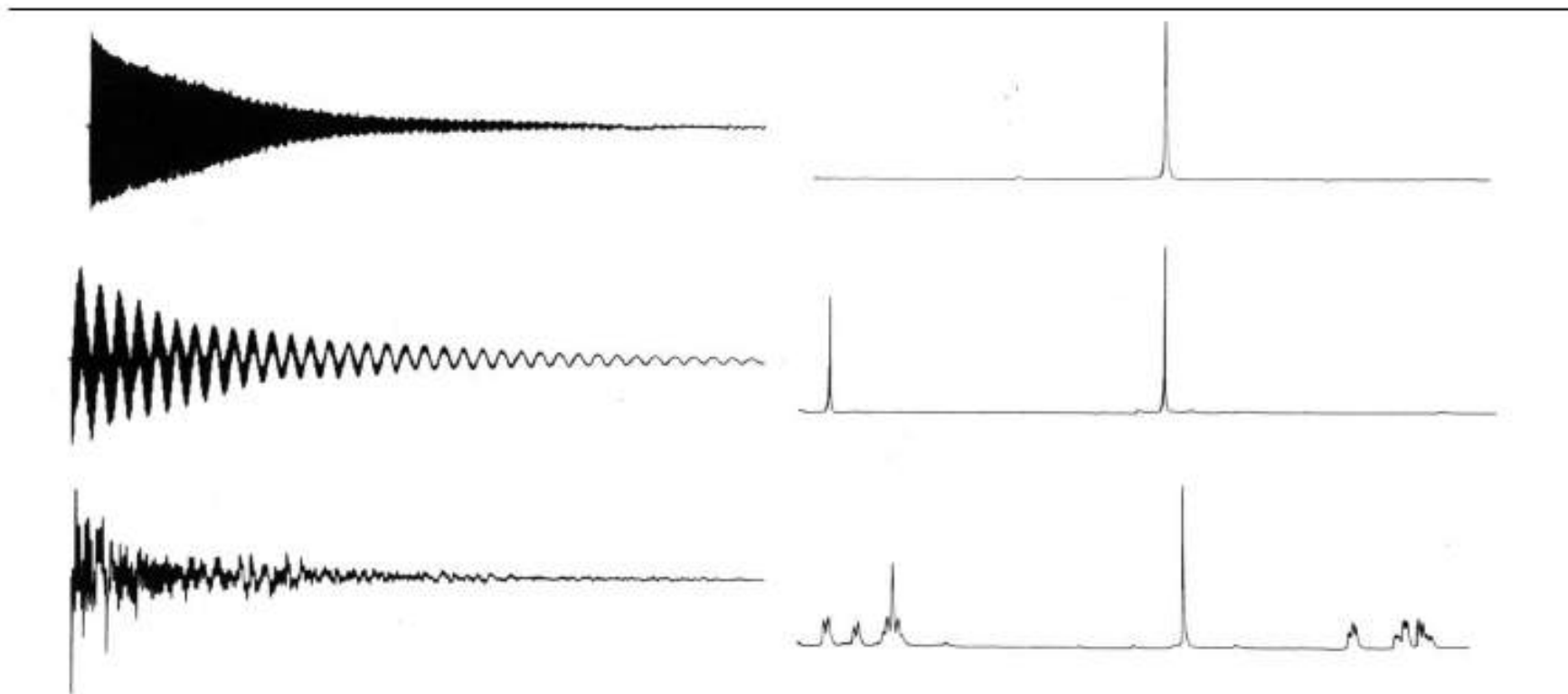
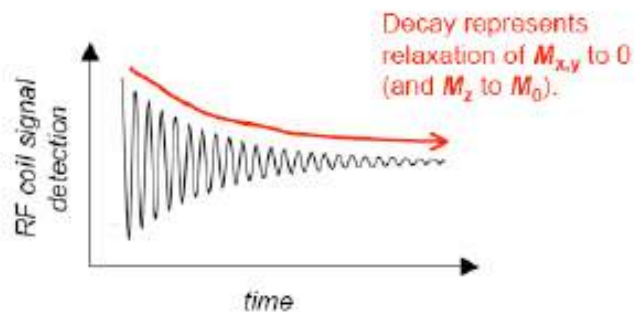


Figure 1.7. The free induction decay (FID) is on the left and its Fourier transform (usual frequency spectrum) is on the right.

FID and relaxation time T_2^*

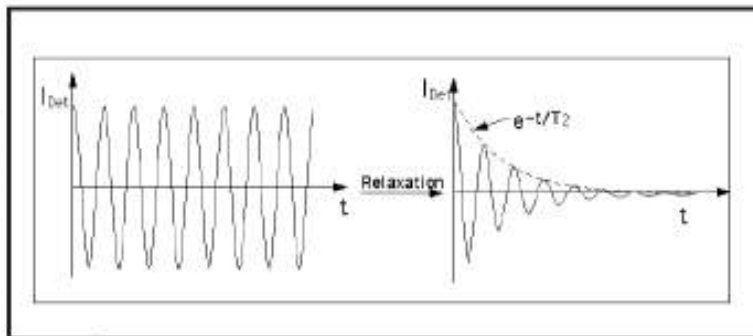
Free Induction Decay and T_2^*

The Free Induction Decay



Two mechanisms for signal decay:

1. Spin flipping that restores M_0 . (timescale T_1)
2. Decoherence of magnetization due to \mathbf{B}_0 inhomogeneity. (timescale T_2) Affected by sample prep.



Right: Signal in absence of transverse relaxation, right: real FID (free induction decay)

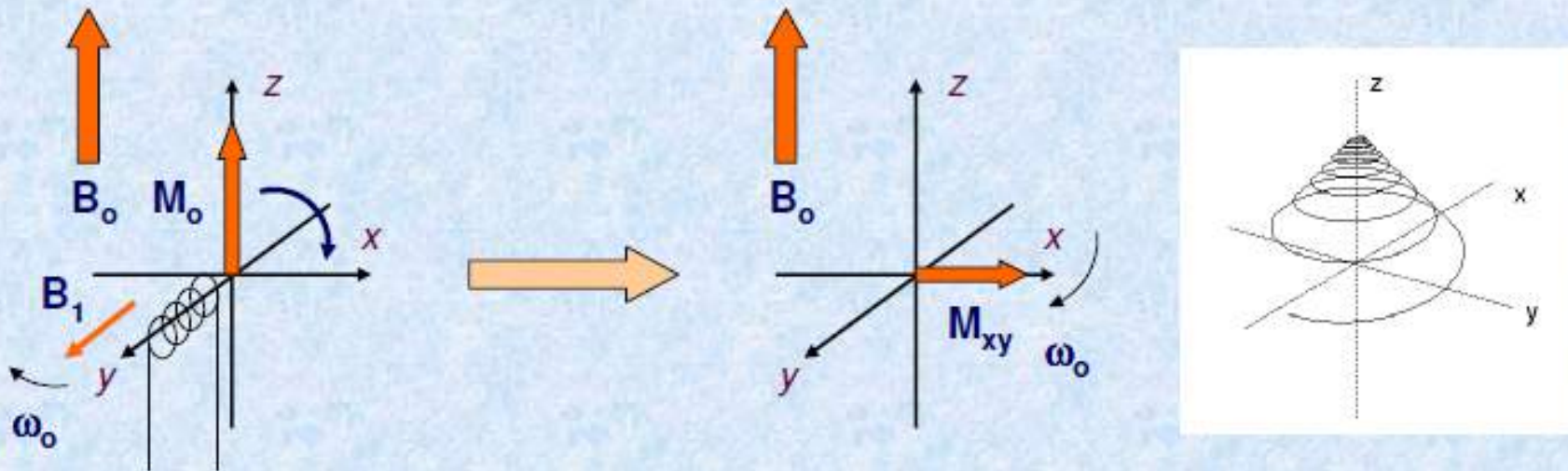
The damping of the Free Induction Decay (FID) is governed by the relaxation time T_2^* , which is greatly dependant on field homogeneities.

In practice, the FID will only last a few tens of milliseconds and the signal must be acquired very quickly if it is to be used in imaging.

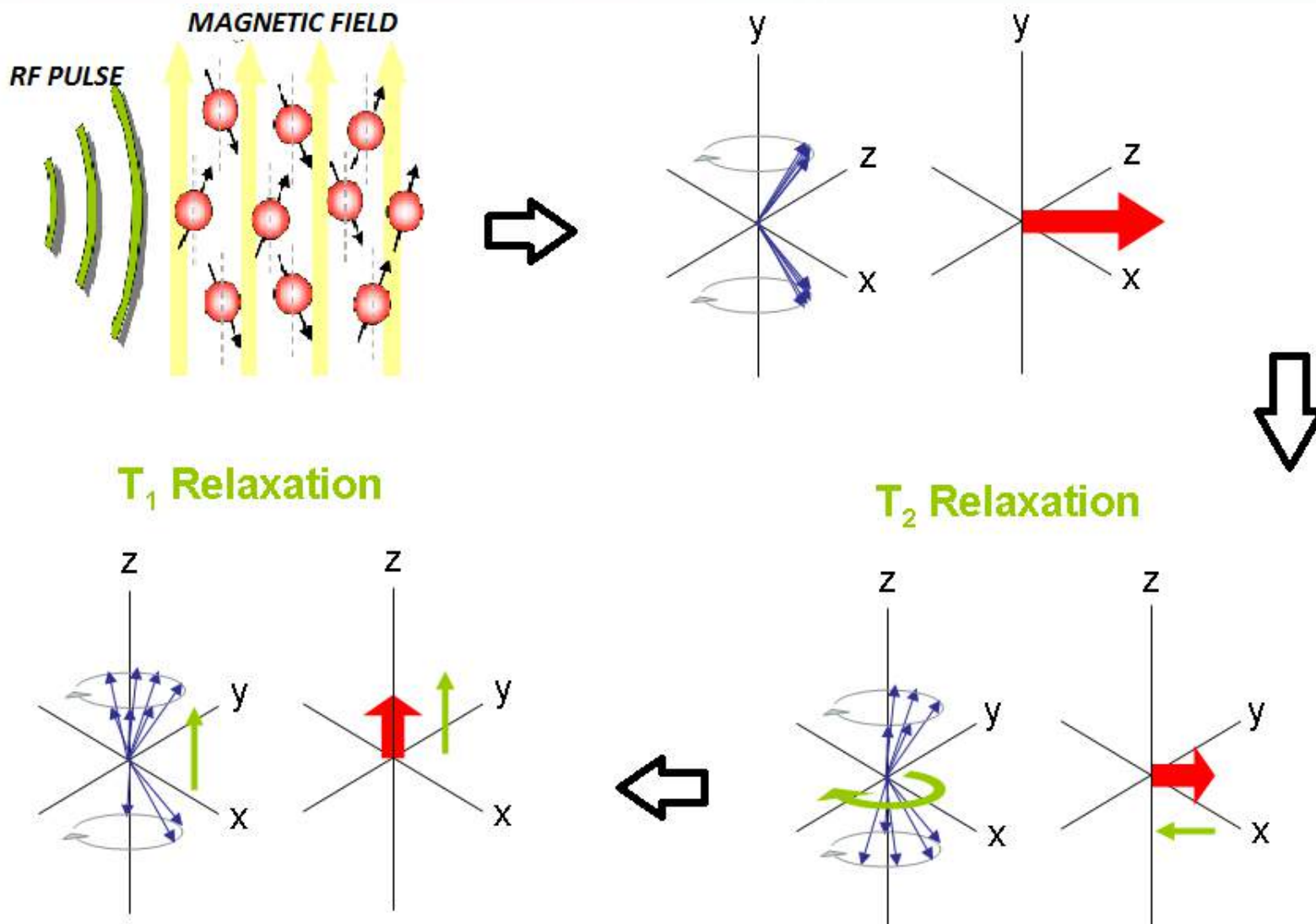
Logitudinal Relaxation time T1 (spin-lattice)

NMR excitation

When the frequency of the alternating current is ω_0 , the frequency of the right vector of \mathbf{B}_1 is ω_0 and we achieve a **resonant condition**. The alternating magnetic field and all the μ 's interact, there's a torque generated, and they rotate. Since they all rotate the same amount, the macroscopic effect is that \mathbf{M}_0 rotates around the **y** axis (in this case...), and we generate **transverse magnetization** (\mathbf{M}_{xy}):



Net magnetization relaxation



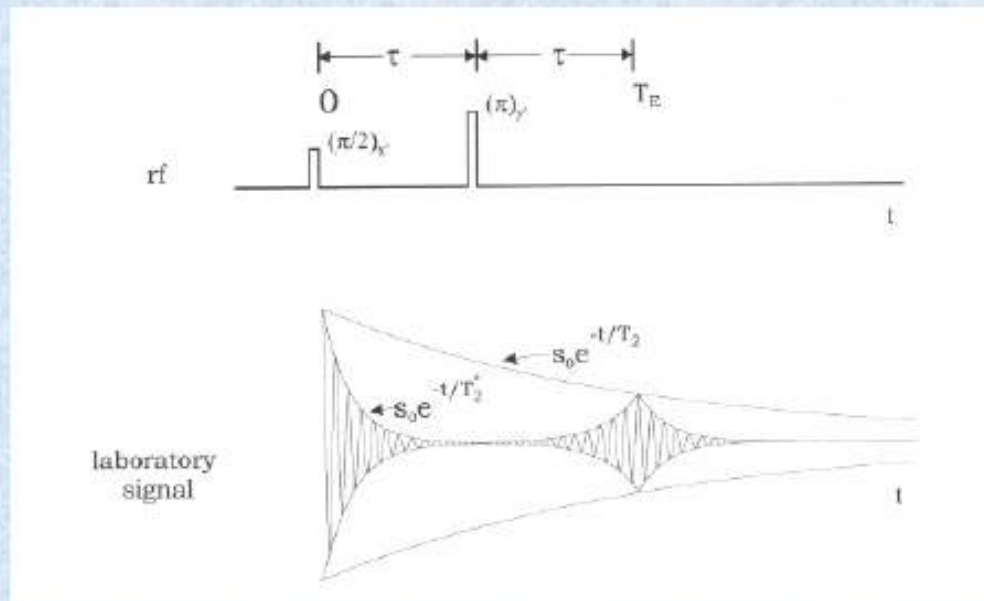
<https://mrimaster.com/>

Transverse Relaxation time T2 (spin-spin)

The Spin Echo Method and T2 Measurements

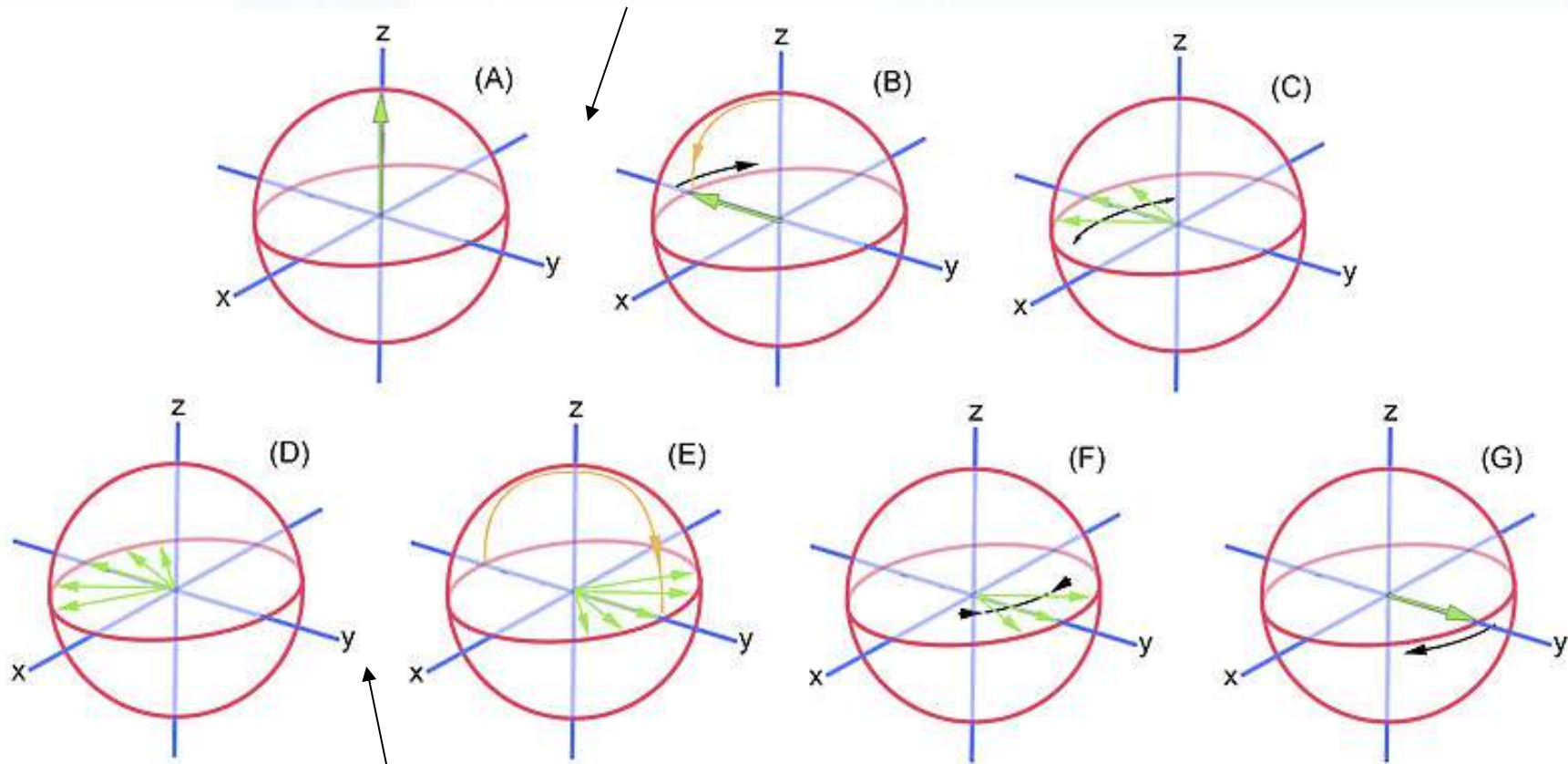
In order to facilitate the acquisition of the NMR signal and to reduce the influence of magnet field heterogeneties a more complex rf pulse sequence has been developed, the spin echo method.

The spin echo sequence is based on the application of two rf pulses : a $\pi/2$ -pulse followed by a π -pulse (or 'refocussing pulse')



Spin-echo (rotating frame)

$\pi/2$ RF pulse

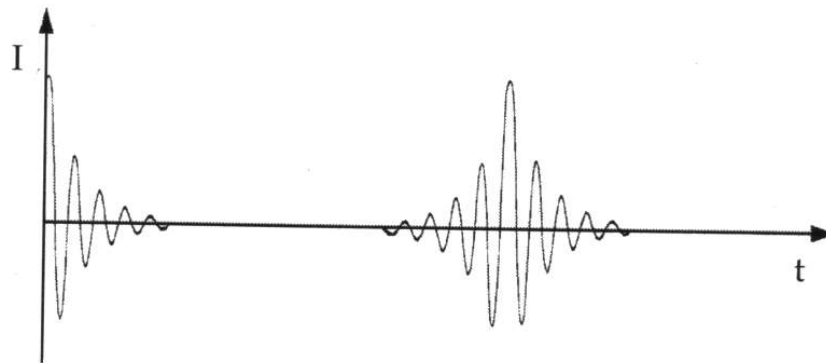
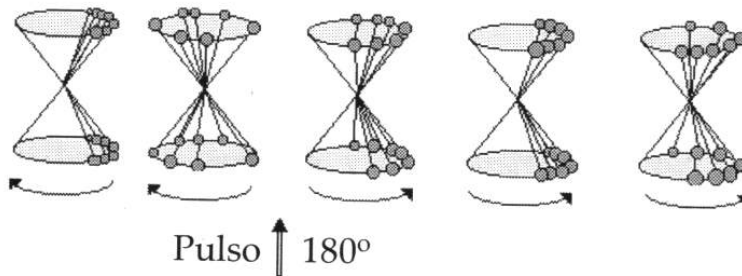


Pulso RF π

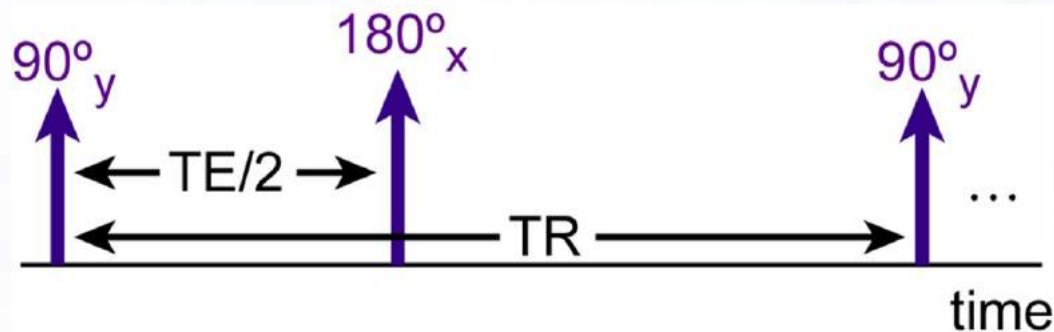
http://pages.physics.cornell.edu/p510/G-7A_Pulsed_NMR:_Spin_Echo



Spin-echo (TR and TE)

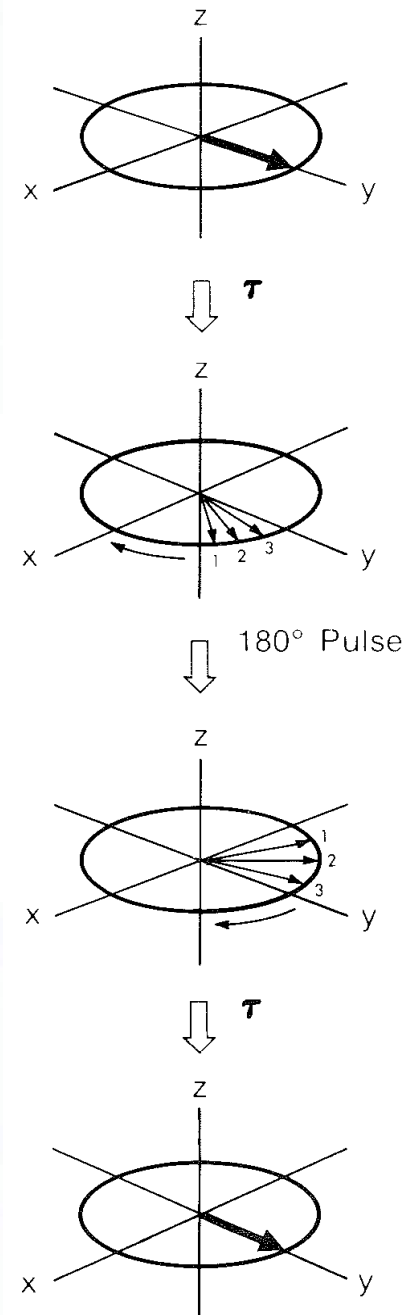
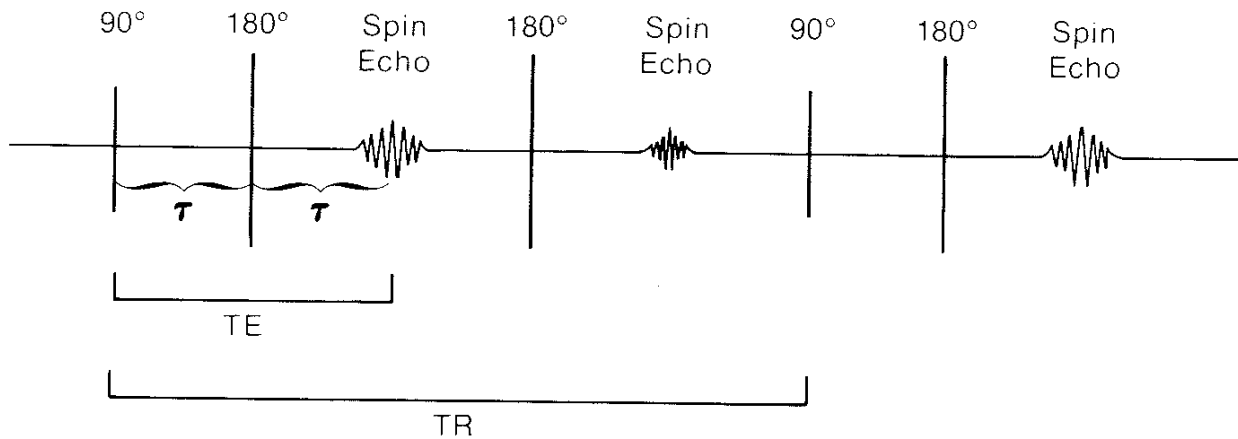


TR: Repetition Time
TE: Echo Time



<http://www-mrsrl.stanford.edu/~brian/bloch/>

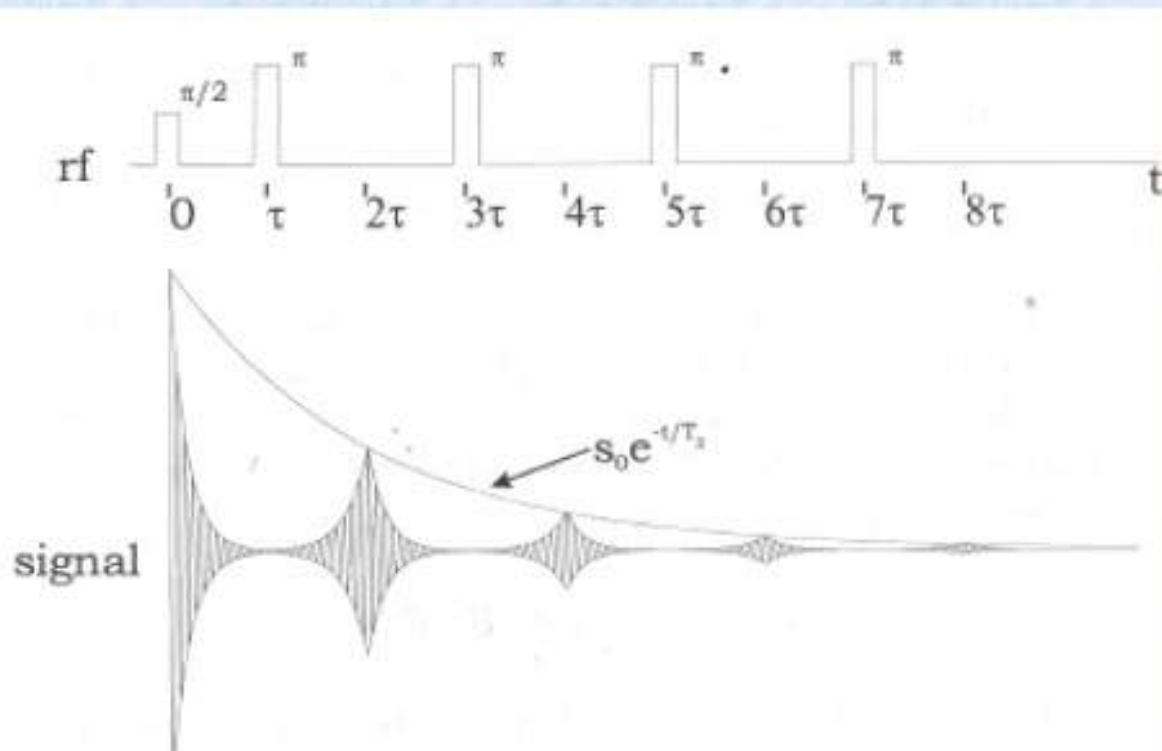
Spin echo (TR and TE)



<http://mriquestions.com/fse-parameters.html>

T2

The Spin Echo Method : multiple rf pulses



The signal arising from multiple spin echoes generated by regularly repeated π -pulses.

The signal decreases as a function of T_2 : shown by the exponential envelope.

MRI intensity: PD, T1- and T2-weighted image

MRI contrast: Spin-echo equation

$$I = N \cdot f(\nu) \cdot \left(e^{-\left(\frac{TE}{T2}\right)} \right) \cdot \left(1 - e^{-\left(\frac{TR}{T1}\right)} \right)$$

I: image intensity (pixel brightness)

N: proton density (tissue)

f(ν): flux function (tissue)

TE: echo time (fixed at the machine)

TR: repetition time (fixed at the machine)

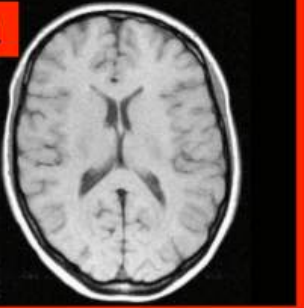
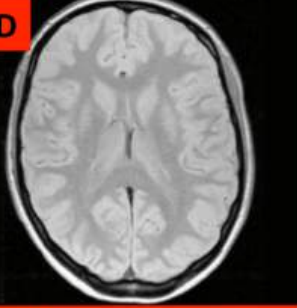
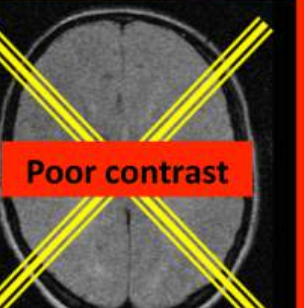

T1: longitudinal relaxation time (tissue)

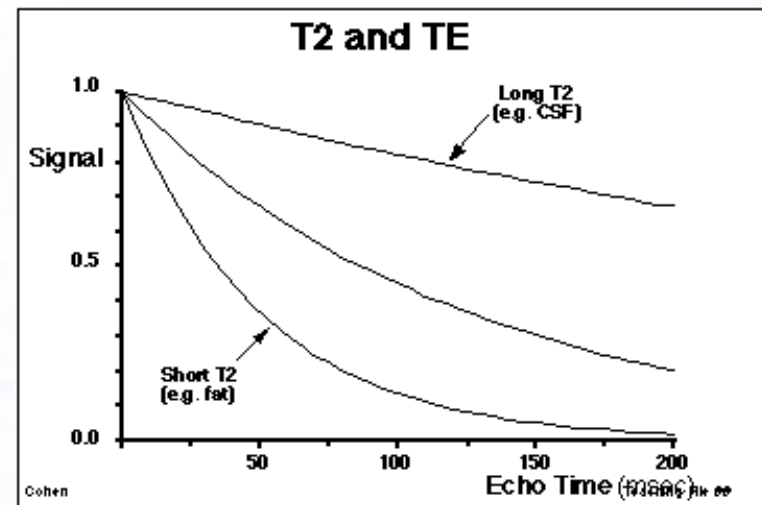
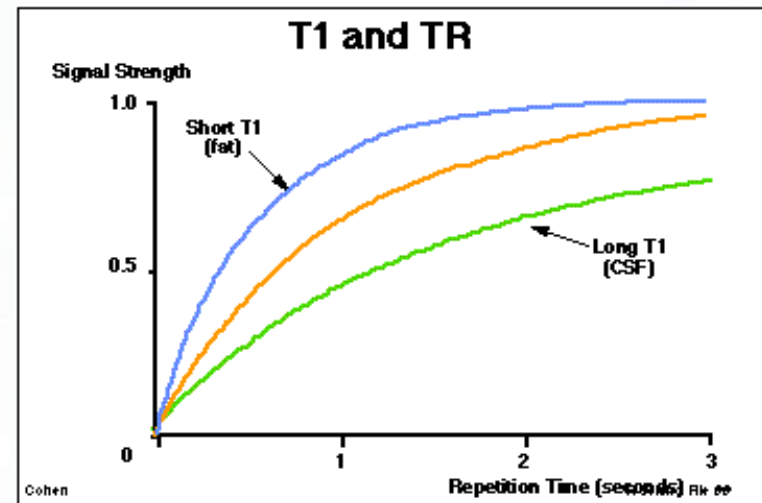
T2: transversal (spin-spin) relaxation time (tissue)

Proton density: water and lipids

T1 and T2 values for tissues

T1 and T2 values at 1.5 Tesla.		
Tissue	T1 (ms)	T2 (ms)
Muscle	870	47
Liver	490	43
Kidney	650	58
Grey Matter	920	100
White Matter	790	92
Lung	830	80
CSF	2,400	160

	Short TR	Long TR
Short TE	T1 	PD 
Long TE	 Poor contrast	T2 

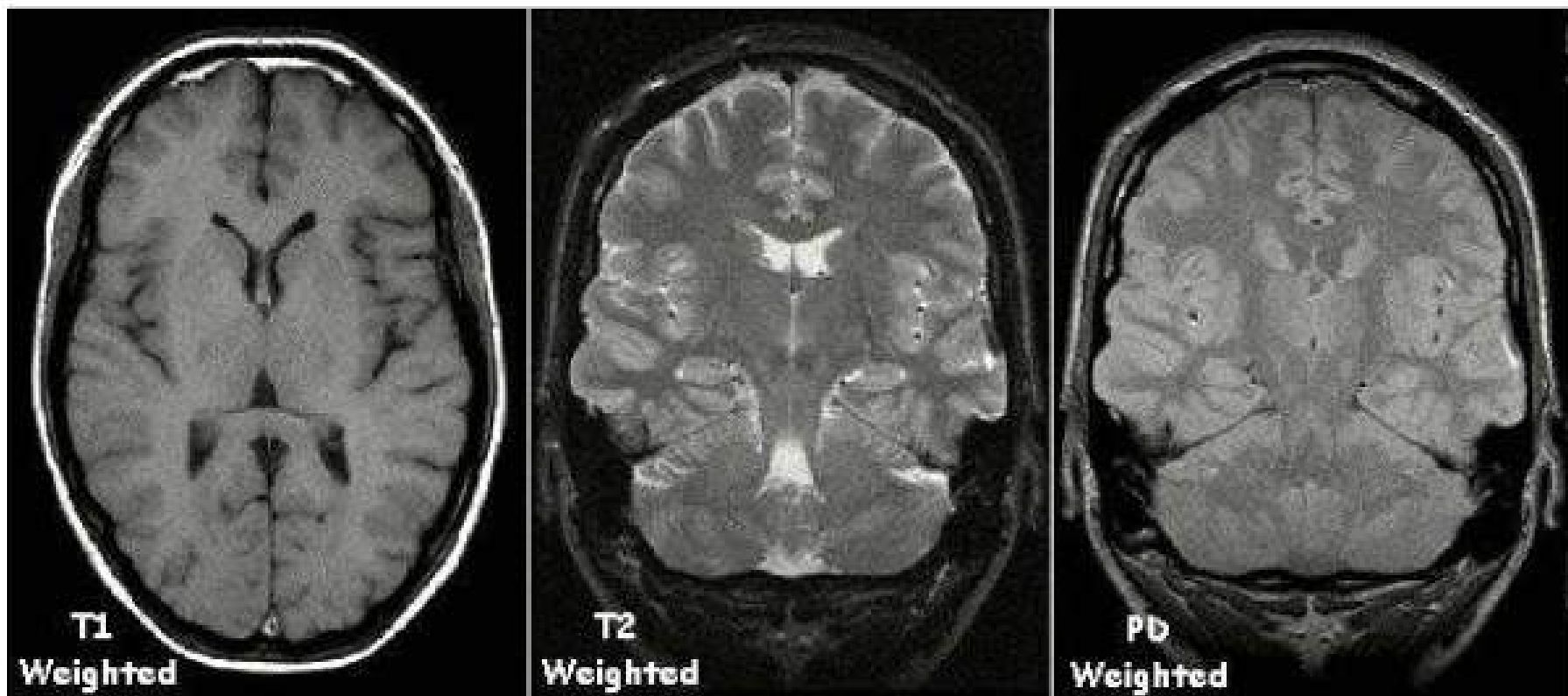


<http://mriquestions.com/image-contrast-trte.html>

T1- and T2-weighted Images

<u>TISSUE</u>	<u>T1W</u>	<u>T2W</u>
<u>FAT</u>	BRIGHT	INT/DARK
<u>BRAIN</u>		
WHITE MATTER	BRIGHT	DARK
GREY MATTER	DARK	BRIGHT
CSF	VERY DARK	VERY BRIGHT
<u>GADOLINIUM CHELATE</u>		
LOW CONCENTRATION	VERY BRIGHT	BRIGHT
HIGH CONCENTRATION	INT/DARK	VERY DARK
<u>HEMATOMA</u>		
HYPERACUTE(<6 HRS)	INT	INT
ACUTE(6-24 HRS)	INT/DARK	DARK
SUBACUTE(1DAY-1MONTH)	BRIGHT RIM	BRIGHT
CHRONIC(>1 MONTH)	DARK RIM WITH OR WITHOUT A BRIGHT CENTRE	DARK RIM WITH OR WITHOUT A BRIGHT CENTRE

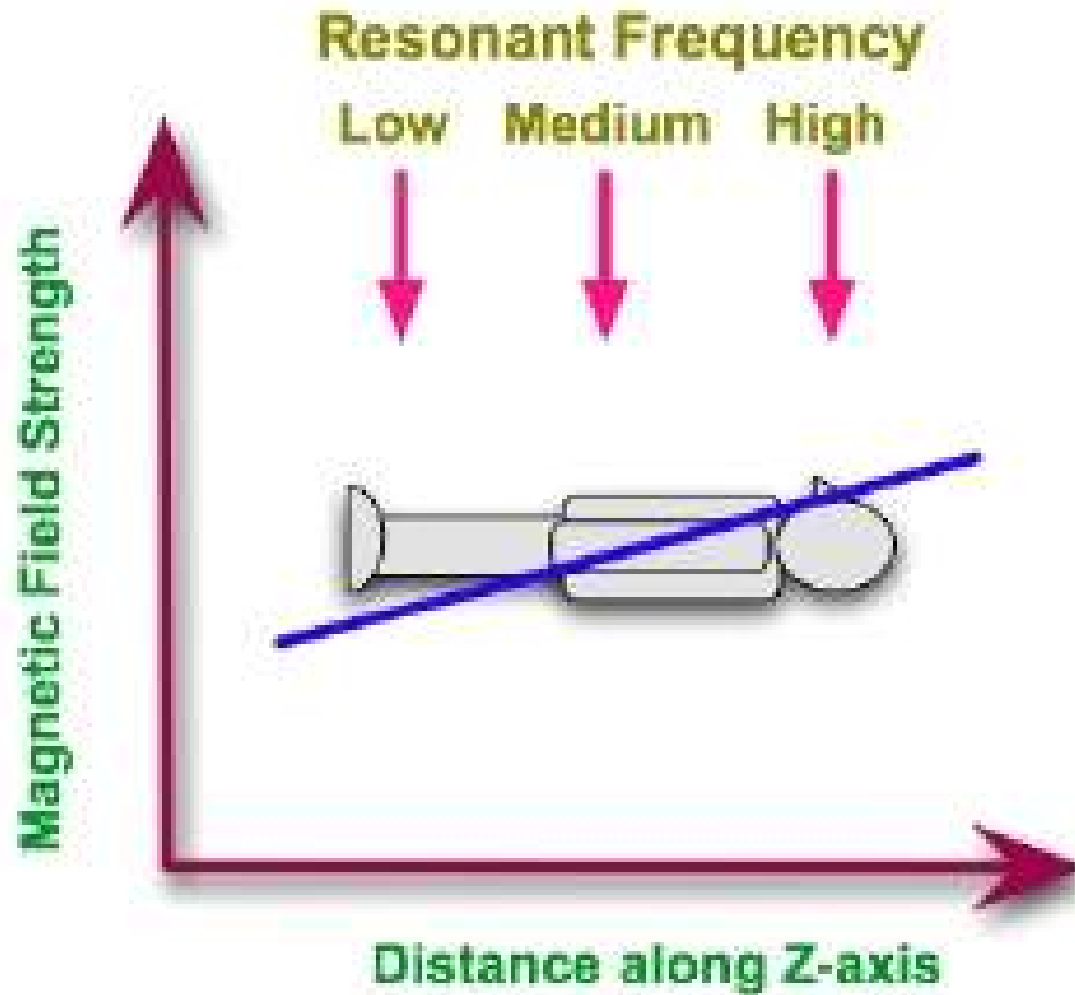
<http://casemed.case.edu/clerkships/neurology/NeurLrngObjectives/MRI.htm>



Three types of MR image: the T1 weighted image depicts relatively bright grey matter and dark CSF; the T2 weighted image highlights the CSF, while the PD weighted image shows little contrast between tissues.

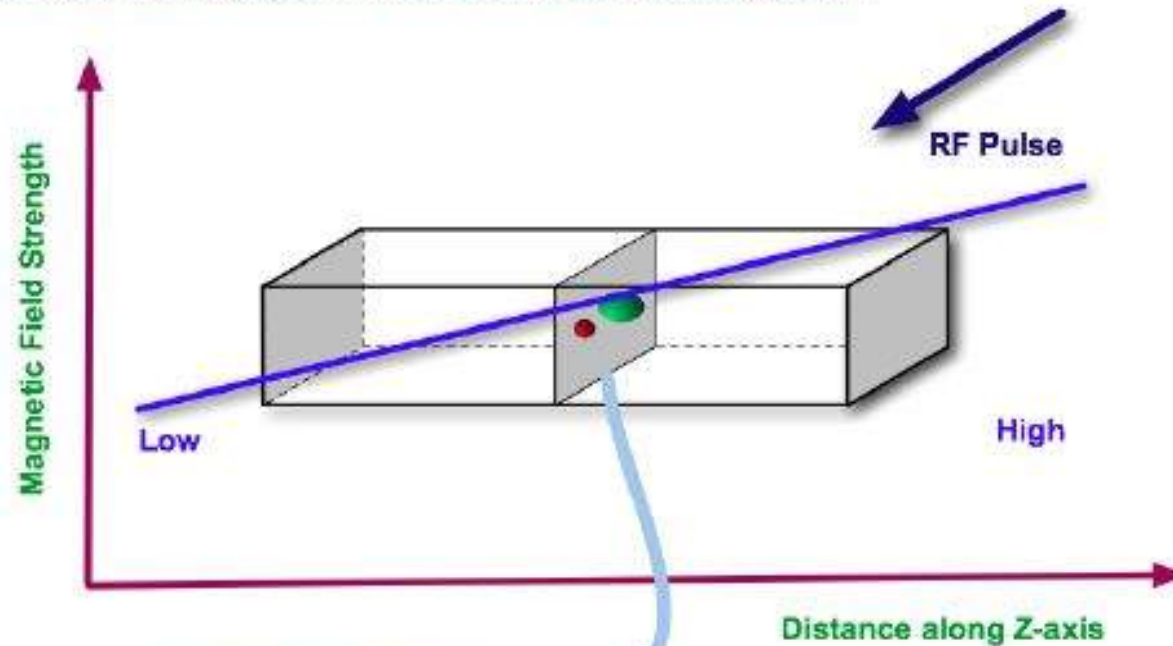
- A long TR and short TE sequence is usually called Proton Density -weighted
 - A short TR and short TE sequence is usually called T1-weighted
 - A long TR and long TE sequence is usually called T2-weighted
- CSF: Cerebro-Spinal Fluid

Image



Imagem

1. Select slice during excitation phase using a longitudinal gradient:



2. Apply a transverse gradient during the emission phase to acquire one projection:



Image formation

K-space properties:

- Center of k-space center corresponds to low spatial frequencies (structure of image)
- Boundary of k-space corresponds to high spatial frequencies (details of image)

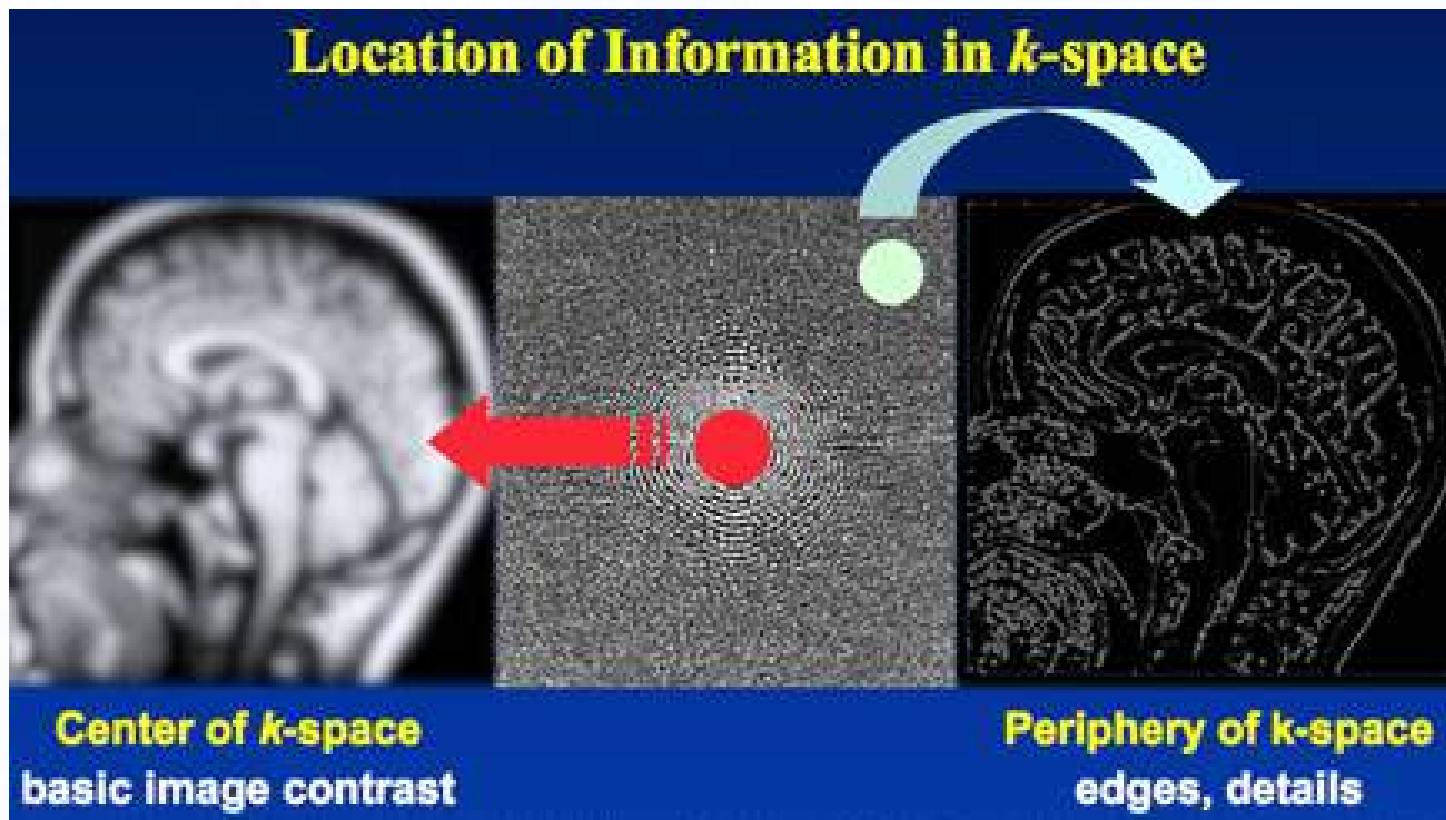


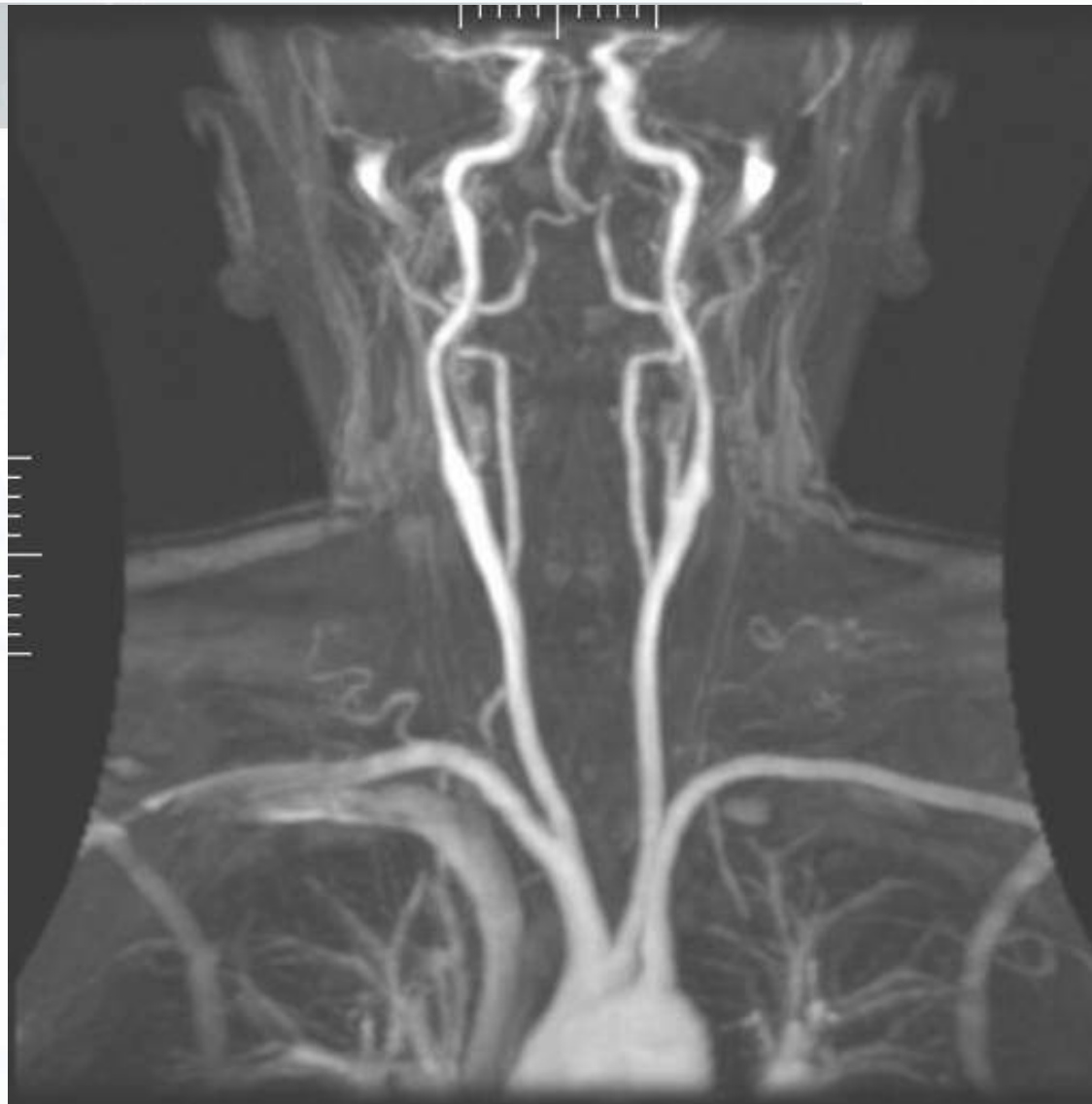
TABLE 31.3 Medical Imaging Techniques

Technique	Resolution
Conventional X-ray	$\frac{1}{2}$ mm
CT scan, X-ray	$\frac{1}{2}$ mm
Nuclear medicine (tracers)	1 cm
SPET	1 cm
PET	3–5 mm
NMR	$\frac{1}{2}$ –1 mm

1.5 tesla scanners often cost between \$1 million and \$1.5 million USD. 3.0 tesla scanners often cost between \$2 million and \$2.3 million USD.

MRI: 800 a 1000 reais

CT (adomen) : 400 a 600 reais



Magnetic resonance angiography - contrast with Gd

Author: Ofir Glazer, Bio-Medical Engineering Department, Tel-Aviv University, Israel. Part of M.Sc. final project, tutored by Dr. Hayit Greenspan.



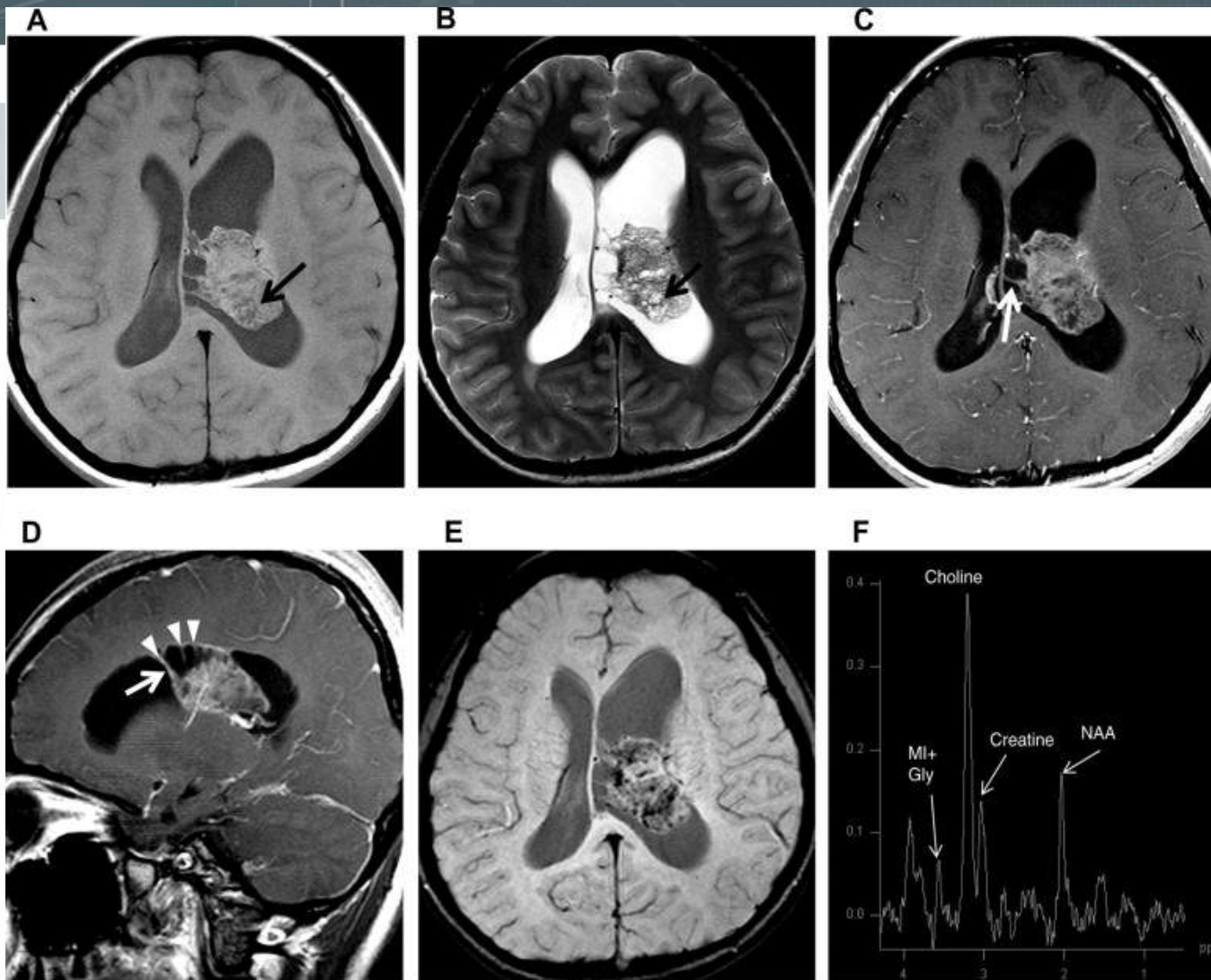


Fig. 1. Patient 1 - MRI findings: (A) axial T1-weighted, (B) axial T2-weighted, (C) postcontrast axial T1-weighted and (D) postcontrast sagittal T1-weighted MRI. The tumour is composed of a moderately enhanced solid portion that has a soap bubble or spongy appearance (black arrows) and multiple cysts interfacing between the solid part of the tumour and the lateral ventricular wall. Spicules (white arrows) formed by the cyst wall appear to form a connection between the solid part of the tumour and the undulated lateral ventricular wall (arrowheads). (E) Susceptibility-weighted axial MRI showing multiple low-intensity dots that reflect calcification and vessels. (F) Magnetic resonance spectroscopy showing high choline peaks and low N-acetyl aspartate and myoinositol and/or glycine peaks.

A) T1-weighted

B) T1-weighted
With Gd

C) T2-weighted

D) Susceptibility

E) Diffusion
coefficient map

F) CT

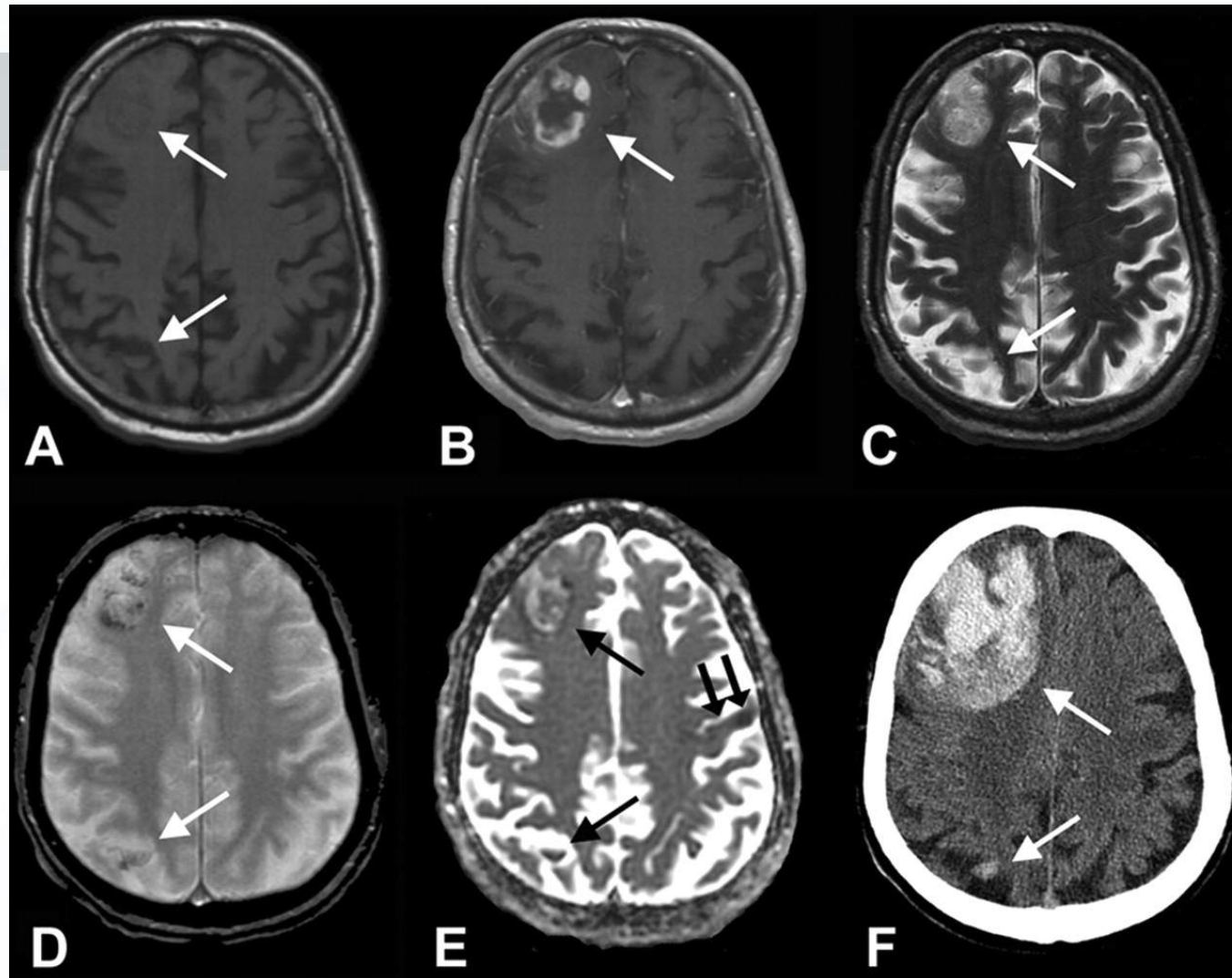
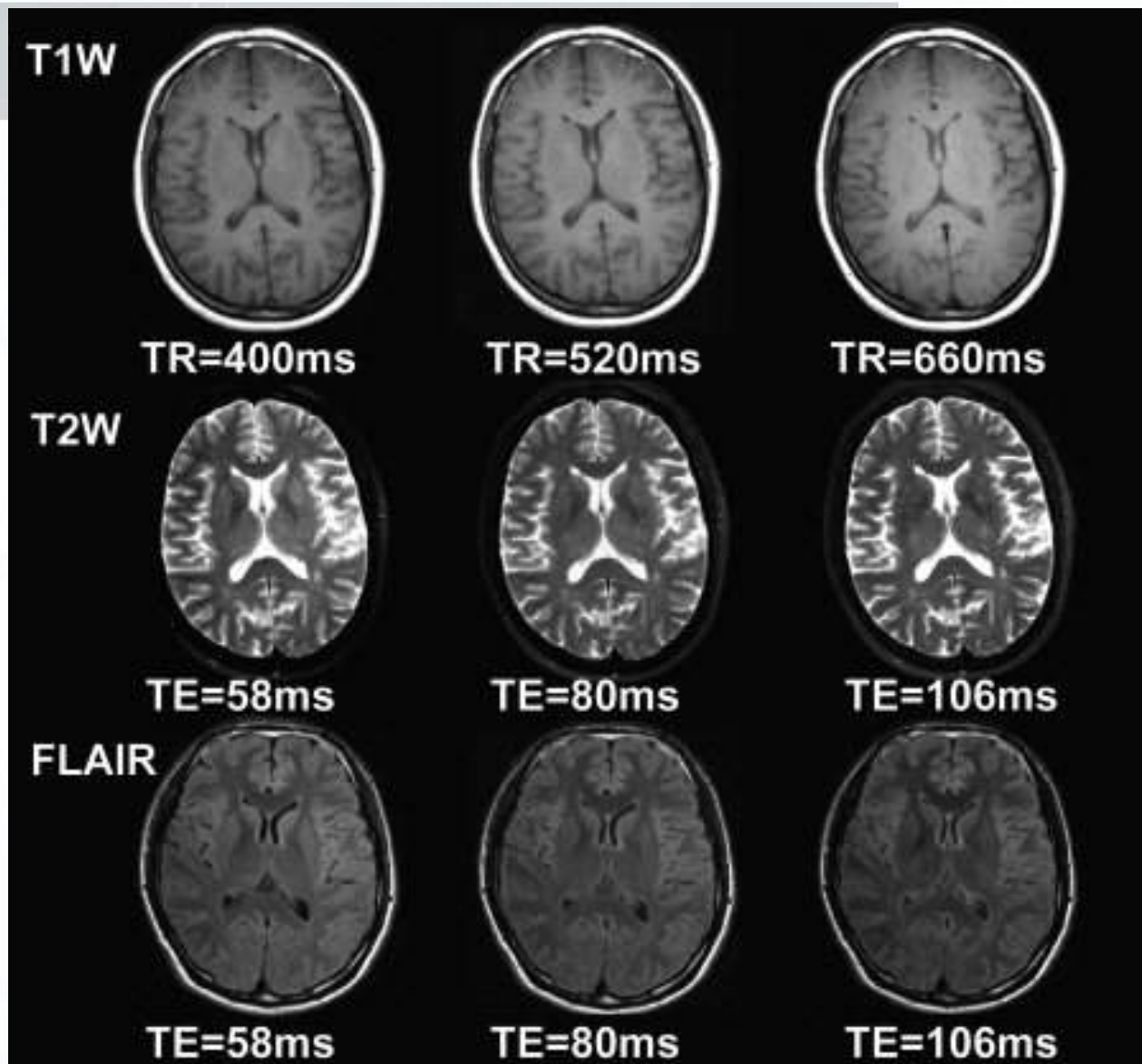


Figure. MRI T1-weighted (A), T1-weighted with gadolinium (B), T2-weighted (C), and susceptibility-weighted (D) sequences show hyperacute hemorrhages in the right frontal lobe and right parietal lobe (arrows). There is marked peripheral nodular gadolinium enhancement within the right frontal hemorrhage (B, arrow). The apparent diffusion coefficient map (E) shows hyperintensity within the right frontal hemorrhage (arrow) and hypointensity due to acute infarction in the left precentral gyrus (double arrow). CT scan (F) 5.5 hours following MRI shows enlargement of the right frontal hemorrhage and no change in size of the right parietal hemorrhage (arrows).

Nguyen T N et al. Neurology 2006;66:E30-E30



J Magn Reson Imaging. 2005 Jul;22(1):13-22.
Routine clinical brain MRI sequences for use at 3.0 Tesla.
Lu H1, Nagee-Poetscher LM, Golay X, Lin D, Pomper M, van Zijl PC.

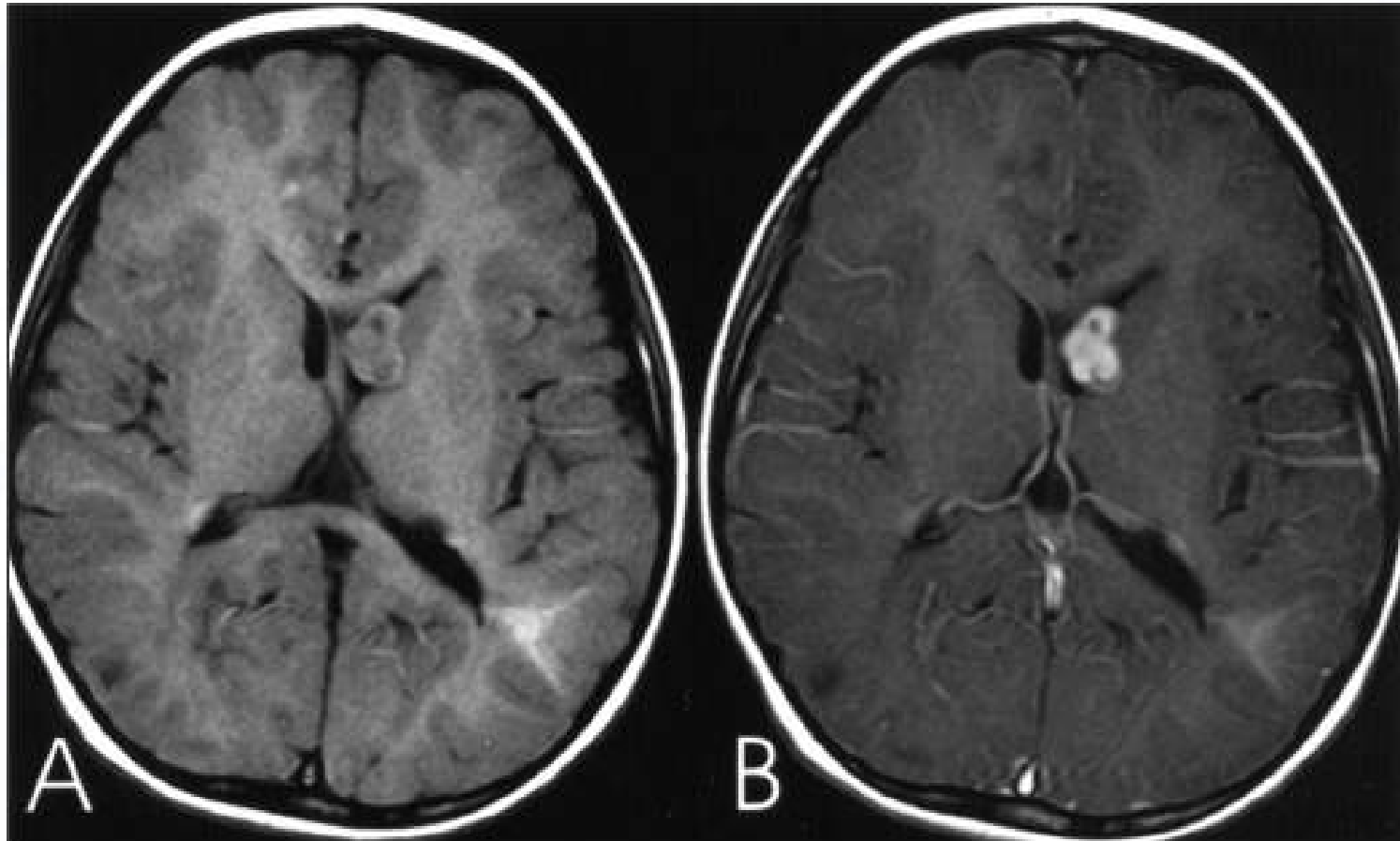
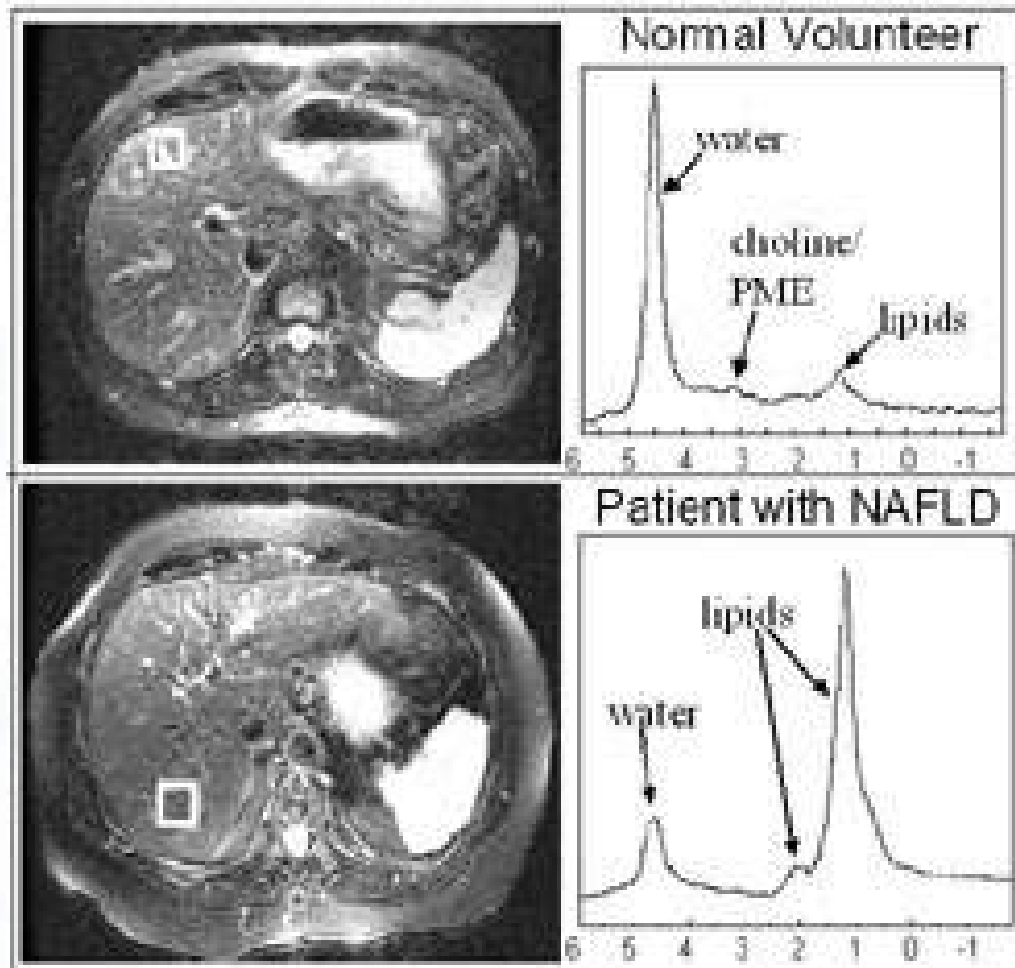


Fig 1. (A) Axial T1 weighted MRI before contrast administration shows a large left foraminal nodule promoting mild left lateral ventricle enlargement. Bilateral cortical tubers are also seen. (B) Axial T1 weighted MRI post-contrast administration demonstrates strong enhancement of the left Monro foramen nodule.

MRI spectroscopy mode : nonalcoholic fatty liver disease (NAFLD)



<http://www.radiology.ucsf.edu/apmri/home>

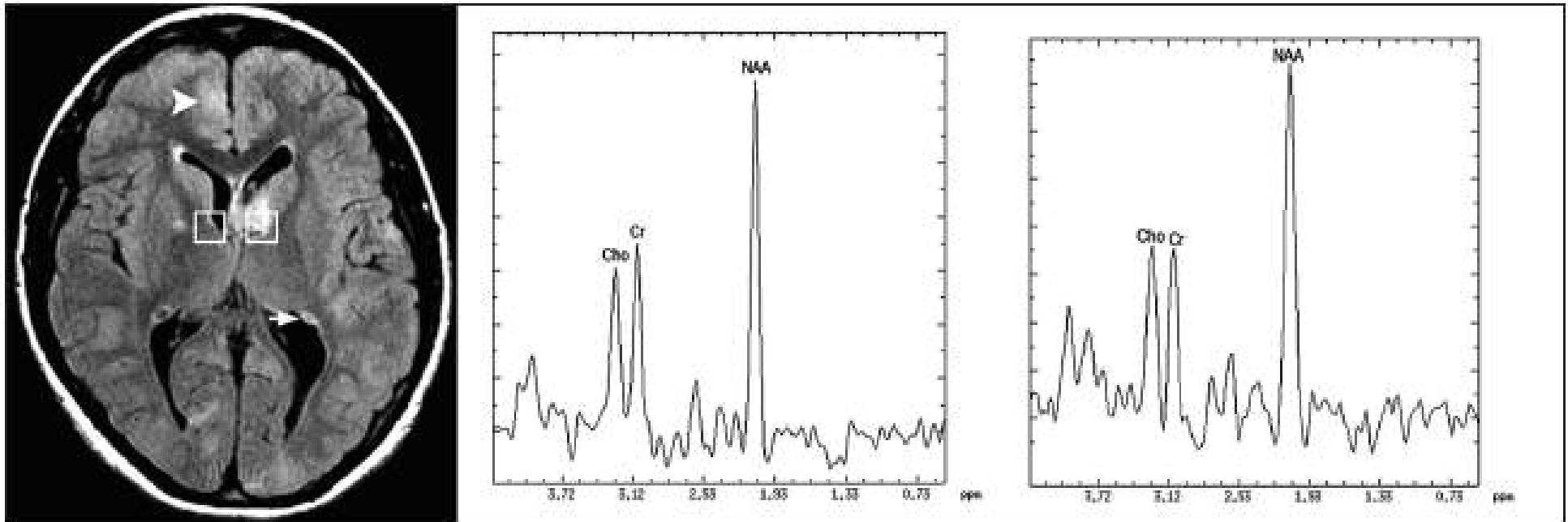


Figure. (A) FLAIR sequence at the level of the foramen of Monro shows cortical tubers (arrowhead) and subependymal nodules (arrow) in the temporal horns of the lateral ventricles and at the left foramen of Monro region. The selected volumes of interest are shown at the right and left foramen of Monro region. 1H-MRS obtained at the right (B) and left (C) foramen of Monro region.

Arq. Neuro-Psiquiatr. vol.66 no.2b São Paulo June 2008
doi: 10.1590/S0004-282X2008000300003

Proton MR spectroscopy of the foramen of Monro region in patients with tuberous sclerosis complex

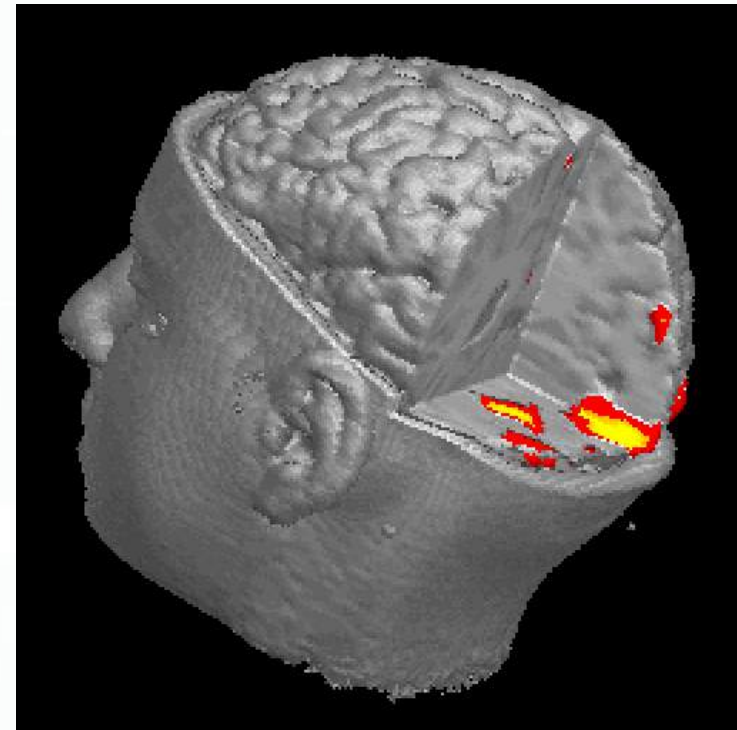
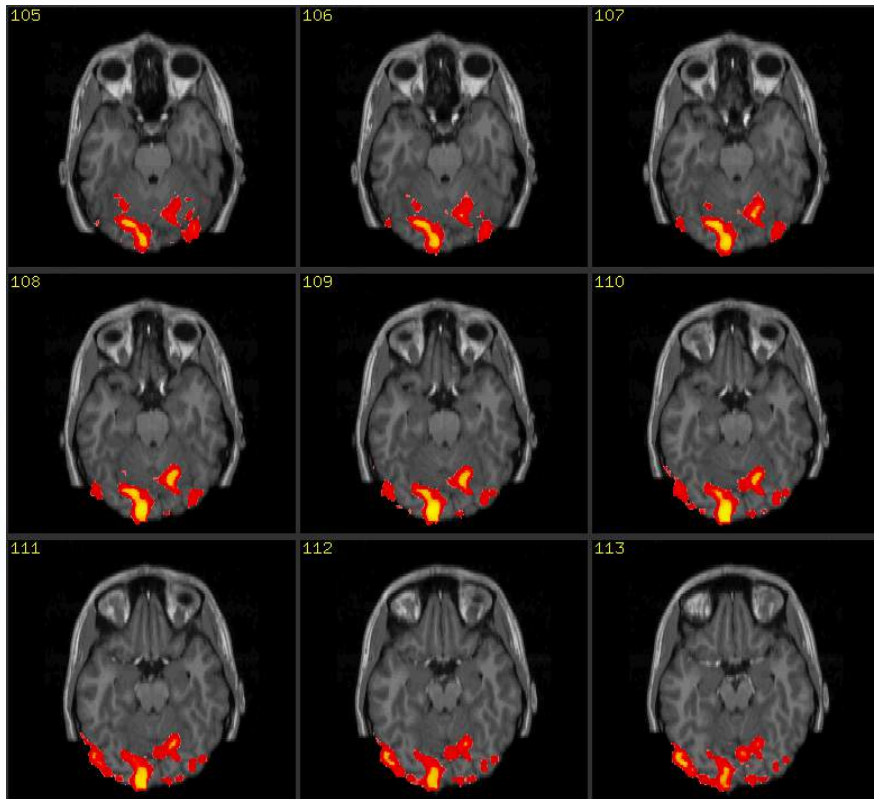
Arnolfo de Carvalho-Netoⁱ; Isac Bruckⁱⁱ; Sérgio A. Antoniukⁱⁱⁱ; Edson Marchioriⁱⁱⁱ; Emerson L. Gasparettoⁱⁱⁱ

ⁱDepartment of Radiology, University of Parana, Curitiba PR, Brazil

ⁱⁱDepartment Neuropediatrics, University of Parana, Curitiba PR, Brazil

ⁱⁱⁱUniversity of Parana, Curitiba PR, Brazil, and Department of Radiology, University of Rio de Janeiro, Rio de Janeiro RJ, Brazil

fMRI (funcional MRI)



- $T2^*$ per voxel is sensitive to the ratio of deoxygenated hemoglobin and oxygenated
- Increase in metabolic activity in the brain causes vasodilation and increased flow of oxygenated blood, $T2^*$ and increases voxel intensity increases
- fMRI detects difference of 3%
- BOLD signal (Blood Oxygen Level-Dependent)
- oxygenated hemoglobin: diamagnetic
- deoxygenated hemoglobin: Paramagnetic

References

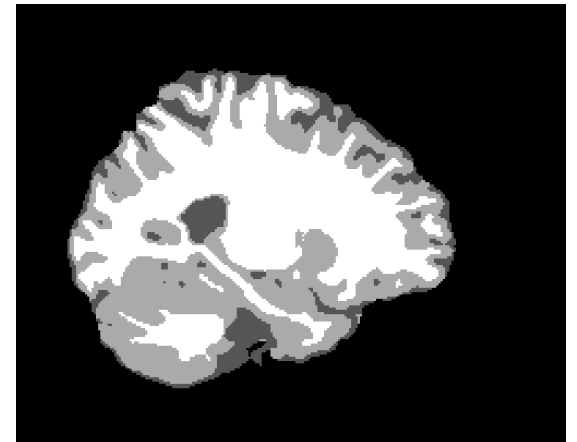
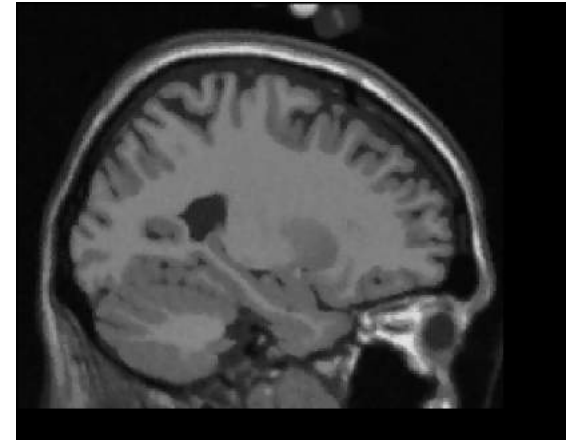
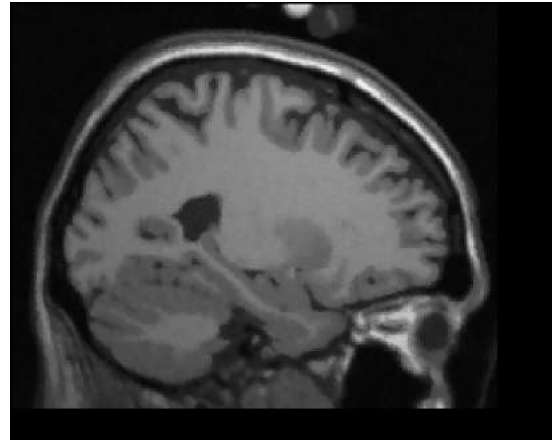
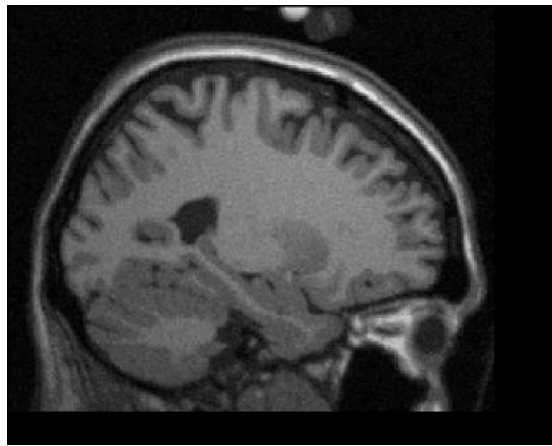
E. Purcell, H. Torrey, and R. Pound, "Resonance absorption by nuclear magnetic moments in a solid," *Physical Review*, vol. 69, pp. 37–38, 1946.

P. C. LAUTERBUR, "Image formation by induced local interactions: Examples employing nuclear magnetic resonance," *Nature*, vol. 242, pp. 190–191, 1973.

Plewes, D. B. and Kucharczyk, W " A Primer of MRI, *Journal of Magnetic Resonance Imaging*, vol. 35, p. 10381054, 2012.

Currie, S., Hoggard, N., Craven, I.J. Hadjivassiliou, M. and Wilkinson, I.D., *Basic MR physics for physicians*, *Postgrad Medical Journal*, vol. 89, p. 209223, 2013.

Magnetic Resonance Image Processing and Analysis



Fábio Cappabianco – Institute of Science and Technology, Federal University of São Paulo
fcappabianco@gmail.com

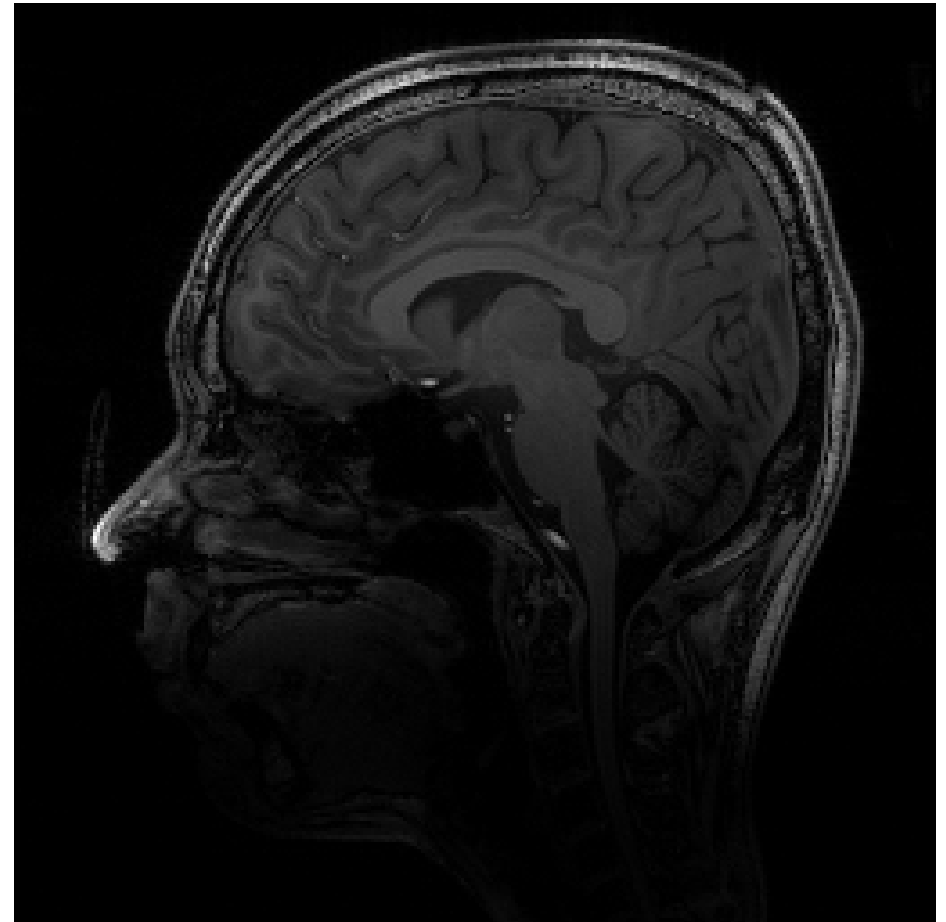
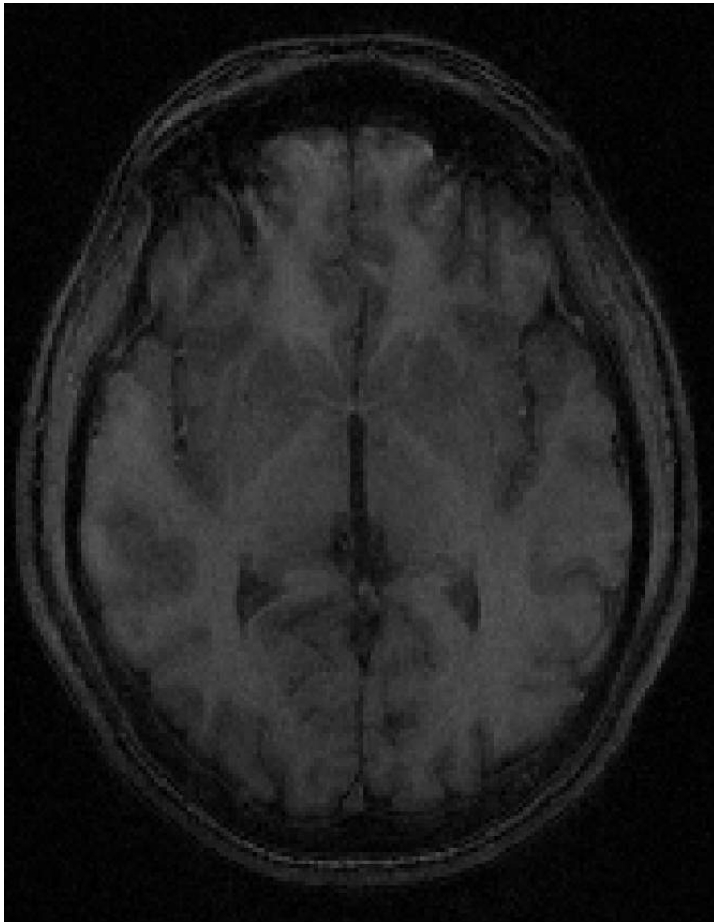
Outline

- MRI intensity regularization
 - High-frequency noise filtering
 - Intensity normalization
 - Inhomogeneity effect removal
- MRI segmentation – brain imaging case study
 - Skull stripping
 - Tissue segmentation/classification
 - Small structure segmentation

Before we start ...

- For the exercises:
 - Softwares:
 - **FSL** - <https://fsl.fmrib.ox.ac.uk/fsl/fslwiki/>
 - **3DSlicer** - <https://www.slicer.org/>
 - Freesurfer - <https://surfer.nmr.mgh.harvard.edu/>
 - SPM - <http://www.fil.ion.ucl.ac.uk/spm/>
 - **BIAL** - <https://github.com/GIBIS-UNIFESP/BIAL>
 - BrainSuite - <http://brainsuite.org/>
 - Databases:
 - **BrainWeb** - <http://brainweb.bic.mni.mcgill.ca/brainweb/>
 - IBSR 18 - <https://www.nitrc.org/projects/ibsr>

MRI Intensity Regularization



High-frequency Noise Filtering

- In MRI → Rician distribution.

– PDF:

$$f(x|v, \sigma) = \frac{x}{\sigma^2} \exp\left(\frac{-(x^2 + v^2)}{2\sigma^2}\right) I_0\left(\frac{x\sigma}{\sigma^2}\right)$$

$$I_0(x) = \sum_{m=0}^{\infty} \frac{1}{m! \Gamma(m+1)} \left(\frac{x}{2}\right)^{2m}$$

$$\Gamma(x) = (x-1)!$$

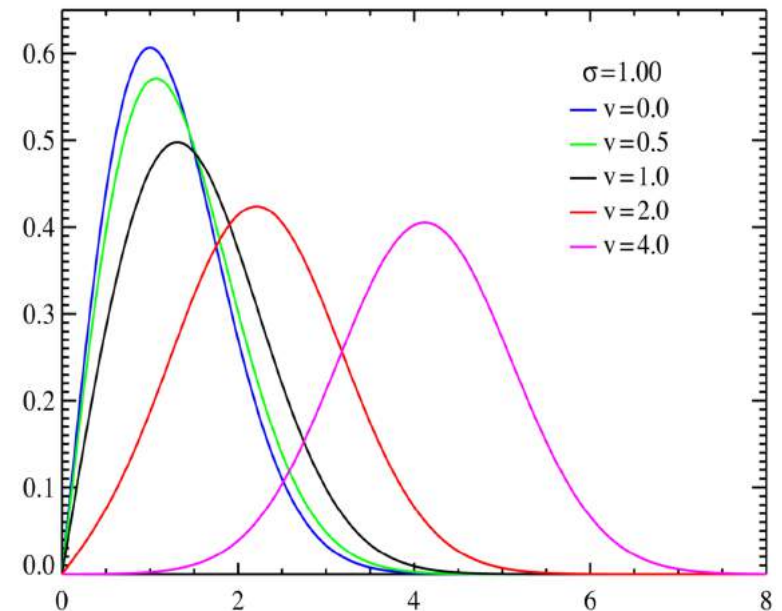
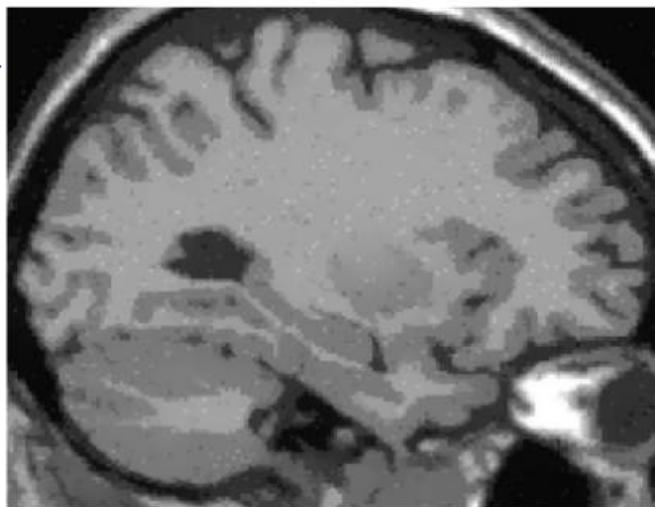
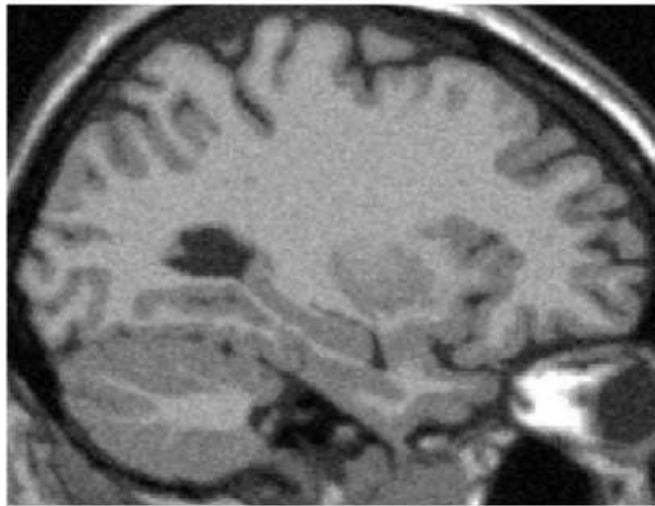
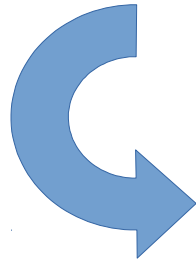


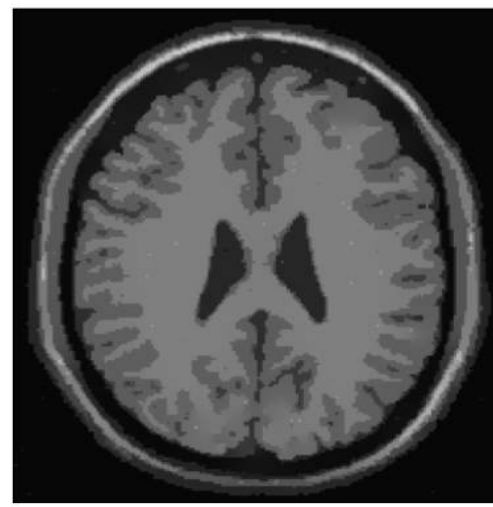
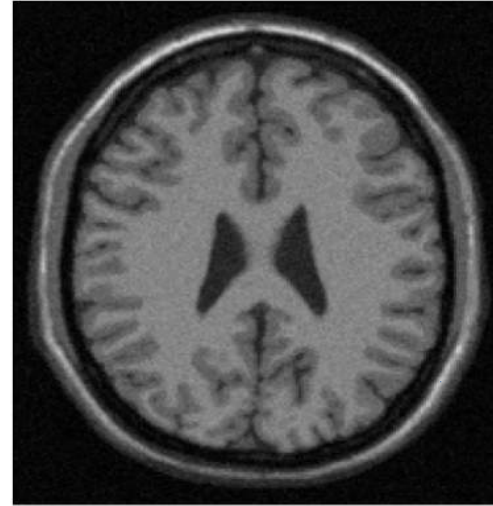
Image from: https://en.wikipedia.org/wiki/Rice_distribution#/media/File:Rice_distributiona_PDF.png

High-frequency Noise Filtering

Weak filtering



Strong filtering



High-frequency Noise Filtering

- 1st generation of filters: isotropics
 - e.g. Mean, median, gaussian
- 2nd generation of filters: local anisotropics
 - e.g. diffusion, bilateral [Smith 1997]
- 3rd generation of filters: non-local anisotropics
 - e.g. non-local means [Tristan-Vega 2012], BM3D, PLOW

High-frequency Noise Filtering

- Isotropic filters:
 - Same operation over all pixels.
 - Simplest → convolution.
 - Fastest → $O(n*a)$
 - Worst → borders also blurred.

High-frequency Noise Filtering

- Local anisotropic filters:
 - Adaptive filter, depending on pixel adjacency contents.
 - Relatively simple, mostly iterative process.
 - Reasonably fast $\rightarrow O(n*a*i)$
 - Much better results – stronger edges preserved.

High-frequency Noise Filtering

- Non-local anisotropic filters:
 - Tries to get more information from adjacencies with similar intensities or patterns of the filtered pixel.
 - Very complex → requires clustering pixel patches.
 - Very slow → $O(n^{\alpha} \cdot a^i)$.
 - Best results → Estimates noise and removes it.
- Newest:
 - http://www.nitrc.org/snapshots.php?group_id=518
 - [Tristan-Vega 2012]
 - Compile with itk and add as module of 3DSlicer.

High-frequency Noise Filtering

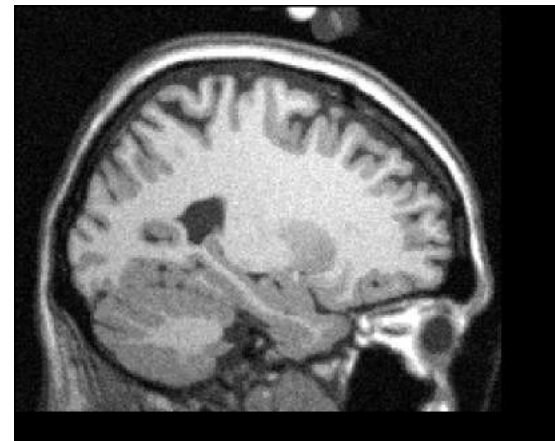
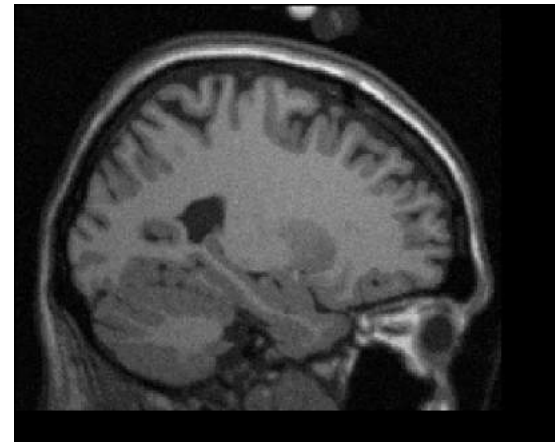
- Exercise:
 - Open 3D slicer
 - Run gradient anisotropic filtering over t1_pn5_rf40.
 - Open FSL
 - Run Susan filtering over t1_pn5_rf40.
 - Compare results and execution time.

High-frequency Noise Filtering

- Evaluation
 - PSNR, MSE → global.
 - SSIM and variations such as MSSIM. [Wang 2004] → structural.
- Today's use...
 - MRI is becoming almost noise free.
 - 7 Tesla images are nice and clear ... in some ways!
 - Even supervised training with patches from multiple images was tested
 - In medical images may generate incorrect results.

Intensity Normalization

- Used to standardize intensity range and distribution of a set of images.
- Based on landmarks.
 - Normally, just mean and quartiles are enough.
 - [Zhuge 2006]



Intensity Normalization

- Two steps method
 - 1st – training: find landmarks in the histogram of input image.
 - 2nd – transformation: find landmarks in target images and map them to the ones of the training image.

Intensity Normalization

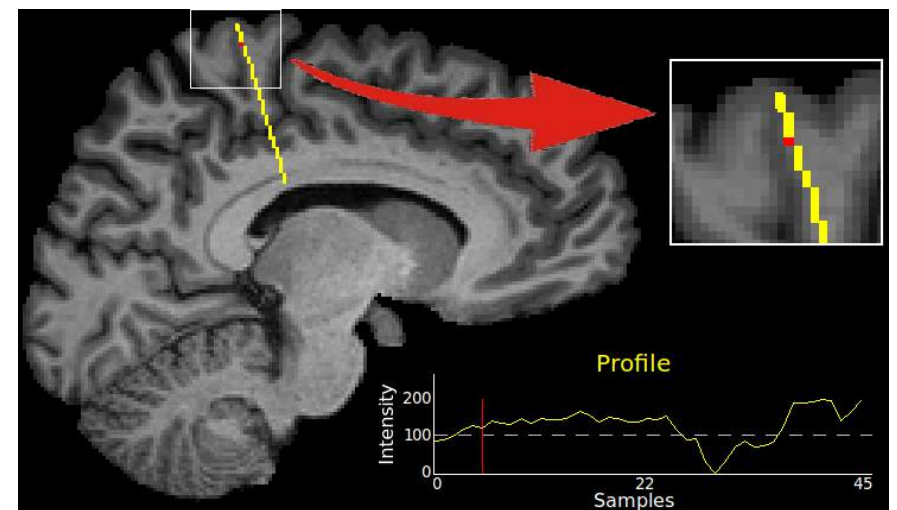
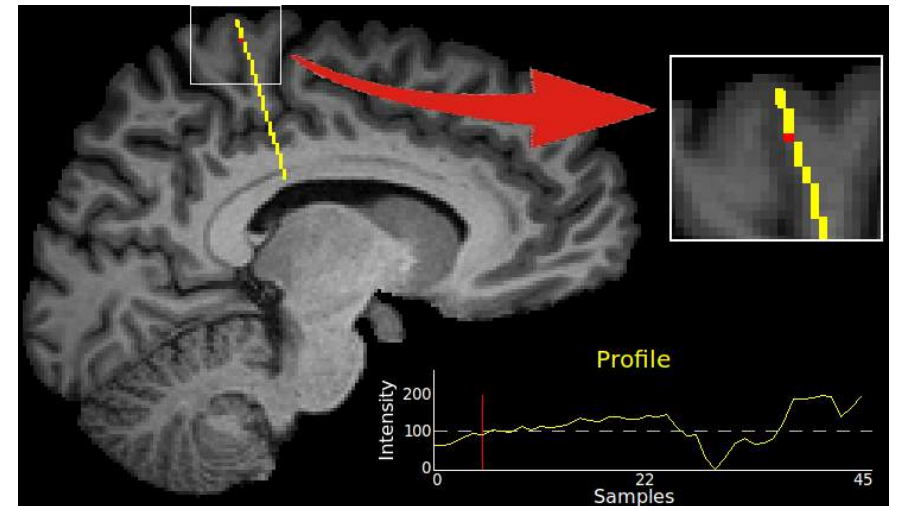
- Consequences:
 - Improves inhomogeneity correction.
 - May improve segmentation process based on expected intensity ranges.

Intensity Inhomogeneity Correction

- Consists of a multiplicative low-frequency noise.
 - $I(s) = \hat{I}(s) * B(s) + \eta(s)$
- Depends on:
 - Magnetic field or scanner features
 - Scanned subject

Intensity Inhomogeneity Correction

- Affects:
 - Segmentation process
 - Statistic measurements
 - Human interpretation



Intensity Inhomogeneity Correction

- General methods:
 - N3 [Sled 1998], N4 [Tustison 2010]
 - Used over any kind of images.
- Brain specific methods:
 - BFC, FAST (also segments tissues)
 - Used over skull stripped brain images.

Intensity Inhomogeneity Correction

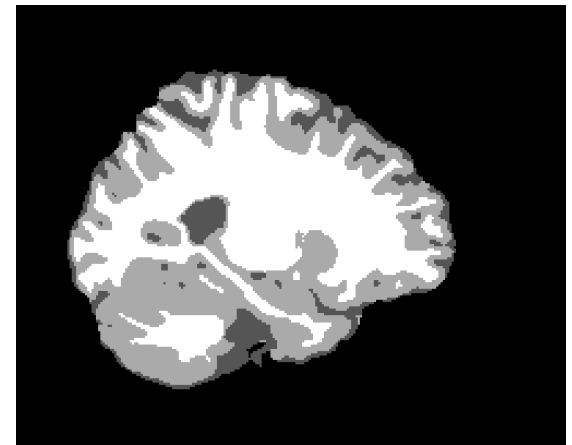
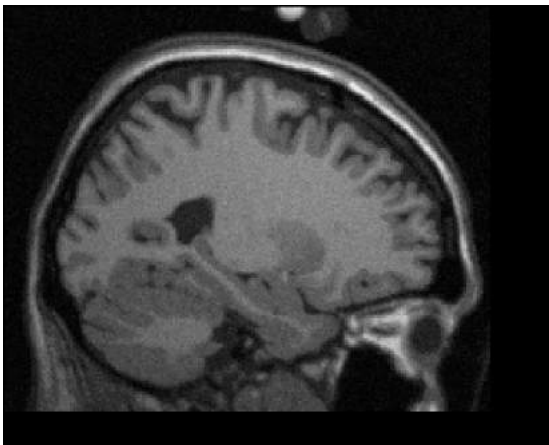
- Exercise
 - Open 3D slicer
 - Run N4itk inhomogeneity correction over t1_pn5_rf40.
 - Run N4itk inhomogeneity correction over t1_pn5_rf40 denoised.
 - Run gradient anisotropic filtering over t1_pn5_rf40 unbiased.
 - Compare results.

Intensity Inhomogeneity Correction

- Evaluation:
 - Using phantom.
 - Post-segmentation results.
- Results:
 - Even generic methods work better over mask.
 - 7T images have even greater inhomogeneity.
 - Not improved since N4 [Tustison 2010].
 - Not a huge improvement since N3 from [Sled 1997]!!!

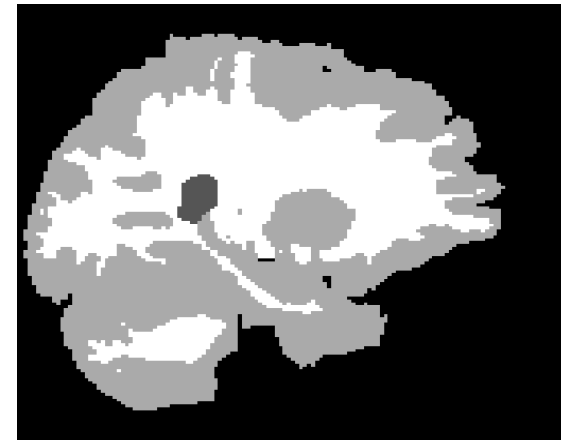
MRI Segmentation

- Why?
 - Improved visualization.
 - Statistical analysis.
 - fMRI.
 - 3D modeling.



Skull Stripping

- Ill posed problem.
 - Extract everything that does not belong to the brain.
 - What about CSF?
 - Optical nerve?
 - Where does the brain ends?



Skull Stripping

- Methods:
 - Surface fitting:
 - BET from FSL [Smith 2002].
 - BSE from BrainSuite.
 - Region growing:
 - Hibrid watershed from Freesurfer. [Ségonne 2004]
 - Mixed histogram matching:
 - SPM (also segments tissues)

Skull Stripping

- Exercise
 - Open FSL
 - Run bet over t1_pn5_rf40.
 - Run bet over t1_pn5_rf40 denoised and unbiased.
 - Run bet with COG correction over t1_pn5_rf40 denoised and unbiased.
 - Compare results
 - Inhomogeneity correction effects [Miranda 2013]

Skull Stripping

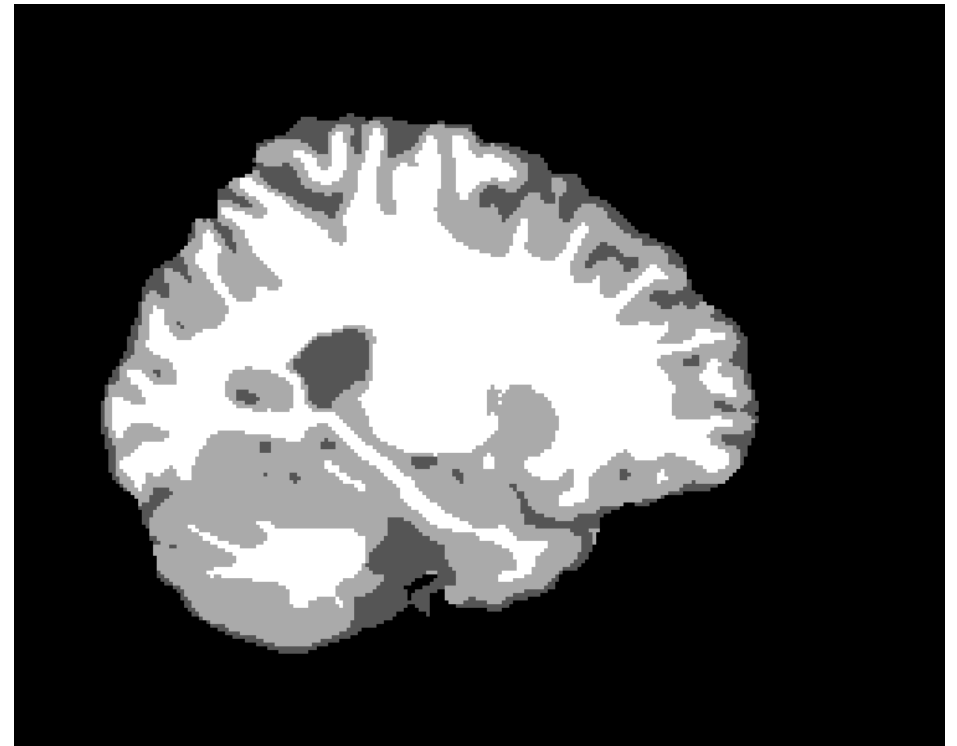
- Evaluation:
 - Compare to manual segmentation. [Fennema-Notestine 2006]
 - Still, depends on human perception or goal application.
- Open questions:
 - No method generates perfect segmentation.
 - Depends on inhomogeneity correction for high magnetic field MRI [Cappabianco 2012].
 - Harder for pathological cases.

Tissue Segmentation

- Definition:
 - Label pixels into GM, WM, and CSF.
- Goal:
 - Allow quantization, analysis, fMRI studies.
- Issues:
 - What about partial volume pixels?

Tissue Segmentation

- Methods:
 - OPF clustering
 - Gaussian mixture
 - Markov random fields [Zhang 2001]
 - K-means



Tissue Segmentation

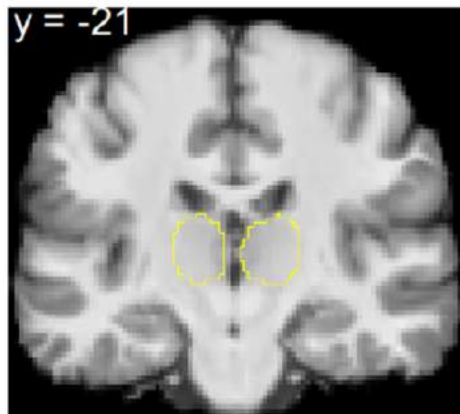
- Exercise
 - Open FSL
 - Run FAST with partial volume option
 - Run c-means
 - Run OPF clustering
- Compare results

Tissue Segmentation

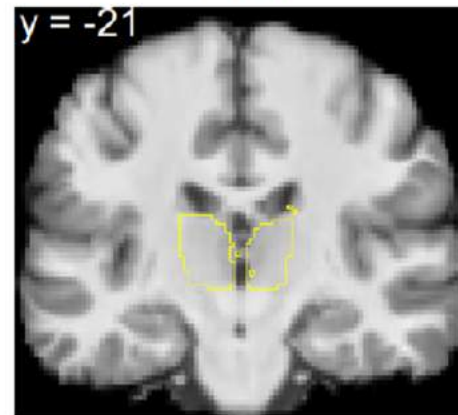
- Evaluation:
 - Area comparison metrics:
 - Dice, Jaccard, Kappa.
 - Parameter evaluation metrics:
 - ROC curves. [Cappabianco 2012b]
- Open problems:
 - How to generate the ground-truth?
 - Manual or semi-automatic segmentation is still impossible today.
 - Evaluation without ground-truth [Boiux 07].

Small Structure Segmentation

- Segmentation of sub-cortical or cortical structures.



Ground Truth



OPF

Small Structure Segmentation

- User iteration types
 - Automatic
 - Manual
 - Semi-automatic
- Implementation types
 - Region growing
 - Edge delineation

Other operations

- Pose estimation.
- Brain alignment.
- Surface extraction.
- Hemisphere symmetry analysis
- Registration
- ...

References

- [Smith 1997] Smith, Stephen M., and J. Michael Brady. "SUSAN—a new approach to low level image processing." *International journal of computer vision* 23.1 (1997): 45-78.
- [Black 1998] Black, Michael J., et al. "Robust anisotropic diffusion." *IEEE Transactions on image processing* 7.3 (1998): 421-432.
- [Sled 1998] Sled, John G., Alex P. Zijdenbos, and Alan C. Evans. "A nonparametric method for automatic correction of intensity nonuniformity in MRI data." *IEEE transactions on medical imaging* 17.1 (1998): 87-97.
- [Zhang 2001] Zhang, Yongyue, Michael Brady, and Stephen Smith. "Segmentation of brain MR images through a hidden Markov random field model and the expectation-maximization algorithm." *IEEE transactions on medical imaging* 20.1 (2001): 45-57.
- [Smith 2002] Smith, Stephen M. "Fast robust automated brain extraction." *Human brain mapping* 17.3 (2002): 143-155.
- [Ségonne 2004] Ségonne, Florent, et al. "A hybrid approach to the skull stripping problem in MRI." *Neuroimage* 22.3 (2004): 1060-1075.
- [Wang 2004] Wang, Zhou, et al. "Image quality assessment: from error visibility to structural similarity." *IEEE transactions on image processing* 13.4 (2004): 600-612.
- [Fennema-Notestine 2006] Fennema-Notestine, Christine, et al. "Quantitative evaluation of automated skull-stripping methods applied to contemporary and legacy images: Effects of diagnosis, bias correction, and slice location." *Human brain mapping* 27.2 (2006): 99-113.

References

- [Zhuge 2006] Zhuge, Ying, et al. "An intensity standardization-based method for image inhomogeneity correction in MRI." Medical Imaging. International Society for Optics and Photonics, 2006.
- [Bouix 2007] Bouix, Sylvain, et al. "On evaluating brain tissue classifiers without a ground truth." Neuroimage 36.4 (2007): 1207-1224.
- [Tustison 2010] Tustison, Nicholas J., et al. "N4ITK: improved N3 bias correction." IEEE transactions on medical imaging 29.6 (2010): 1310-1320.
- [Cappabianco 2012] Cappabianco, Fábio AM, et al. "Unraveling the compromise between skull stripping and inhomogeneity correction in 3T MR images." 2012 25th SIBGRAPI Conference on Graphics, Patterns and Images. IEEE, 2012.
- [Cappabianco 2012b] Cappabianco, Fábio AM, et al. "Brain tissue MR-image segmentation via optimum-path forest clustering." Computer Vision and Image Understanding 116.10 (2012): 1047-1059.
- [Miranda 2013] Miranda, Paulo AV, Fábio AM Cappabianco, and Jaime S. Ide. "A case analysis of the impact of prior center of gravity estimation over skull-stripping algorithms in mr images." 2013 IEEE International Conference on Image Processing. IEEE, 2013.
- [Tristán-Vega 2012] Tristán-Vega, Antonio, et al. "Efficient and robust nonlocal means denoising of MR data based on salient features matching." Computer methods and programs in biomedicine 105.2 (2012): 131-144.

Extras

Anisotropic Diffusion Filtering

- Iterative process simulating thermal energy flow.

$$I_s^{t+1} \approx I_s^t + \frac{\lambda}{|\eta_s|} \sum_{p \in \eta_s} g(|\nabla I_{s,p}^t|, \gamma) \nabla I_{s,p}^t \quad (1)$$

- I_s^t – intensity of pixel s in instant t
- λ – constant related to diffusion rate
- η_s – pixels adjacent to s
- $\Delta I_{s,p}^t$ or x – magnitude of intensity directional gradient from s to p
- $g(\cdot)$ – edge stopping function

Anisotropic Diffusion Filtering

- Edge stopping functions:

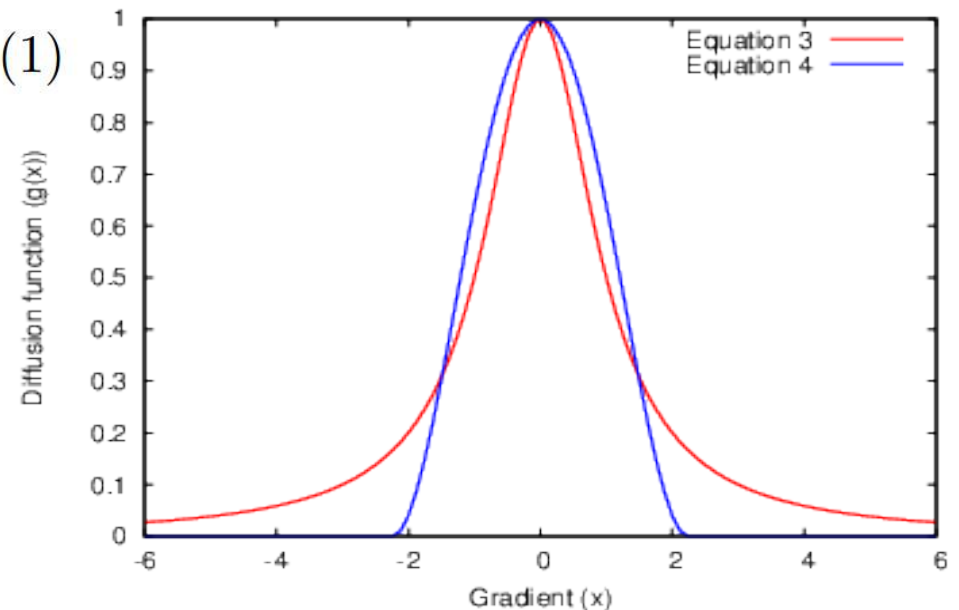
$$I_s^{t+1} \approx I_s^t + \frac{\lambda}{|\eta_s|} \sum_{p \in \eta_s} g(|\nabla I_{s,p}^t|, \gamma) \nabla I_{s,p}^t \quad (1)$$

Let $\gamma = \lambda / |\eta_s|$

$$g(x, \gamma) = \exp(-x^2 / 2\gamma^2) \quad (2)$$

$$g(x, \gamma) = \left[1 + (x/\gamma)^2\right]^{-1} \quad (3)$$

$$g(x, \gamma) = \begin{cases} \left[1 - (x^2 / 5\gamma^2)\right]^2 & |x| \leq \gamma\sqrt{5} \\ 0, & \text{otherwise} \end{cases} \quad (4)$$



[Black 1998]

Bilateral Filter

- Goal: average the intensity of pixels based on intensity and spatial proximity

$$- BF [I(p)] = \frac{1}{W_p} \sum_{q \in Adj} G_{\sigma_s}(\|p - q\|) G_{\sigma_r}(|I(p) - I(q)|) I(q)$$

- W_p is a factor of normalization.
- G_x are Gaussian functions.

Non-local Means

- Same idea as bilateral filter, but use information from other image locations.
- Use patches to compare similar image locations.
- Estimate intensity distance function based on N-Dimensional vector, where N depends on the patch size.

$$- NLM[I(p)] = \frac{1}{W_p} \sum_{q \in Adj} G_{\sigma_s}(\|p - q\|) G_{\sigma_r}(\|Adj(p) - Adj(q)\|) I(q)$$

MSSIM

- Mean structural similarity index.

- $SSIM(x, y) = [l(x, y)]^\alpha \cdot [c(x, y)]^\beta \cdot [s(x, y)]^\gamma$

- Compares:

- Luminance

- $l(x, y) = \frac{2\mu_x\mu_y + C_1}{\mu_x^2 + \mu_y^2 + C_1}$

- Contrast

- $c(x, y) = \frac{2\sigma_x\sigma_y + C_2}{\sigma_x^2 + \sigma_y^2 + C_2}$

- Structure

- $s(x, y) = \frac{\sigma_{xy} + C_3}{\sigma_x\sigma_y + C_3}$

- MSSIM → Mean value of SSIM over local windows.

Nonparametric Nonuniformity Normalization (N3)

- Find a smooth, slowly varying, multiplicative field which maximizes the frequency the input signal.
 - Unknown frequency/distribution
 - Large search space.
 - Hard to estimate related measures (e.g. Entropy)
- Strategy:
 - Sharpening input signal.
 - Estimate true signal.
- Assumptions:
 - Bias has unimodal Gaussian distribution.
 - Zero noise.

Nonparametric Nonuniformity Normalization (N3)

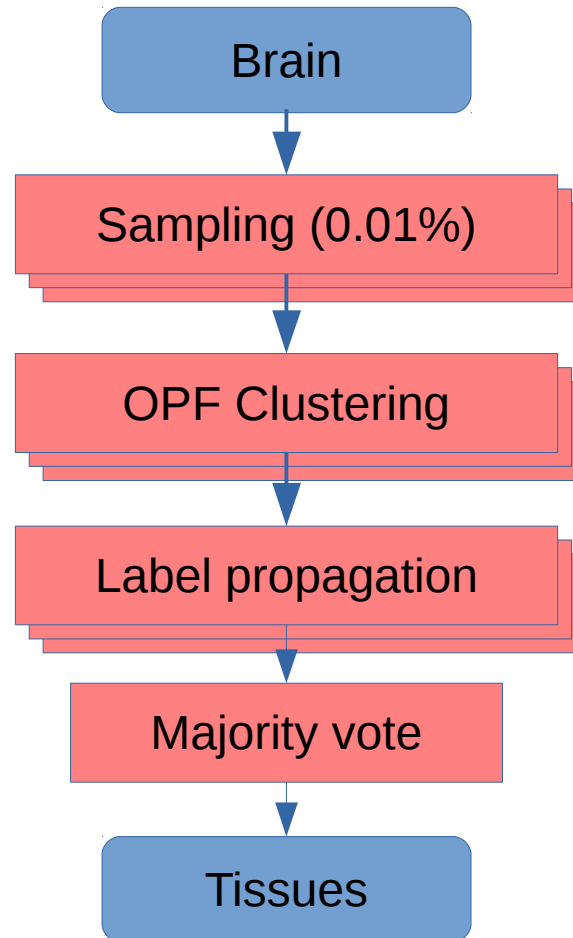
- Computing the filtered image:
- Considered model:
 - $I(s) = J(s) * B(s)$
- Correction:
 - $\tilde{G}(x) = \frac{\tilde{B}^*(x)}{|\tilde{B}(x)|^2 + C^2}$
 - $\tilde{I}(s) = \tilde{J}(s) * \tilde{G}(s)$
- Iterative process applied to different scales.
- Use B-Spline to smooth the final result.

Brain Extraction Tool

- Method:
 - Computes robust lower and upper intensity values.
 - Estimate center-of-gravity using weighted intensity values.
 - Initialize a sphere composed of triangle mesh.
 - Deform mesh until it fits image borders.

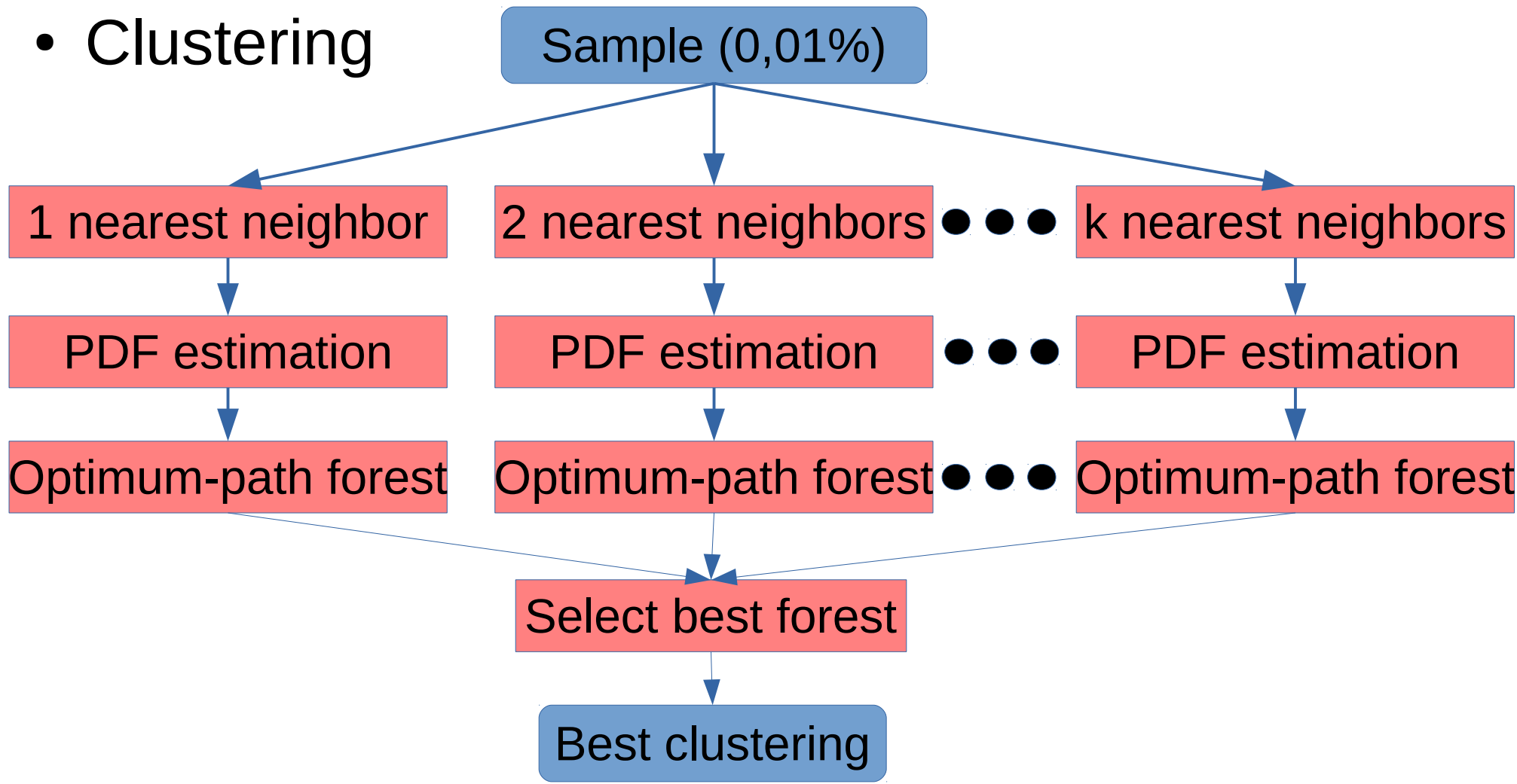
Optimum Path Forest Clustering

- Overview

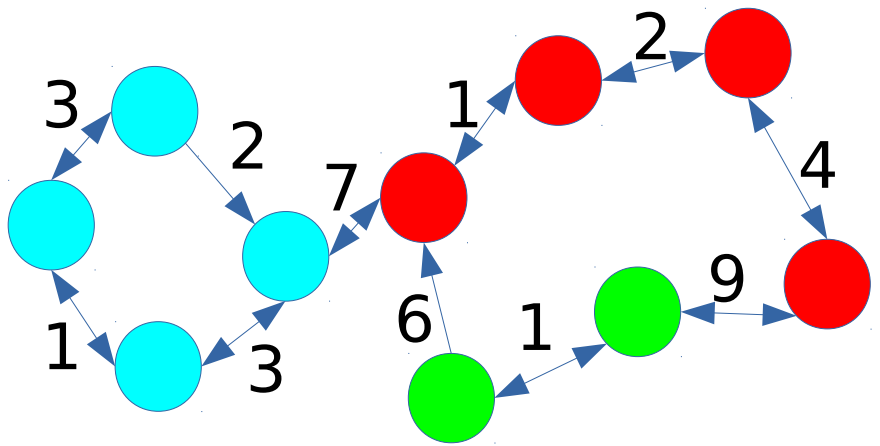


Optimum Path Forest Clustering

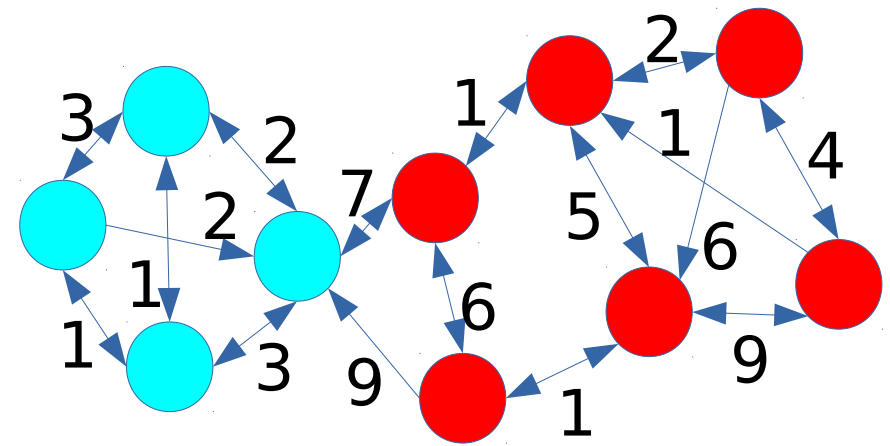
- Clustering



Optimum Path Forest Clustering



$k=2, c=3$

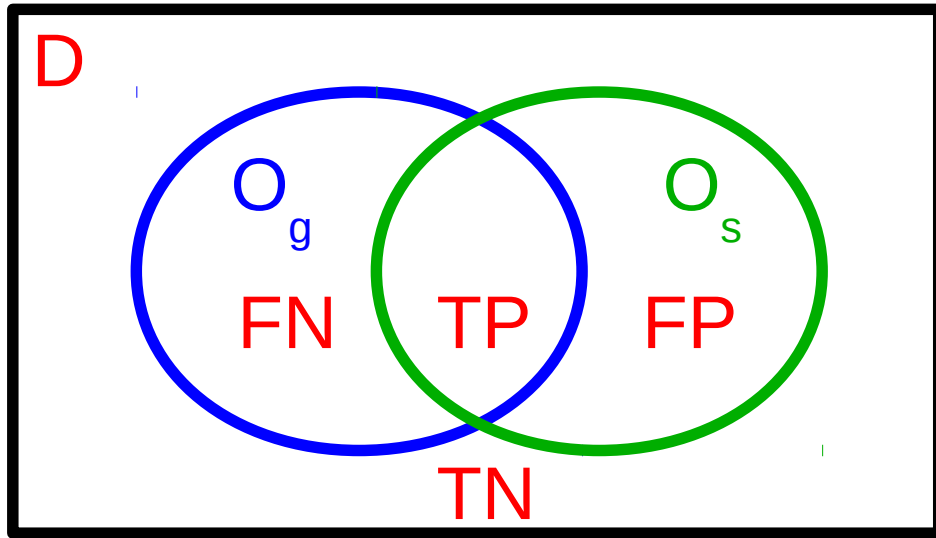


$k=3, c=2$

$$C(k) = \sum_{i=1}^c \frac{V_i}{W_i + V_i},$$

V_i e W_i are the sum of the weights of intra and inter cluster edges, respectively.

Accuracy Metrics



D: Image domain

O_g: Ground-truth object pixels

O_s: Segmentation object pixels

TP: $O_g \cap O_s$

TN: $D - (O_g \cup O_s)$

FP: $O_s - (O_s \cap O_g)$

FN: $O_g - (O_s \cap O_g)$

$$FNN: \frac{|FN|}{|FN| + |VP|} \quad FPN: \frac{|FP|}{|FP| + |VN|}$$

$$dice: \frac{2|TP|}{2|TP| + |FP| + |FN|}$$

$$jaccard: \frac{|TP|}{|TP| + |FP| + |FN|}$$

V. POSE AND SPATIAL STANDARDIZATION



Sibigrapi – São José dos Campos
2016

Claudio Shida

Email: shida@unifesp.br

Summary

- A. Image interpolation
- B. Motion correction
- C. Image registration

A. Image interpolation

Definition: Interpolation is used to find intensity values between grid points

It is essential for a variety of medical imaging processing, such as,

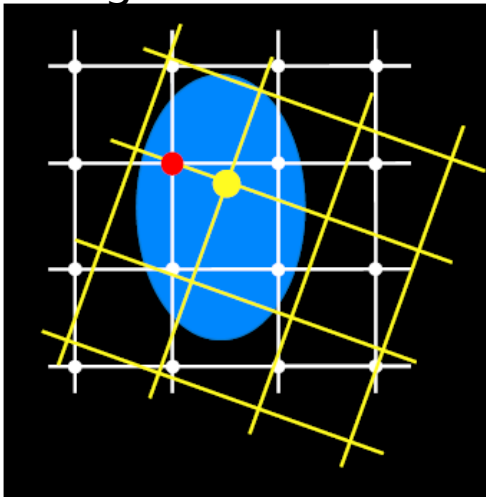
- image generation,
- compression or resampling,
- subpixel translation,
- elastic deformation or warping,
- magnification or minification
- geometrical correction
- image registration and proper volume visualization.

Image interpolation is a more consolidated issue and the most commonly used interpolation techniques are: nearest neighbor, bilinear, bicubic, B-splines, lanczos2, discrete wavelet transform and Kriging.

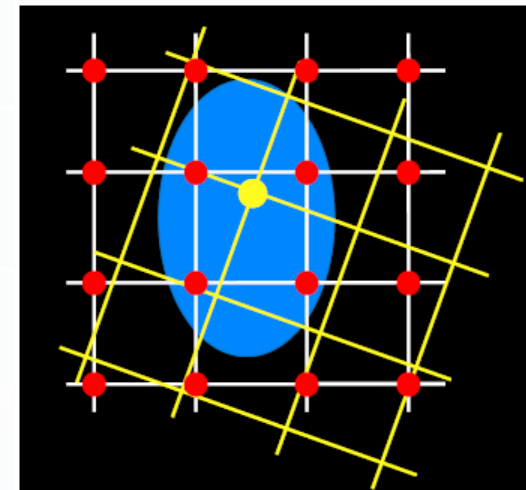
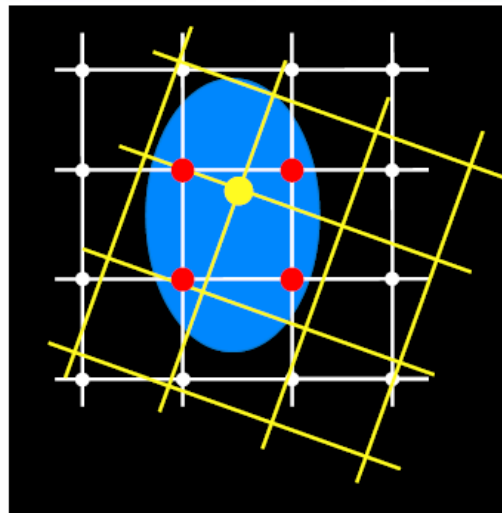
A. Image interpolation

- Spline
- Sinc
- k-Space methods

Nearest
Neighbour



Trilinear



A. Image interpolation - References

J. Ashburner and C. D. Good, "Spatial registration of images," in Quantitative MRI of the Brain: Measuring Changes Caused by Disease, P. Tofts, Ed. John Wiley & Sons, 2003, ch. 15, pp. 503-532.

T. M. Lehmann, C. Gonner, and K. Spitzer, "Survey: Interpolation methods in medical image processing," IEEE TRANSACTIONS ON MEDICAL IMAGING, vol. 18, no. 11, pp. 1049-1075, 1999.

E. H. W. Meijering, "Spline interpolation in medical imaging: comparison with other convolution-based approaches," Proceedings of EUSIPCO 2000, M. Gabbouj and P. Kuosmanen (eds.), vol. IV, pp. 1989-1996, 2000.

A. Amanatiadis and I. Andreadis, "A survey on evaluation methods for image interpolation," Measurement Science and Technology, vol. 20, no. 10, p. 104015, 2009.

B. Motion correction

Patient may move the head during a run or between runs, resulting in wrong spatial location.

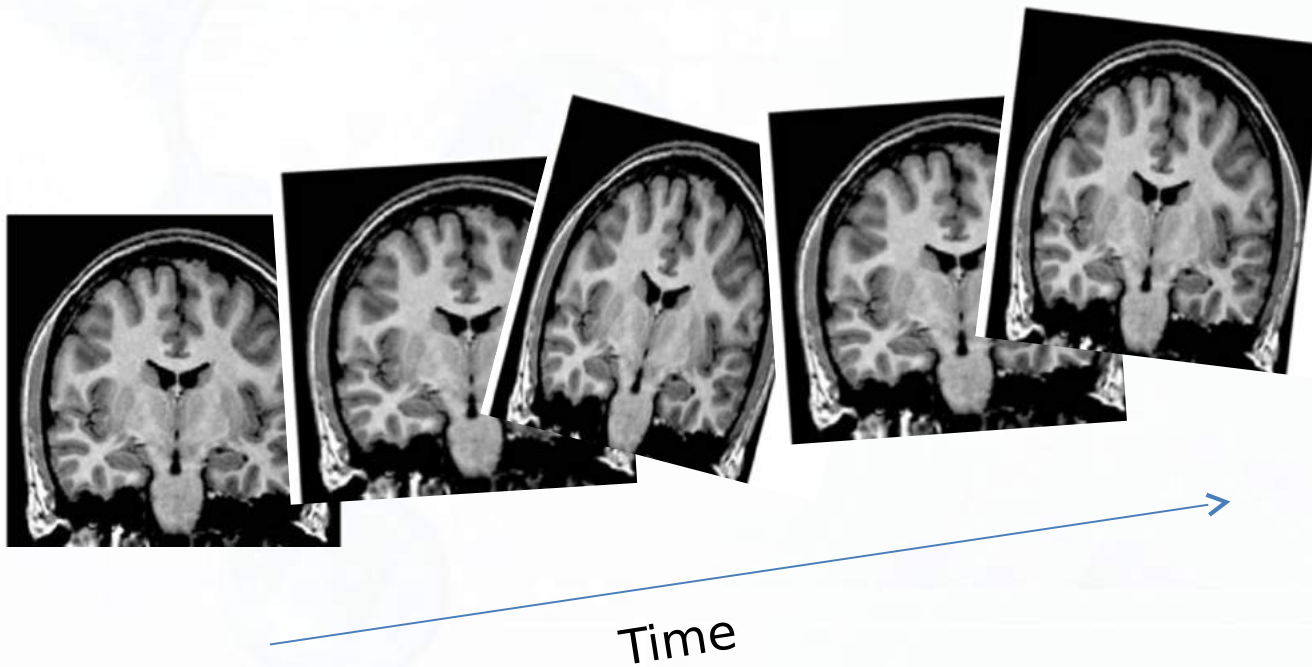
- impossible to avoid movements as small as a few millimeters.
- It will dislevel or distort the image sequence.

The motion correction should be carried out co-registering each volume in the sequence run acquisition to a reference volume.

The reference volume may be:

- i) First volume in the sequence acquisition;
- ii) Middle volume in the sequence acquisition; or
- iii) Average of all the volumes in the sequence acquisition prior to motion correction.

B. Motion correction



B. Motion correction

most commonly used interpolation technique are:

- Earest neighbor,
- bilinear,
- Trilinear,
- bicubic,
- B-splines,
- lanczos2,
- discrete
- wavelet transform and Kriging [89].

C. Image registration

- Image Registration is the process of estimating an optimal transformation between two images.
- Sometimes also known as “Spatial Normalization”

C. Image registration

Applications

- fMRI Specific
 - Motion Correction
 - Correcting for Geometric Distortion in EPI
 - Alignment of images obtained at different times or with different imaging parameters
 - Formation of Composite Functional Maps
- Other Applications
 - Mapping of PET/SPECT to MR Images
 - Atlas-based segmentation/brain stripping
 - And many many many more!

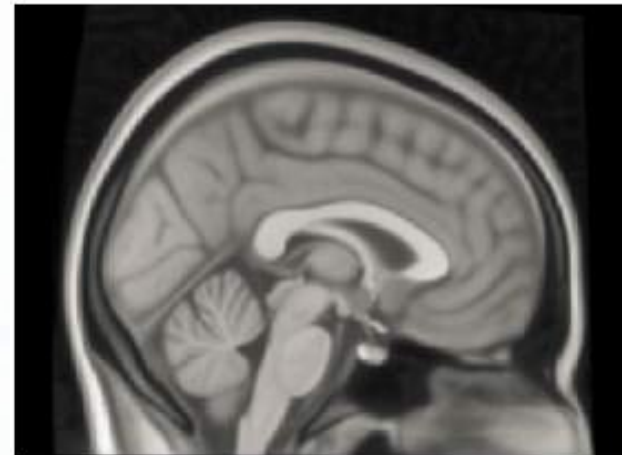
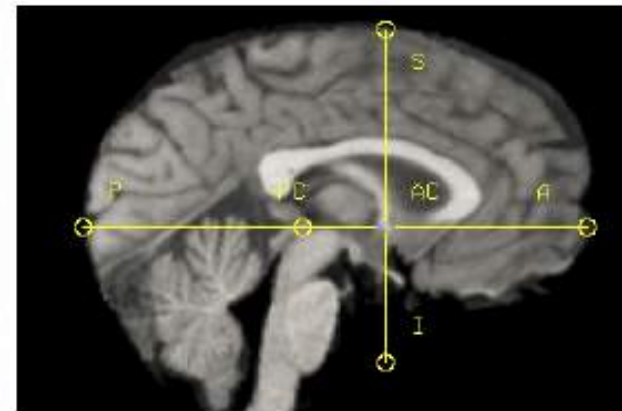
C. Image registration

Components of the Image Registration Process

- Reference and Target datasets.
- Transformation model
- Cost Function
- Optimization Method

C. Image registration - Reference and Target datasets

- Common reference coordinate system for reporting/describing
- Register all members of a group to this space for group Studies
- Original Talairach & Tournoux coords based on one postmortem Brain
- Now use standard images based on non-linear group average (MNI152)
- MNI is not quite Talairach



C. Image registration - Transformation Model

Transformation Model (FSL)

- Rigid
- Affine
- Non-linear

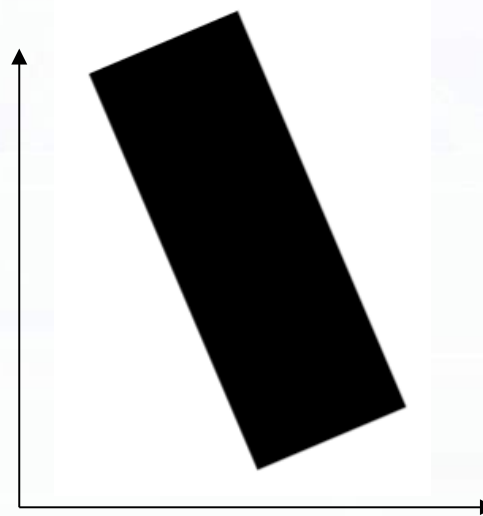
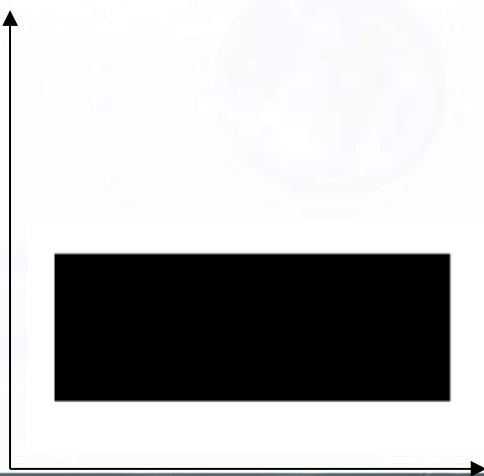
C. Image registration - Rigid Transformation

- Rotation(R)
- Translation(t)
- Similarity(scale)

$$\vec{p}_1 = \begin{bmatrix} x_1 \\ y_1 \end{bmatrix} \quad \vec{p}_2 = \begin{bmatrix} x_2 \\ y_2 \end{bmatrix} \quad \vec{s}_1 = \begin{bmatrix} s_1 \\ s_2 \end{bmatrix} \quad \vec{t}_1 = \begin{bmatrix} t_1 \\ t_2 \end{bmatrix}$$

$$p_2 = t + sRp_1$$

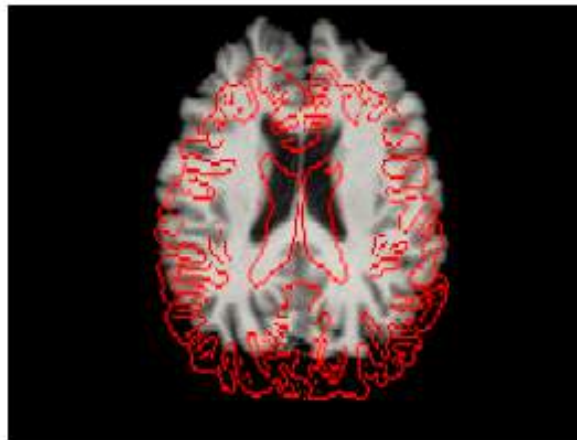
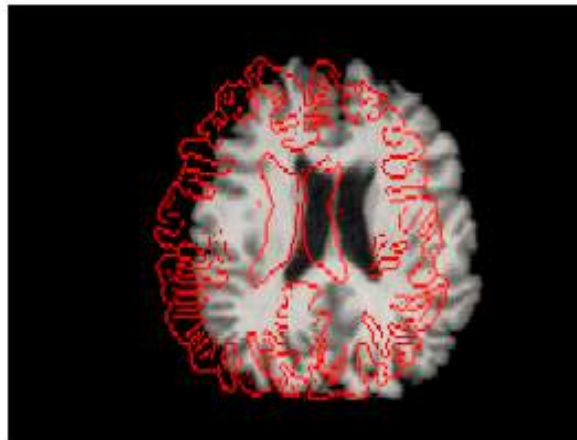
$$R = \begin{bmatrix} \cos(\theta) & -\sin(\theta) \\ \sin(\theta) & \cos(\theta) \end{bmatrix}$$



C. Image registration - Rigid Transformation

- 6 DOF in 3D
- Includes:
 - 3 Rotations
 - 3 Translations

**Used for
within-subject
registrations**



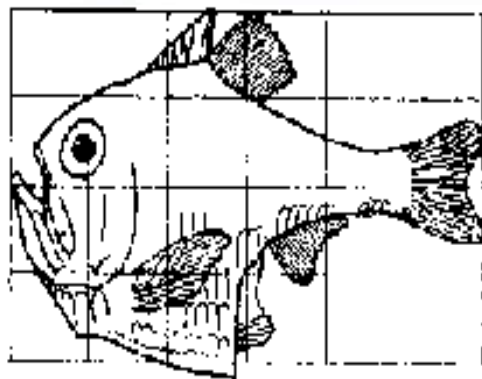
C. Image registration - Affine Transformation

- Rotation
- Translation
- Scale
- Shear

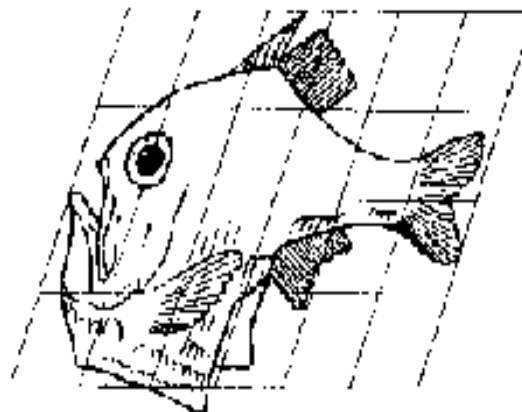
$$\begin{bmatrix} x_2 \\ y_2 \end{bmatrix} = \begin{bmatrix} a_{13} \\ a_{23} \end{bmatrix} + \begin{bmatrix} a_{11} + a_{12} \\ a_{21} + a_{22} \end{bmatrix} \begin{bmatrix} x_1 \\ y_1 \end{bmatrix}$$

No more preservation of lengths
and angles

Parallel lines are preserved



Argyropelecus olfersi.



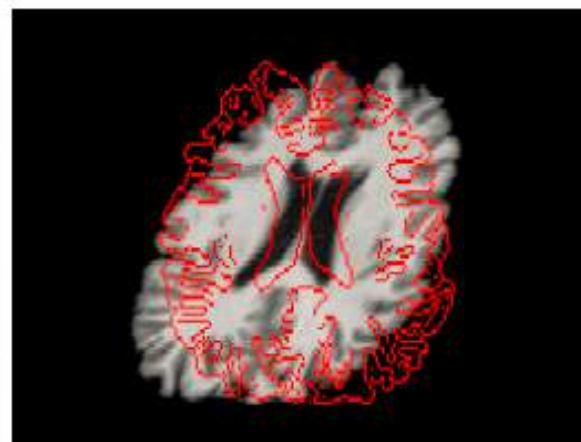
Sternoptyx diaphana.

C. Image registration - Affine Transformation

12 DOF in 3D

- Linear Transf.
- Includes:
 - 3 Rotations
 - 3 Translations
 - 3 Scalings
 - 3 Skews/Shears

**Used for eddy current correction
and initialising non-linear
registration**

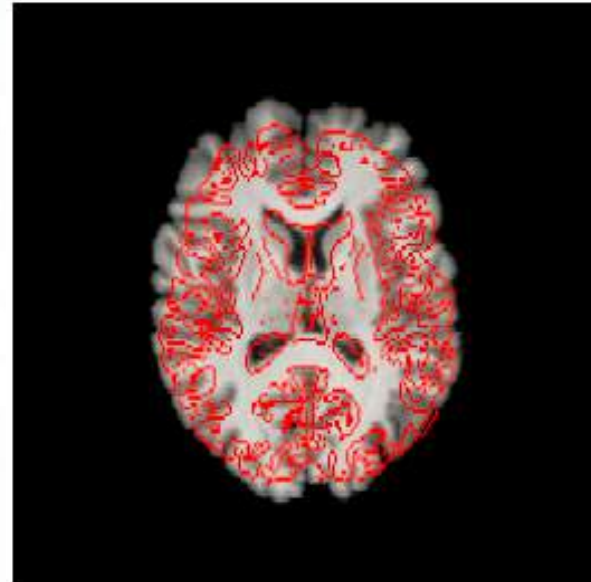


C. Image registration - non linear

More than 12 DOF

- Can be purely local
- Subject to constraints:
 - Basis Functions
 - e.g. B-Splines
 - Regularisation
 - Topology-preservation

Used for good quality between-subject registrations



C. Image registration - What do I use? (FSL)

Rigid body (6 DOF)

- within-subject motion

Non-linear (lots of DOF!)

- high-quality image (resolution, contrast) & same modality of reference/template
- better with a non-linear template (e.g. MNI152_T1_2mm)

Affine (12 DOF)

- needed as a starting point for non-linear
- align to affine template, or using lower quality images, or eddy current correction

More DOF is NOT always better (e.g. within-subject)

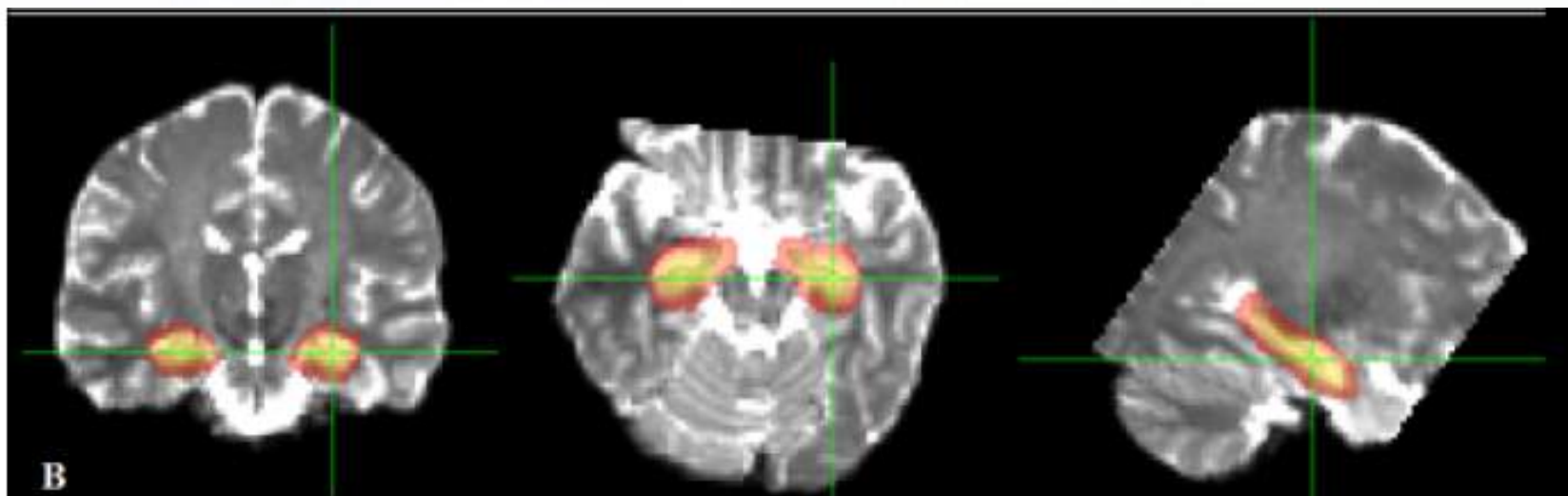
C. Image registration - Cost Function

Measures “goodness” of alignment
Seek the minimum value
Several main varieties



Examples: Least square, normalized correlation, correlation ratio

C. Image registration - Applicationn



C. Image registration

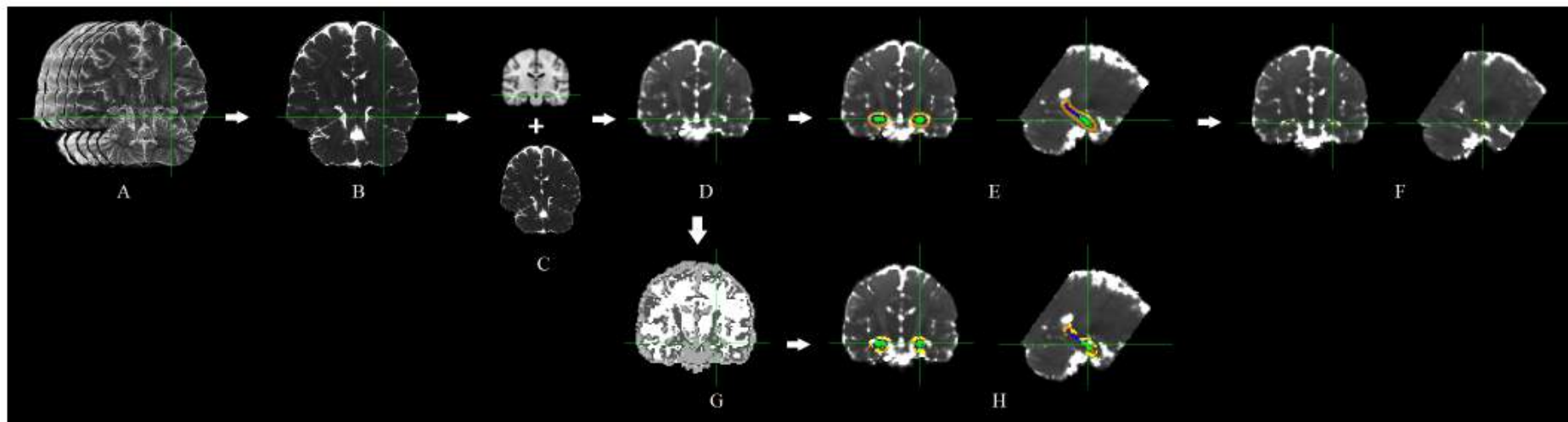
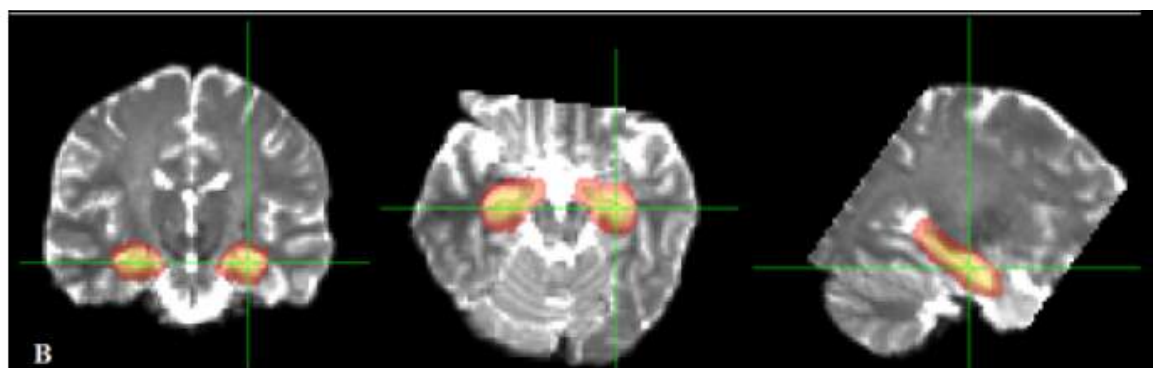


Fig. 1. Procedure for automatic estimation of hippocampal T2 relaxation time. A) Multi-echo T2 input images. B) Computed T2 Relaxometry. C) Illustration of the registration procedure of the T2 Relaxometry image (bottom) with an atlas (top). D) T2 Relaxometry image in the atlas common space. E) Simplest methodology, based on the mask of the hippocampi. F) Experiment using three high probability regions mimicking the manual procedure. G) tissues generated from brain pixel labeling. H) The resultant hippocampus mask composed only by gray matter. The T2 relaxation time is given by the median intensity of the regions in Figures E), F) or H). Different colors in E) and H) are labels achieved applying distinct thresholding values.



Shida CS¹, Santos ACD², Salmon CEG², Leite JP², Ide JS¹

¹Federal University of São Paulo, Institute of Science and Technology, São José dos Campos, Brazil,

²University of São Paulo USP, Ribeirão Preto, Brazil

30th International Epilepsy Congress 2013 Montreal · Abstract: A-577-0009-01248

Purpose

Several neuroimaging studies of epilepsy require the normalization procedure (warping of individual brain images to a common template space) in order to perform a group study. Satisfactory normalization algorithms are available for anatomically normal brains; however, this is not a solved problem for brains with lesions or undergone surgery. Some previous works have shown that MRI normalization of these atypical brains, using different methods can dramatically affect partially or the whole final normalized brains (Ripollés et al., NeuroImage 60, 2002, 1296-1306; Brett et al., NeuroImage 14,2001, 486-500; Crinion et al., NeuroImage 37, 2007, 866-875, 2007).

Method

In this work, we sought to compare two popular methods of MRI T1 image normalization:

•FSL

•SPM8/Dartel

Our patients were separated in 3 groups:

- **Group A:** 8 epilepsy patients that had undergone surgery
- **Group B:** 9 epilepsy patients' candidates for surgery
- **Group C:** 9 healthy patients

Performance evaluation was quantified through variance per voxel and ANOVA test.

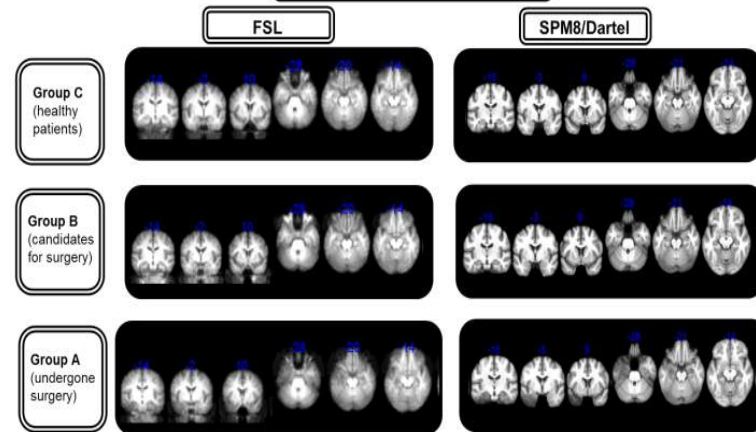
Results

- We have observed visually that SPM8/Dartel perform better than FSL the registration/normalization process, that is, the first present less deformation comparing the images of the 3 groups.
- Statistical analysis of intra- and inter-groups and different registration methods, also, shown that SPM8/Dartel presented the smaller variance in all cases of comparison between methods (Table).

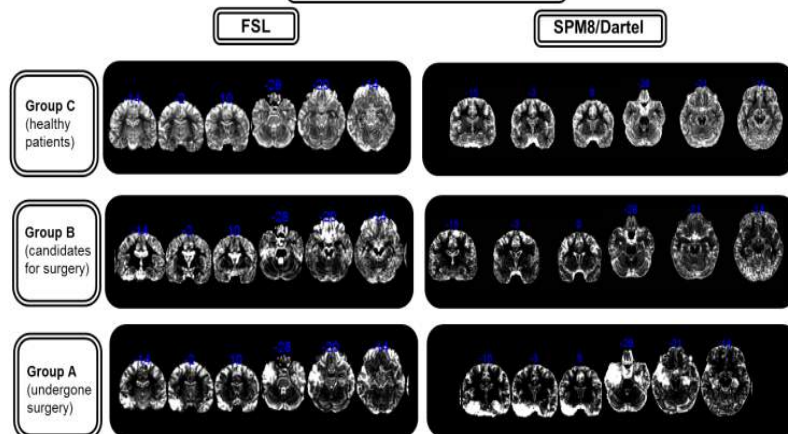
Table: Average variance of the MR normalized images of groups A, B and C. The variance of each normalized patient image was calculated against Single Subject image. Normalized images were obtained using FSL and SPM8/Dartel analysis package.

Groups	SPM8/Dartel (variance)	FSL* (variance)
Group C (9 healthy patients)	1746,2	3659,5
Group B (9 candidates for surgery)	1881,1	4166,6
Group A (Undergone surgery – all 8 patients)	1995,0	4149,8
- Part of Group A - 3 patients undergone right side surgery	2675,8	6815,2
- Part of Group A - 5 patients undergone left side surgery	2091,6	3854,5

Normalized Images (average)



Variance Images (average)



Conclusion

In this work, we observed superior and robust performance of DARTEL algorithm in our MRI data. However, a larger number of patients would be desirable for more statistically significant results.

C. Image registration - References

- P. A. Miranda, F. A. Cappabianco, and J. S. Ide, "A case analysis of the impact of prior center of gravity estimation over skull-stripping algorithms in mr images," in 2013 IEEE International Conference on Image Processing. IEEE, 2013, pp. 675-679.
- M. Brett, I. S. Johnsrude, and A. M. Owen, "The problem of functional localization in the human brain," *Nature reviews neuroscience*, vol. 3, no. 3, pp. 243-249, 2002.
- A. Klein, J. Andersson, B. A. Ardekani, J. Ashburner, B. Avants, M.-C. Chiang, G. E. Christensen, D. L. Collins, J. Gee, P. Hellier, J. H. Song, M. Jenkinson, C. Lepage, D. Rueckert, P. Thompson, T. Vercauteren, R. P. Woods, J. J. Mann, and R. V. Parsey, "Evaluation of 14 nonlinear deformation algorithms applied to human brain mri registration," *NeuroImage*, vol. 46, no. 3, p. 786802, 2009.
- M. Jenkinson, C. F. Beckmann, T. E. Behrens, M. W. Woolrich, and S. Smith, "Fsl," *NeuroImage*, vol. 62, no. 2, pp. 782-790, 2001.
- J. L. Andersson, M. Jenkinson, S. Smith et al., "Non-linear registration, aka spatial normalisation fmrib technical report tr07ja2," *FMRIB Analysis Group of the University of Oxford*, vol. 2, 2007.
- B. B. Avants, N. Tustison, and G. Song, "Advanced normalization tools (ants)," *Insight J*, vol. 2, pp. 1-35, 2009.
- N. J. Tustison, P. A. Cook, A. Klein, G. Song, S. R. Das, J. T. Duda, B. M. Kandel, N. van Strien, J. R. Stone, J. C. Gee et al., "Large-scale evaluation of ants and freesurfer cortical thickness measurements," *Neuroimage*, vol. 99, pp. 166-179, 2014.
- S. Klein, M. Staring, K. Murphy, M. A. Viergever, and J. P. Pluim, "Elastix: a toolbox for intensity-based medical image registration," *IEEE transactions on medical imaging*, vol. 29, no. 1, pp. 196-205, 2010.
- J. West and et al., "Comparison and evaluation of retrospective intermodality brain image registration techniques," *Journal of Computer Assisted Tomography*, vol. 21, no. 4, pp. 554-566, 1997.
- M. Jenkinson and S. Smith, "A global optimisation method for robust affine registration of brain images," *Medical Image Analysis*, vol. 5, pp. 143-156, 2001.
- M. Jenkinson, P. Bannister, M. Brady, and S. Smith, "Improved optimization for the robust and accurate linear registration and motion correction of brain images," *Neuroimage*, vol. 17, no. 2, pp. 825-841, 2002.

Principles of fMRI

Gilson Vieira and Kelly Cotosck
Ph. D. in Bioinformatics and Ph. D. student in Neuroimaging
at University of São Paulo

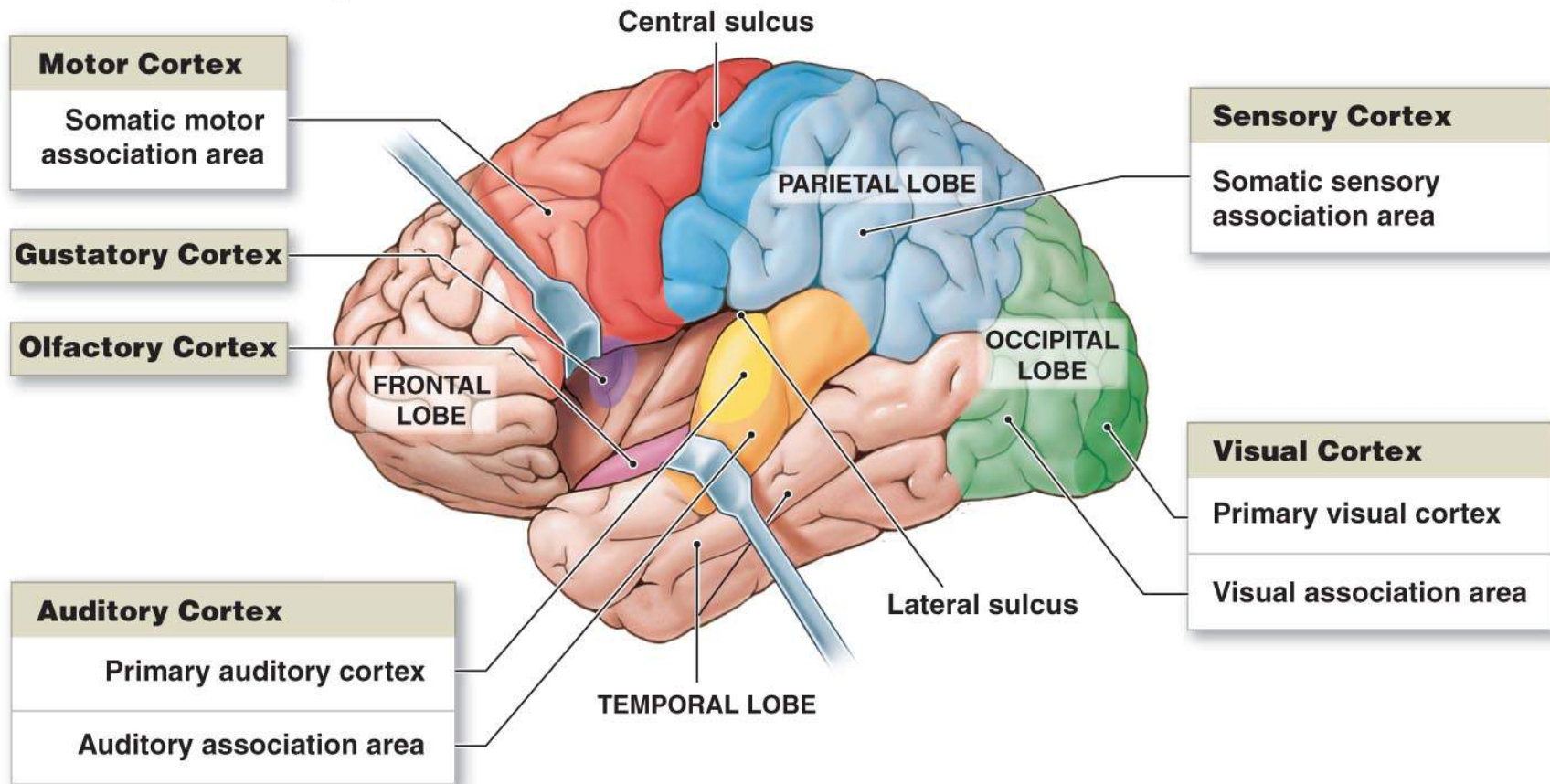


fMRI Image

- ✓ Noninvasive technique used to study brain activity
- ✓ Do not use intravenous contrast
- ✓ Evaluates the oxygen consumption in the brain areas activated
- ✓ The hemodynamic response function:
 - Location
 - Change Location - Brain Mapping

Brain Functional Areas

The motor and sensory cortexes and the association areas for each

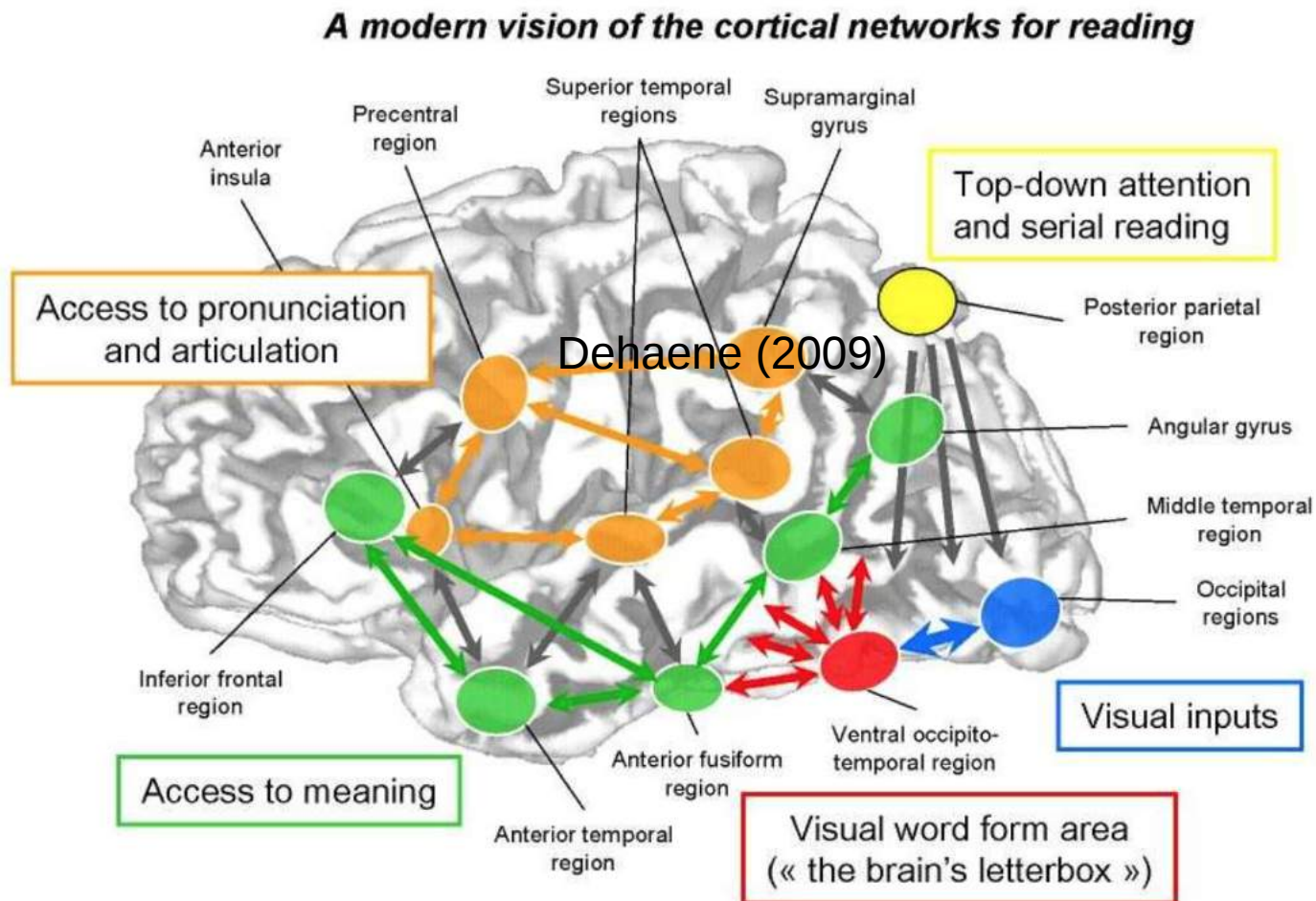


© 2011 Pearson Education, Inc.

Source: <http://www2.highlands.edu/academics/divisions/scipe/biology/faculty/harden/2121/notes/cns.htm>

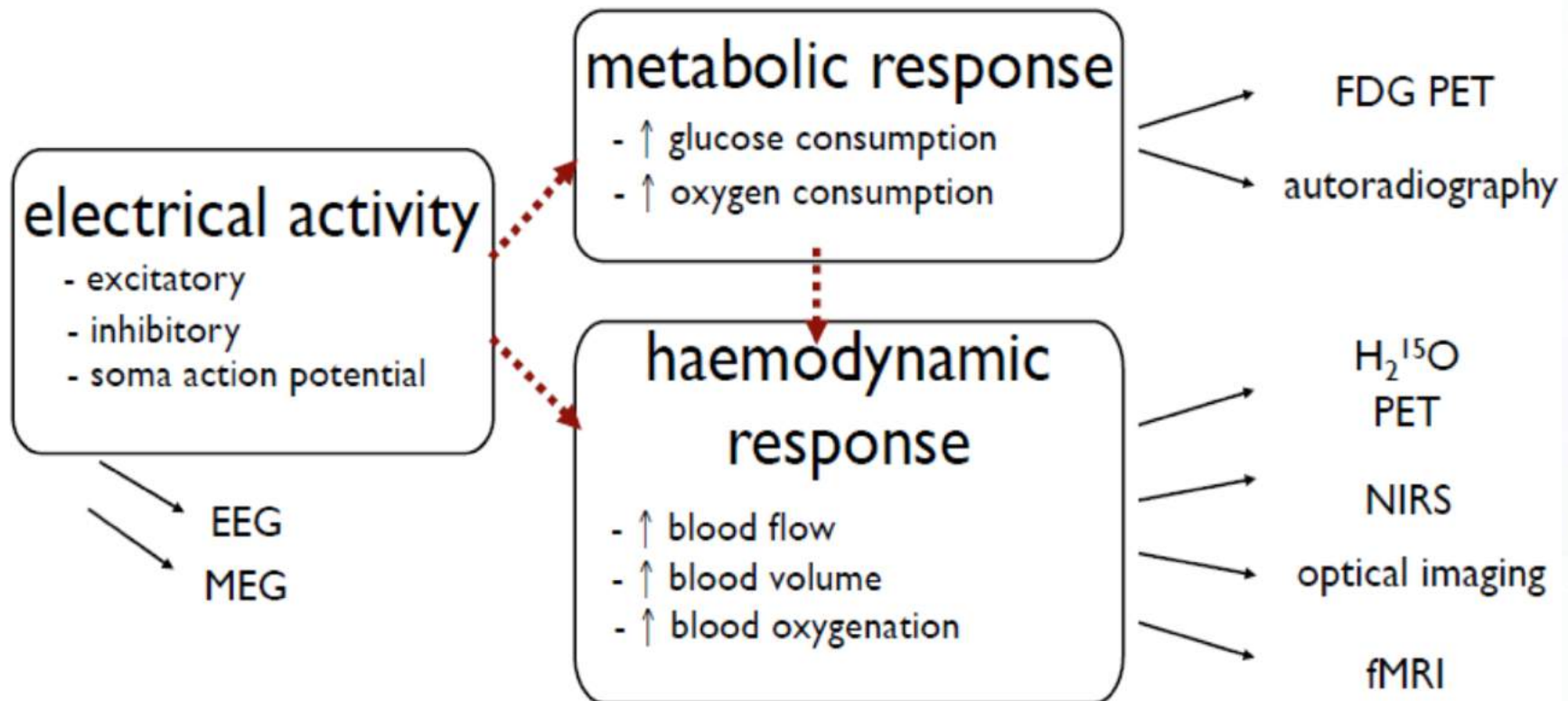


Brain Functional Networks



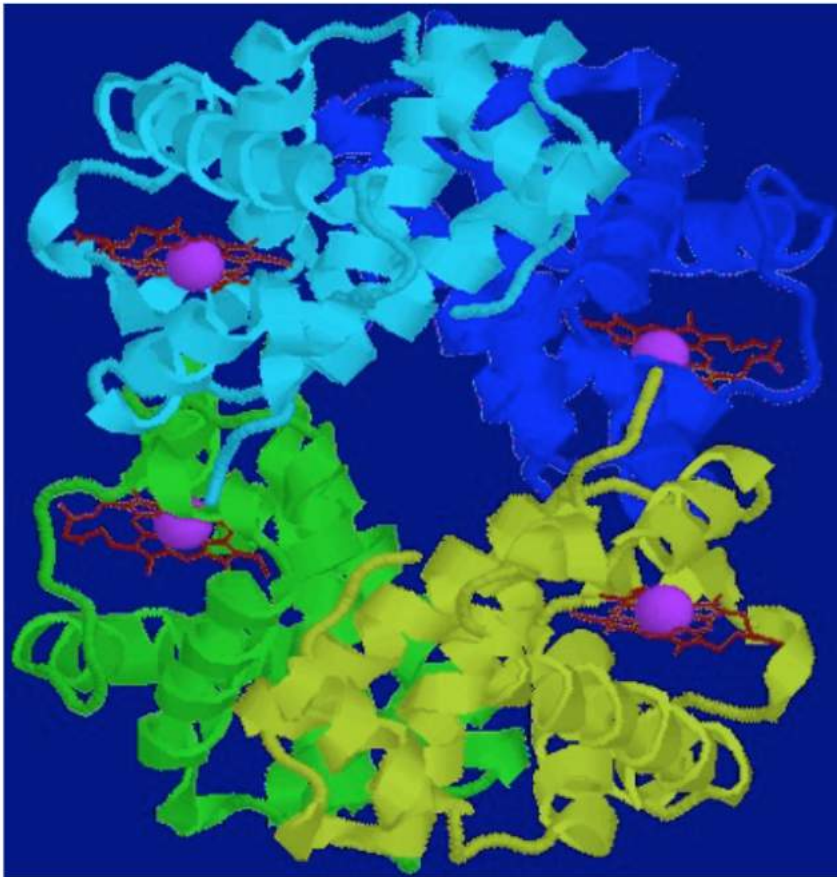
Source: Dehaene (2009)

Physiological correlates of brain electrical activity



Source: http://fsl.fmrib.ox.ac.uk/fslcourse/graduate/WebLearnArchive/2010-2011/Introduction%20to%20fMRI%20_1st%20week%20course/_Intro_to_FSL_Day1_2010.pdf

Magnetic Properties of Haemoglobin



Oxy-haemoglobin
Diamagnetic
(same as tissue)

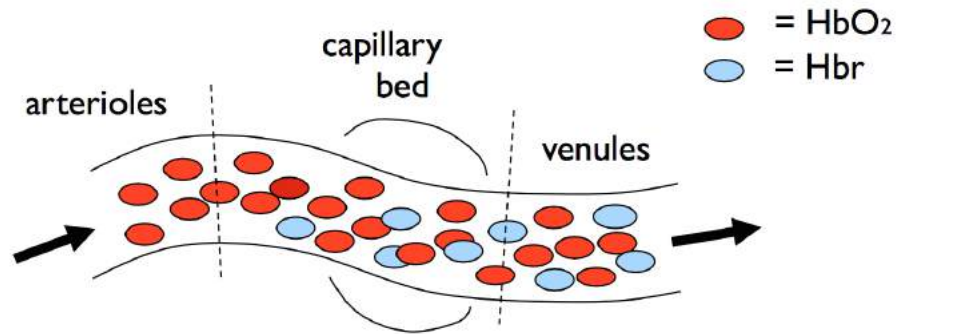
Deoxy- haemoglobin
Paramagnetic
 $\Delta\chi \approx 0.2$ ppm

Source:: http://fsl.fmrib.ox.ac.uk/fslcourse/graduate/WebLearnArchive/2010-2011/Introduction%20to%20fMRI%20_1st%20week%20course_/Intro_to_FSL_Day1_2010.pdf

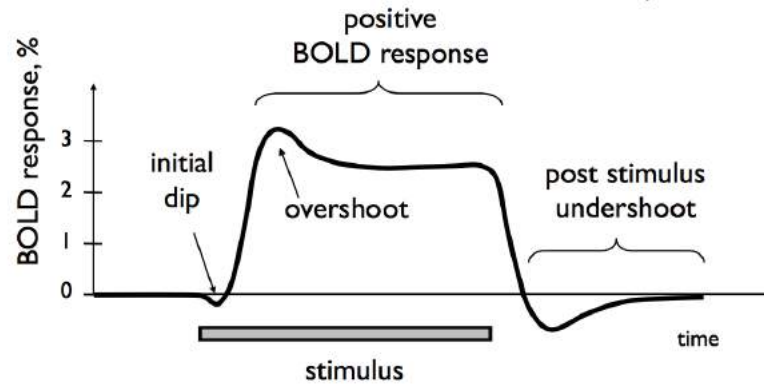
BOLD Effect

Increased Neuronal Activity

CBF ↑
CBV ↑
CMRO₂ ↑

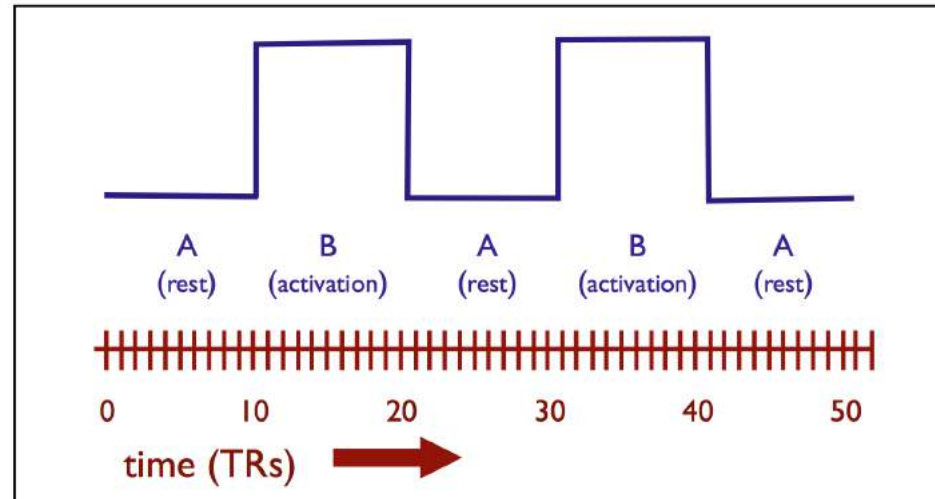


Magnetic field less perturbed
→ Less dephasing
→ More signal



Source: http://fsl.fmrib.ox.ac.uk/fslcourse/graduate/WebLearnArchive/2010-2011/Introduction%20to%20fMRI%20_1st%20week%20course/_Intro_to_FSL_Day1_2010.pdf

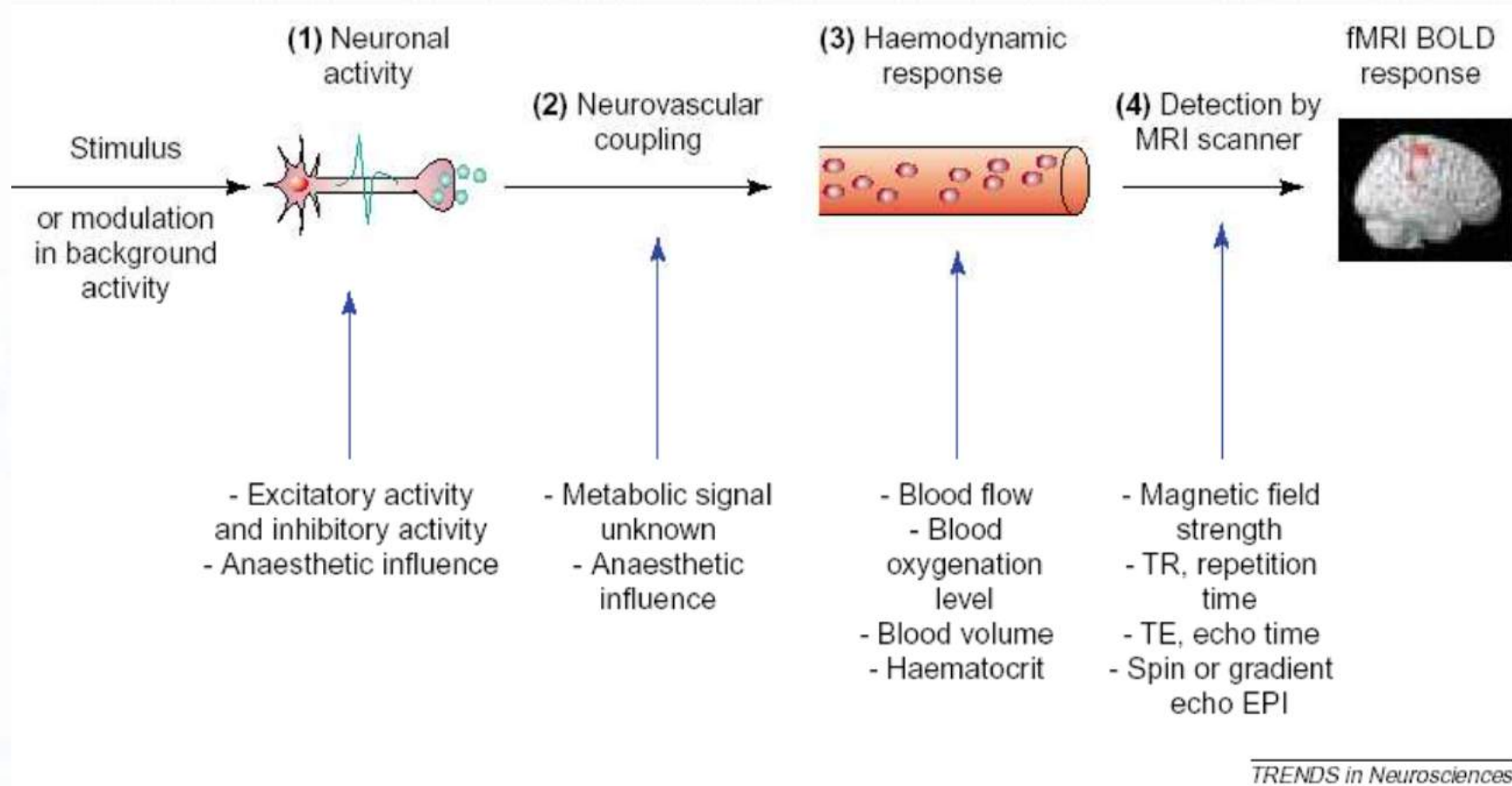
Experimental Design



- Simple paradigm design:
 - stimulus vs baseline
 - constant stimulus “intensity”
 - constant block lengths
 - many repetitions: ABABA
- Need baseline (rest) condition to measure *change*

Source: http://fsl.fmrib.ox.ac.uk/fslcourse/graduate/WebLearnArchive/2010-2011/Introduction%20to%20fMRI%20_1st%20week%20course_/Intro_to_FSL_Day1_2010.pdf

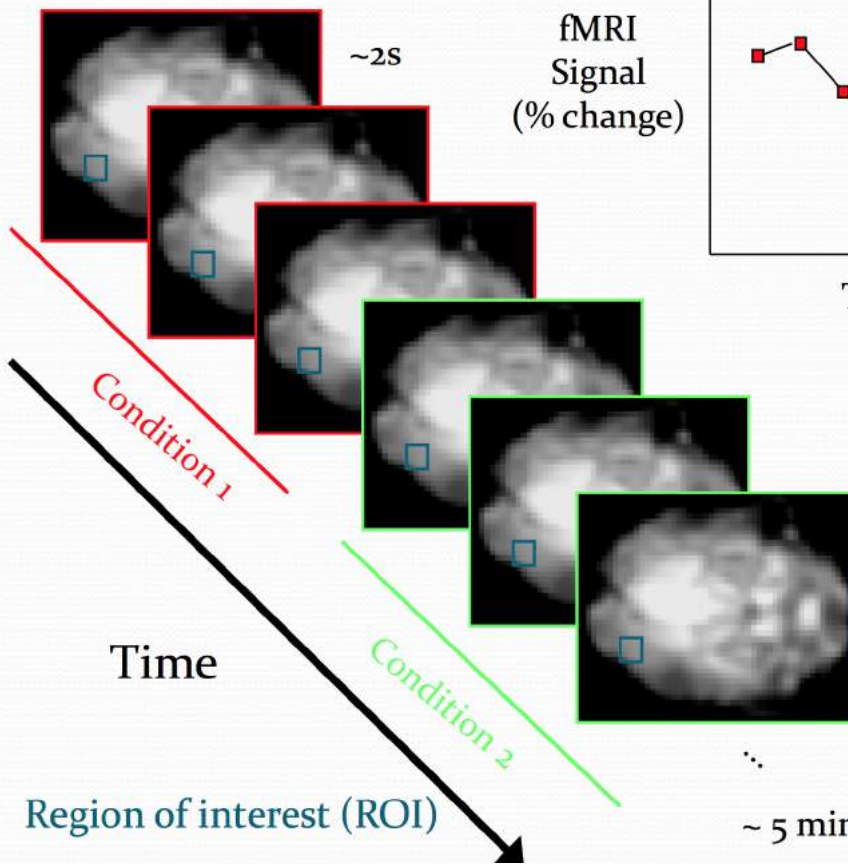
Stimulus to BOLD



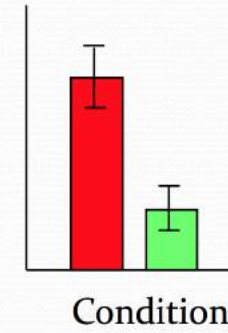
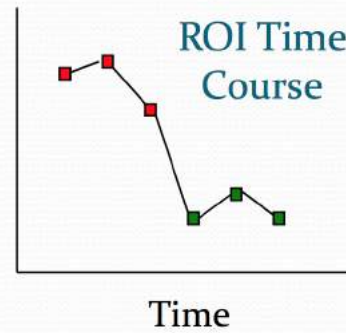
Source: Trend in Neuroscience

Activation Statistics

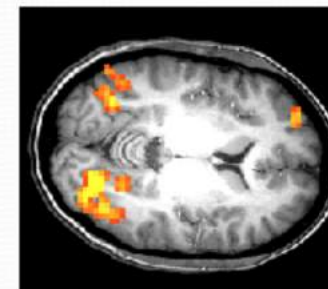
Functional images



fMRI
Signal
(% change)

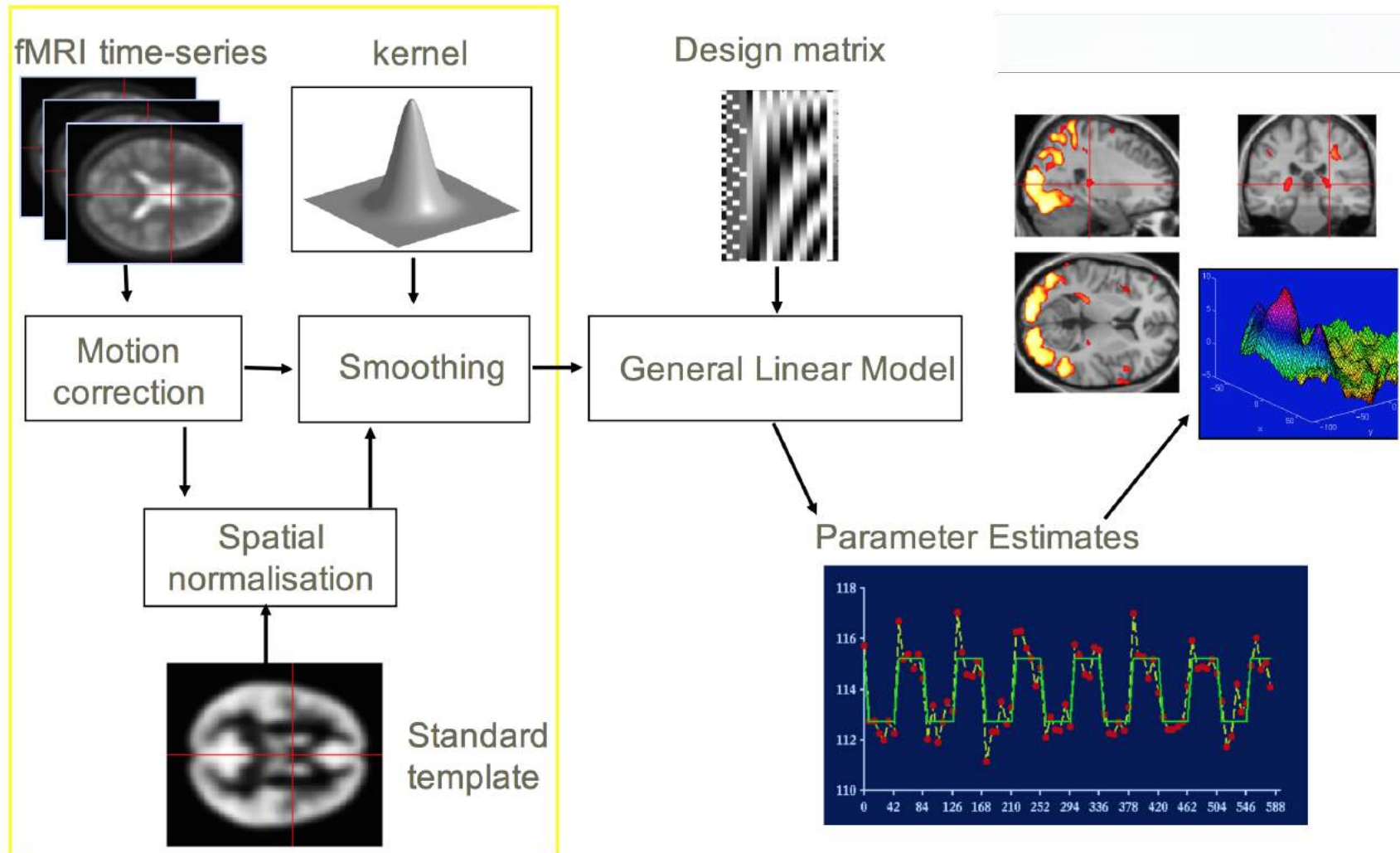


Statistical Map
superimposed on
anatomical MRI image



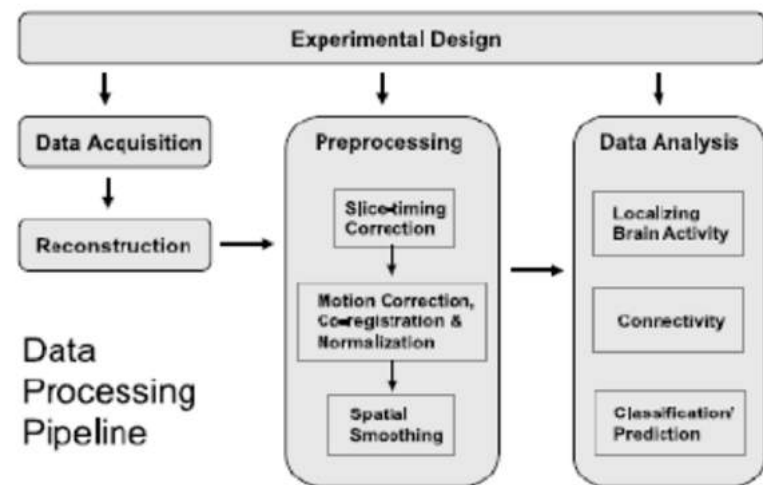
Source: <http://slideplayer.com/slide/4261788/>

Overview fMRI Data Processing



Data Preprocessing

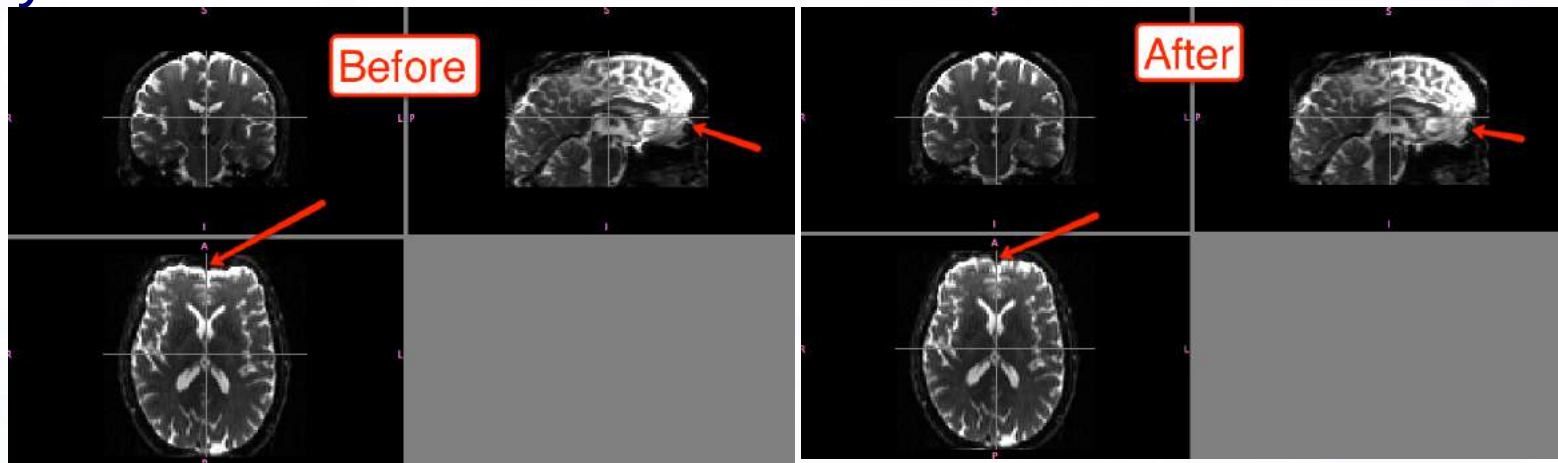
- Preprocessing have two primary goals
 - to reverse displacements of the data in time or space that may have occurred during acquisition
 - to enhance the ability to detect spatially extended signals within or across subjects.



Source: Parida (2013)

Distortion Correction

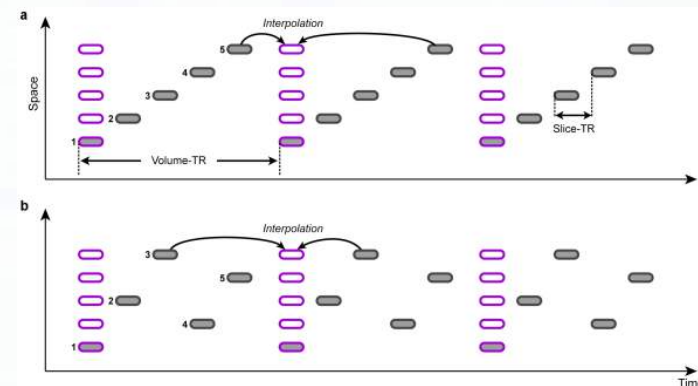
- fMRI data are distorted in space as a result of magnetic field lines at air tissue interfaces.
- To correct for this spatial distortion, methods use a map of the magnetic field
- In most cases, this correction is performed by the scanning system itself



Source: <http://andysbrainblog.blogspot.com.br/>

Slice Acquisition Correction

- In a typical fMRI sequence, each slice samples a slightly different point in time
- Slice-acquisition correction compensates for this staggered order of acquisition by interpolating in-between time points
- The correction works by calculating the signal that would have been obtained if the slice had been acquired at the closest TR
- This preprocessing step is quite important for even-related designs



Temporal High-Pass Filtering

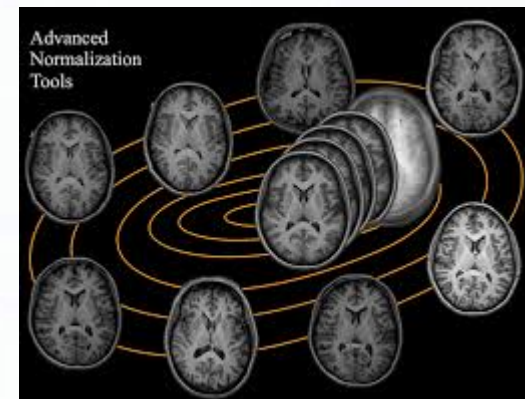
- The fMRI signal often show low-frequency drifts caused by physiological noise as well as by scanner-related noise
 - these drifts reduce substantially the power of statistical analysis invalidating event-related averaging
- The removal of low-frequency drifts is one of the most important preprocessing steps and should be always performed
 - This preprocessing can be "dangerous" as condition-related signals may be removed if correction is not properly applied

Motion Correction

- A common data preprocessing step is to correct for the effects of motion by realigning the image of the brain obtained at each point in time back to the first or median image
- Most methods treat the brain as a rigid body and calculate the six possible movement parameters which minimize the difference between the realigned brain and the brain in its reference position
- Motion correction of this kind does not completely remove the effects of movement upon the fMRI signal
- Statistical analysis of fMRI data often will consider the six movement parameters measured during realignment to account for changes in the signal within voxels that are correlated with the movement of the head

Spatial Normalization

- To test a hypothesis regarding a certain area of the brain within a population spatial normalization is needed
 - This is done by warping the anatomical structure of the brain of one subject to match a template brain within a standard defined space
- An alternative to anatomical registration is functional identification
 - The approach is first to identify a region across subjects by its functional responses to test other types of stimuli across subjects within this area



References

- Faro, Scott H., and Feroze B. Mohamed, eds. *BOLD fMRI: A guide to functional imaging for neuroscientists*. Springer Science & Business Media, 2010.
- Parida, Shantipriya, and Satchidananda Dehuri. "Applying Machine Learning Techniques for Cognitive State Classification." *IJCA Proceedings on International Conference in Distributed Computing and Internet Technology (ICDCIT), ICDCIT*. 2013.